UNIVERSITA' VITA-SALUTE SAN RAFFAELE

CORSO DI DOTTORATO DI RICERCA INTERNAZIONALE
IN MEDICINA MOLECOLARE
Curriculum in Medicina Clinica e Sperimentale

ROLE OF CHROMOGRANIN A-DERIVED FRAGMENTS AND OTHER BIOMARKERS IN PANCREATIC NEOPLASMS: FOCUS ON NEUROENDOCRINE TUMORS

DoS: Prof. Angelo Corti
Second Supervisor: Dott.ssa Ilaria Marinoni

Tesi di DOTTORATO DI RICERCA di Valentina Andreasi
Matr. 013847
Ciclo di dottorato XXXIV
SSD MED/18

Anno Accademico 2020/2021



CONSULTAZIONE TESI DI DOTTORATO DI RICERCA

La sottoscritta / *I* Valentina Andreasi

Matricola / *registration number* 013847

nata a / *born at* Milano

il / *on* 20/06/1993

autore della tesi di Dottorato dal titolo / *author of the PhD thesis titled* "**Role of chromogranin A-derived fragments and other biomarkers in pancreatic neoplasms: focus on neuroendocrine tumors**"

☐ **AUTORIZZA** la Consultazione della tesi / AUTHORIZES *the public release of the thesis*

☒ **NON AUTORIZZA** la Consultazione della tesi per 6 mesi / DOES NOT AUTHORIZE *the public release of the thesis for 6 months*

a partire dalla data di conseguimento del titolo e precisamente */ from the PhD thesis date, specifically*

Dal / *from* .../.../... Al / *to* .../.../...

Poiché /*because*:

□ l'intera ricerca o parti di esssa sono potenzialmente soggette a brevettabilità /*The whole project or part of it might be subject to patentability;*

X ci sono parti di tesi che sono già state sottoposti a un editore o sono in attesa di pubblicazione / *Parts of the thesis have been or are being submitted to a publisher or are in press;*

□ la tesi è finanziata da enti esterni che vantano dei diritti su di esse e sulla loro pubblicazione / *the thesis project is financed by external bodies that have rights over it and on its publication.*

E' fatto divieto di riprodurre, in tutto o in parte, quanto in essa contenuto / *Copyright the contents of the thesis in whole or in part is forbidden*

Data 13/10/2021 Firma Valentina Andreasi.....

DECLARATION

This thesis has been composed by myself and has not been used in any previous application for a degree. Throughout the text I use both 'I' and 'We' interchangeably. All the results presented here were obtained by myself, at San Raffaele Scientific Institute (Milan, Italy) and at the Institute of Pathology (Bern, Switzerland), except for:

1) *Chromogranin A and NETest measurements (aim 4, p.73) were performed at Wren laboratories, Branford, CT, USA.*

2) *Cell isolation and culture for patient-derived islet-like tumoroids were performed by Mr. Simon-Leonhard April-Monn (Institute of Pathology, Bern, Switzerland).*

3) Immunohistochemistry set-up for Chromogranin A (CgA) and CgA-derived fragments was performed in collaboration with Dr. Josè Galvàn (Translational Research Unit, Institute of Pathology, Bern, Switzerland).

Some of the contents of the present Thesis have been already published, in collaboration with the co-authors included in the publications listed below:

Andreasi V, Partelli S, Manzoni M, Muffatti F, Colombo B, Corti A, Falconi M. Association between preoperative Vasostatin-1 and pathological features of aggressiveness in localized nonfunctioning pancreatic neuroendocrine tumors (NF-PanNET). Pancreatology 2019.

Partelli S*, **Andreasi V***, Muffatti F, Schiavo Lena M, Falconi M. Circulating Neuroendocrine Gene Transcripts (NETest): A Postoperative Strategy for Early Identification of the Efficacy of Radical Surgery for Pancreatic Neuroendocrine Tumors. Ann Surg Oncol 2020. *Co-first authors.

Andreasi V, Muffatti F, Guarneri G, Falconi M, Partelli S. Surgical Principles in the Management of Pancreatic Neuroendocrine Neoplasms. Curr Treat Options Oncol 2020.

Reni M, **Andreasi V**, Gasparri AM, Dugnani E, Colombo B, Macchini M, Bianco M, Dallatomasina A, Citro A, Assi E, Protti MP, Esposito E, Falconi M, Curnis F, Piemonti L, Corti A. Circulating Chromogranin A Is Cleaved Into Vasoregulatory Fragments in Patients With Pancreatic Ductal Adenocarcinoma. Front Oncol 2020.

Andreasi V, Partelli S, Manzoni MF, Muffatti F, Di Filippo L, Crippa S, Corti A, Falconi M. Role of chromogranin A-derived fragments after resection of non-functioning pancreatic neuroendocrine tumors. Currently under submission.

All sources of information are acknowledged by means of reference.

ACKNOWLEDGEMENTS

The research conducted on the role of chromogranin-A derived fragments in pancreatic neuroendocrine neoplasms was supported by the European Neuroendocrine Tumor Society (ENETS) Translational Medicine Fellowship Grant 2019.

We are also grateful to Gioja Bianca Costanza Fund for supporting the present PhD scholarship.

Alla mia Mamma,
che è stata sempre al mio fianco

E al mio Papà,
che oggi mi guarda dall'alto e che,
come promesso, non mi ha mai abbandonata

ABSTRACT

Introduction: The lack of valid biomarkers represents a major unmet clinical need in pancreatic neuroendocrine neoplasms (PanNENs). Chromogranin A (CgA) is the most commonly measured PanNEN biomarker, despite relevant limitations related to variable sensitivity, poor specificity and lack of assay standardization. Therefore, novel biomarkers are needed to improve diagnosis, detect disease recurrence and assess treatment response. In this project, the role of CgA-derived fragments as PanNEN biomarkers was investigated, focusing on the N-terminal peptide vasostatin-1 (VS-1). A multianalyte biomarker, NETest, was also assessed as PanNEN biomarker. Given the role of CgA-derived fragments in tumor vascular biology, their tissue expression was correlated with pathological features in PanNENs. Finally, the role of CgA-derived fragments was investigated in the setting of pancreatic ductal adenocarcinoma (PDAC).

Methods: The project was developed according to different tasks: 1) CgA-derived fragments and total-CgA were measured in patients who underwent surgery for PanNENs; 2) NETest was evaluated as biomarker evaluate the efficacy of surgical resection in patients with PanNENs; 3) The site of CgA cleavage was investigated and CgA-derived fragments tissue expression was assessed; 4) The role of CgA fragmentation in terms of prognosis was assessed in patients with PDAC.

Results: *Aim 1.* VS-1 is significantly correlated with tumor size, aggressiveness features and risk of disease relapse in patients with localized non-functioning (NF) PanNENs. VS-1 is not affected by proton pump inhibitors treatment. *Aims 2-3*. VS-1 is able to early assess surgical effectiveness in patients with NF-PanNETs, especially in those with aggressive tumors. Total-CgA, VS-2 and pancreastatin are not useful in this context. *Aim 4.* NETest seems able to provide a proper evaluation of the initial postoperative disease status in setting of PanNENs. *Aim 5.* CgA processing occurs within neuroendocrine tumor cells. VS-1 tissue expression is a marker of tumor differentiation. *Aim 6.* C-terminal CgA cleavage is enhanced in PDAC and it is associated with poorer survival outcomes.

Conclusions: VS-1 has been identified as a promising biomarker for PanNENs. CgA C-terminal fragmentation is enhanced in PDAC, whereas N-terminal cleavage seems more relevant in PanNENs. Whether CgA fragmentation in PanNENs is just a disease epiphenomenon or plays a role in tumor vascular biology remains an open point.

Table of Contents

Acronyms and abbreviations **5**

List of figures **8**

Introduction **11**

Neuroendocrine neoplasms **11**

Pancreatic neuroendocrine neoplasms **12**

Epidemiology ***12***

Tumor grading ***13***

Genomic landscape ***14***

Prognosis ***15***

Angiogenesis in PanNENs ***17***

Treatment options and follow-up ***18***

Biomarkers in neuroendocrine tumor disease **19**

Assessment of tumor response: imaging is not enough ***19***

Monoanalyte versus multianalyte biomarkers: pros and cons ***20***

Overview of monoanalyte NET biomarkers ***21***

Overview of multianalyte NET biomarkers ***22***

Chromogranin A (CgA) and CgA-derived fragments **24**

Structure and function ***24***

Role of CgA and CgA-derived fragments in the process of angiogenesis ***25***

CgA and CgA-derived fragments in normal subjects ***27***

CgA as neuroendocrine biomarker: more flaws than strengths? ***27***

Vasostatin-1 as neuroendocrine biomarker ***31***

NETest: a promising multianalyte biomarker **32**

NETest: clinical utility ***33***

Pancreatic ductal adenocarcinoma **34**

Premises for investigating CgA and CgA-derived fragments in PDAC ***35***

Aims **37**

Biomarkers in PanNENs **37**

Biological role of CgA and CgA-derived fragments in PanNENs **37**

CgA and CgA-derived fragments as PDAC biomarkers 37

Aim 1 - To evaluate VS-1, compared with total-CgA, as biomarker for patients submitted to surgery for localized NF-PanNETs, by assessing the association with pathological features of aggressiveness and with survival outcomes 38

Results 38

Study population 38

Correlation of VS-1 and total-CgA with pathological features of aggressiveness 40

Survival analysis 49

Discussion 49

Materials and methods 53

Study design 53

Participants 53

Test methods 54

Samples and data collection 54

Statistical analysis 55

Aims 2 and 3 - To evaluate the ability of VS-1, compared with total-CgA, to assess the effectiveness of surgical resection in patients with NF-PanNETs. To investigate PST and vasostatin-2 (VS-2) as potential biomarkers for NF-PanNETs. 57

Results 57

Study population 57

AIM 2 - Test results: total-CgA and VS-1 59

AIM 3 - Test results: VS-2 and PST 62

Determinants of high (> 0.390 nM) preoperative VS-1 63

VS-1 postoperative decrease in patients with and without features of aggressiveness 64

Discussion 65

Materials and Methods 69

Study design 69

Participants 69

Test methods 69

Samples and data collection 70

Statistical analysis *71*

Aim 4 - To investigate NETest as biomarker for patients undergoing surgery for PanNETs by assessing its effectiveness in defining the extent and efficacy of surgical resection and in predicting disease recurrence. **72**

Results **72**

Study cohort *72*

Test results: NETest *74*

Test results: CgA *77*

Determinants of preoperative NETest scores *78*

Discussion **80**

Study Design *83*

Patients *84*

Test Methods *84*

Samples and data collection *85*

Statistical Analysis *86*

Aim 5 – To investigate the biological role of CgA and CgA-derived fragments in PanNENs, by assessing the site of production and cleavage using *in vitro* models and evaluating the relationship between their tissue expression, MVD and other immunohistochemical markers. **87**

Results **87**

PanNEN cell lines and patient-derived islet-like tumoroids produce and secrete CgA and CgA-derived fragments *87*

Immunohistochemistry set-up and scoring for CgA and CgA-derived fragments *89*

Correlation between pathological features and histological scores *94*

Correlation with MVD and hypoxia marker CA-9 ..... *96*

Correlation between plasma and tissue levels of VS-1 ..... *97*

Determinants of VS-1 tissue score and plasma levels *97*

Discussion **99**

Materials and methods **102**

Patients *102*

Cell culture *102*

Cell lysis *102*

Patient-derived islet-like tumoroids *102*

CgA and CgA-derived fragments immunoassays *103*

Immunohistochemistry *103*

Data and samples collection *104*

Statistical analysis *104*

Aim 6 - To investigate CgA and CgA-derived fragments as biomarkers in patients with PDAC, by correlating their plasma levels with survival outcomes. **106**

Results **106**

Study partecipants *106*

CgA and CgA-derived fragments can be measured in healthy subjects *107*

CgA fragmentation and PPI *108*

CgA C-terminal cleavage predicts progression-free survival (PFS) and OS in patients with PDAC *109*

Discussion **111**

Materials and methods **113**

Patients and plasma samples *113*

CgA and CgA-derived fragments immunoassays *113*

Statistical analysis *115*

Conclusions **116**

References **117**

Acronyms and abbreviations

AUC: area under the curve

BMI: body mass index

CA-9: carbohydrate antigen 9

CgA: chromogranin A

CI: confidence interval

CT: computed tomography

CTCs: circulating tumor cells

cfDNA: circulating free DNA

ctDNA: circulating tumor DNA

DAB: 3,3-diaminobenzidine

DFS: disease-free survival

ECs: endothelial cells

EDTA: ethylenediaminetretaacetic acid

ELISA: Enzyme-Linked ImmunoSorbent Assays

ENETS: European Neuroendocrine Tumor Society

epCAM: epithelial cell adhesion molecule

FDG: fluorodeoxyglucose

FGF-2: fibroblast growth factor 2

GEP-NENs: gastroenteropancreatic neuroendocrine neoplasms

GLUT-1: glucose transporter type 1

HIF: hypoxia inducible factor

IHC: immunohistochemistry

IQR: interquartile range

mAb: monoclonal antibody

miRNA: microRNA

MEN-1: multiple endocrine neoplasia type 1

MRI: magnetic resonance imaging

MVD: microvessel density

NENs: neuroendocrine neoplasms

NF-1: neurofibromatosis type 1

NF-PanNENs: non-functioning pancreatic neuroendocrine neoplasms

NIH: National Institutes of Health

NRP-1: neuropilin-1

NSE: neuron-specific enolase

OD: odds ratio

OS: overall survival

PAI-1: plasminogen activator inhibitor-1

PanNECs: pancreatic neuroendocrine carcinomas

PanNENs: pancreatic neuroendocrine neoplasms

PanNETs: pancreatic neuroendocrine neoplasms

PDAC: pancreatic ductal adenocarcinoma

PET: positron emission tomography

PFS: progression-free survival

POD: postoperative day

PP: pancreatic polypeptide

PPI: proton pump inhibitors

PRRT: peptide receptor radionuclide therapy

PST: pancreastatin

qPCR: quantitative polymerase chain reaction

RECIST: Response Evaluation Criteria in Solid Tumors

RIPA: radioimmunoprecipitation assay

ROC: Receiver Operating Characteristic

SB-NENs: small bowel neuroendocrine neoplasms

SD: standard deviation

SEER: Surveillance, Epidemiology and End Results

SN: supernatant

SSAs: somatostatin analogues

SSTRs: somatostatin receptors

SUV: standardized uptake value

TACE: transarterial chemoembolization

TMA: tissue microarray

TNFα: tumor necrosis factor alpha

TSC: tuberous sclerosis

uPA: urokinase-type plasminogen activator

VEGF: vascular endothelial growth factor

VHL: Von Hippel Lindau

VS-1: vasostatin-1

WHO: World Health Organization

List of figures

Figure 1. *Genetic pathways altered in well differentiated PanNETs. 15*
Figure 2. *OS stratified according to tumor grade. 16*
Figure 3. *Available circulating neuroendocrine biomarkers (modified from Oberg et al, 2015).....21*
Figure 4. *Schematic representation of full-length CgA and CgA-derived fragments.....25*
Figure 5. *Multistep protocol followed to obtain the NETest score (Modlin et al, 2018 - Open Access publication).....33*
Figure 6. *Matched comparison between preoperative plasma levels of total-CgA and VS-1. .....40*
Figure 7. *Linear regression analysis showing the correlation between VS-1 (A) or total-CgA (B) and tumor size. 41*
Figure 8. *Receiver operating characteristics curve of VS-1 (A) and total-CgA (B) as determinants of tumor size (using a 4 cm cut-off). 43*
Figure 9. *Comparison of the rate of nodal metastases and microvascular invasion between patients with low preoperative VS-1 and those with high preoperative VS-1…45*
Figure 10. *ROC curves of VS-1 (A) and total-CgA (B) as predictors of nodal involvement. 46*
Figure 11. *ROC curves of VS-1 (A) and total-CgA (B) as predictors of microvascular invasion. 46*
Figure 12. *Plasma levels of VS-1 (A) and total-CgA (B) in patients with and without nodal involvement.....47*
Figure 13. *Plasma levels of VS-1 (A) and total-CgA (B) according to the presence or absence of microvascular invasion. 47*
Figure 14. *Comparison of VS-1 and total-CgA plasma levels according to PPI use.....48*
Figure 15. *Bivariate correlation between preoperative plasma levels of VS-1 and total-CgA. 48*
Figure 16. *Comparison of disease-free survival between patients with low preoperative VS-1 plasma levels (n = 34) and patients with high VS-1 plasma levels (n = 16).....49*
Figure 17. *Matched comparison between preoperative total-CgA and VS-1 plasma levels. 59*
Figure 18. *Comparison between preoperative and postoperative VS-1 (A) and total-CgA (B). 60*
Figure 19. *Percentage of patients with VS-1 higher than the predefined cut-off (0.39 nM) preoperatively and postoperatively. 61*
Figure 20. *Comparison between preoperative and postoperative plasma levels of vasostatin-2 (A) and pancreastatin (B). 62*
Figure 21. *Comparison of the rate of nodal metastases and microvascular invasion between patients with low VS-1 (≤ 0.390 nM) and those with high VS-1 (> 0.390 nM). 64*
Figure 22. *Comparison of VS-1 percentage decrease between patients with and without aggressive NF-PanNETs (features of aggressiveness: T3-T4 tumors, nodal/distant metastases, Ki67 >5%, microvascular/perineural invasion, necrosis).....65*
Figure 23. *Relationship between NETest score and surgical resection. 75*
Figure 24. *NETest score changes and surgical resection. 76*
Figure 25. *Relationship between CgA plasma levels and surgical resection. 77*
Figure 26. *CgA changes and surgical resection. 78*

Figure 27. *Comparison of preoperative NETest score (A) and CgA plasma levels between patients with functioning (n = 8) and non-functioning (n = 22) PanNETs.....79*
Figure 28. *Total-CgA and full-length CgA measurement in cell lysate from BON-1, QGP-1 and NT-3. Concentrations are normalized to the amount of total proteins measured in each cell lysate sample.....87*
Figure 29. *VS-1 and $CgA_{1\text{-}372/373}$ measurement in cell lysate from BON-1, QGP-1 and NT-3. Concentrations are normalized to the amount of total proteins measured in each cell lysate sample.....88*
Figure 30. *CgA and CgA-derived fragments measurement in BON-1 supernatant. 88*
Figure 31. *VS-1 measurement in tumoroids, BON-1 and NT-3 supernatant (normalized to the number of plated cells).....89*
Figure 32. *VS-1 staining of NT-3, BON-1 and QGP-1 cell blocks.....90*
Figure 33*. Stainings for full-length CgA (A), total-CgA (B), VS-1 (C) and $CgA_{1\text{-}372/373}$ on normal islets. 91*
Figure 34. *VS-1 staining of two PanNET samples showing different levels of positivity. 92*
Figure 35. *Example of tumor cell detection using a digital pathology software.....92*
Figure 36. *PanNET samples showing increasing VS-1 histological scores.....93*
Figure 37. *A) Comparison of CgA and CgA-derived fragments histological scores according to tumor grade. B) Spearman correlation between histological scores and Ki67 proliferative index. 95*
Figure 38. *Spearman correlation between histological scores and tumor size.....95*
Figure 39. *Comparison of CgA and CgA-derived fragments histological scores according to DAXX/ATRX status.....96*
Figure 40. *Correlation between CgA and CgA-derived fragments histological scores, MVD (A) and hypoxia marker CA-9 (B). 96*
Figure 41. *Correlation between VS-1 plasma and tissue levels, before (A) and after (B) normalization of VS-1 plasma levels for tumor size.....97*
Figure 42. *Plasma levels of full-length CgA (A), $CgA_{1\text{-}373}$ (B) and $CgA_{1\text{-}76}$ (C) in normal subjects and in patients with PDAC.....108*

List of tables

Table 1. *WHO classification for PanNENs (Lloyd RV et al, 2017). 13*
Table 2. *ENETS TNM staging system for PanNENs (Rindi et al, 2006). 13*
Table 3. *Sensitivity and specificity of available NET biomarkers 24*
Table 4. *Conditions associated with increase of CgA plasma levels (Marotta et al, 2012). 29*
Table 5. *Demographic and preoperative features of 50 patients diagnosed with NF-PanNETs.....38*
Table 6. *Pathological features of patients who underwent surgery for NF-PanNETs. ..39*
Table 7. *ROC curve analysis assessing VS-1 and total-CgA plasma levels as predictors of tumor size. 42*
Table 8. *Comparison of clinico-pathological characteristics between patients with low VS-1 plasma levels (≤ 0.39 nM) (n = 34) and those with high preoperative VS-1 (> 0.39 nM) (n = 16). 44*
Table 9. *Demographic and perioperative features of patients submitted to surgery for NF-PanNETs. 57*
Table 10. *Pathological details of patients submitted to surgery for NF-PanNETs. 58*
Table 11. *Univariate logistic regression analysis evaluating demographic, clinical, and pathological determinants of "high" (>0.390 nM) preoperative VS-1. .....63*
Table 12. *Demographic and perioperative features of 30 patients with histologically confirmed PanNETs. 72*
Table 13. *Pathological features of patients who underwent surgery for PanNETs.....73*
Table 14. *Univariate linear regression analysis assessing the determinants of preoperative NETest score. 78*
Table 15. *Clinico-pathological features of 62 patients who underwent surgical resection for NF-PanNETs.....94*
Table 16. *Univariate and multivariate analysis investigating determinants of VS-1 histological scores. 98*
Table 17. *Univariate and multivariate analysis investigating determinants of VS-1 histological scores. 98*
Table 18. *Demographics and clinical features of 172 patients with PDAC and 37 healthy subjects. 106*
Table 19. *Comparison of CgA and CgA-derived fragments plasma levels between healthy subjects and patients with PDAC. 107*
Table 20. *Comparison of CgA and CgA-derived fragments plasma levels in patients with PDAC according to PPI treatment.....108*
Table 21. *Univariate Cox regression analysis assessing the determinants of PFS and OS in patients with PDAC (n=172).....109*
Table 22. *Multivariate Cox regression analysis assessing the determinants of PFS and OS in patients with PDAC (n=172).....110*
Table 23. *Analyte specificity of CgA ELISAs based on different antibodies. 114*

Introduction

Neuroendocrine neoplasms

Neuroendocrine neoplasms (NENs) are heterogeneous tumors originating from secretory cells of the diffuse neuroendocrine system.

NENs have been traditionally considered as uncommon lesions, but their incidence has faced a 6.4-fold increase over the last four decades, growing from 1.09 per 100'000 in 1973 to 6.98 per 100'000 in 2012 (Dasari *et al*, 2017). This rise in incidence has occurred across all primary sites and stages of disease, but it has been significantly greater for patients with localized, low-grade tumors (Dasari *et al*, 2017). The reasons underlying this rapid incidence growth are still unclear. The widespread use of high-quality radiological and endoscopic techniques as well as the improved recognition of the neuroendocrine histology probably played a crucial role in this context (Chauhan *et al*, 2020). On the other hand, the survival of patients diagnosed with NENs has improved over time, probably due to the higher proportion of relatively indolent tumors and to the advances in NENs management (Das & Dasari, 2021; Cives & Strosberg, 2018).

The majority of NENs (55-70%) arise within the gastroenteropancreatic tract, with small bowel (~ 31%), rectum (~ 26%), colon (~ 18%) and pancreas (~ 12%) being the most frequent primary sites (Frilling *et al*, 2012). Consistently, gastroenteropancreatic NENs (GEP-NENs) show the second highest prevalence among gastrointestinal neoplasms, after colon cancer (Cives & Strosberg, 2018; Howlader N *et al*, 2019). The locations of primary tumors within the gastroenteropancreatic tract vary by race and gender. Male patients are more likely to have NENs originating from duodenum, pancreas, small bowel and rectum, whereas female patients more frequently present with tumors arising from stomach, appendix and cecum (Yao *et al*, 2008).

GEP-NENs display a variable biological behaviour, as they comprise both slow-growing, low-grade, incidentally discovered lesions as well as malignant tumors presenting at an advanced stage of disease, with nodal/distant metastases and/or invasion of nearby organs and vessels. GEP-NENs aggressiveness varies according to disease stage, tumor grade and primary tumor site. In particular, NENs arising in rectum and appendix display the best oncological outcomes, with overall survival (OS) rates greater than 20 years from diagnosis. On the contrary, pancreatic NENs display the worst prognosis and patients survive approximately 3 years from diagnosis (Dasari *et al*, 2017).

Pancreatic neuroendocrine neoplasms

Pancreatic neuroendocrine neoplasms (PanNENs) represent approximately 2-3% of all pancreatic lesions and originate from the cells of the islets of Langerhans. These tumors are globally regarded as less aggressive compared to pancreatic ductal adenocarcinoma (PDAC), although they can encompass a wide spectrum of aggressiveness.

Epidemiology

Data from the Surveillance, Epidemiology and End Results Program (SEER) have reported that the incidence of PanNENs has risen from 0.4 per 100'000 inhabitants in the early '00 to 0.8 per 100'000 inhabitants in 2012 (Dasari *et al*, 2017). As reported for GEP-NENs, the growth in incidence has been greater for asymptomatic early-stage lesions, especially for well-differentiated pancreatic neuroendocrine tumors (PanNETs) $\leq$ 2 cm (Kuo & Salem, 2013). Moreover, a decreased mortality and a reduced rate of metastatic disease have been described, probably due to the increased use of cross-sectional imaging modalities. Consistently, PanNENs take the second place as indication for pancreatic resection, after PDAC (Pulvirenti *et al*, 2020). However, the epidemiological data derived from population-based studies are still far from those described in autoptic and surgical series, where a prevalence of incidental PanNETs between 1.5% and 4% has been reported (Kimura *et al*, 1991; Kishi *et al*, 2012; Partelli *et al*, 2019).

Clinical features

Heterogeneity characterizes PanNENs, both from a clinical and biological standpoint. The majority of these neoplasms (80-90%) arise in a sporadic setting, between the sixth and the eighth decade. However, PanNENs can also be diagnosed in the context of a hereditary syndrome, such as multiple endocrine neoplasia type 1 (MEN-1), von Hippel Lindau syndrome (VHL), tuberous sclerosis (TSC) and neurofibromatosis type 1 (NF-1).

According to the presence or absence of a clinical syndrome related to hormonal overproduction, PanNENs are defined as functioning or non-functioning (NF-PanNENs). Functioning PanNENs (e.g. insulinoma, glucagonoma, VIPoma) become rapidly symptomatic due to uncontrolled hormonal secretion and patients are usually diagnosed early in the clinical course. Non-functioning tumors represent the vast majority of PanNENs (60-90%) and frequently remain asymptomatic for a long time (Lloyd RV *et*

al, 2017). Therefore, their diagnosis is often delayed until symptoms related to nearby structures invasion or distant metastases appear (Falconi *et al*, 2016).

Tumor grading

The latest World Health Organization (WHO) classification categorizes PanNENs in two groups, based on tumor cells morphology: 1) well differentiated PanNETs, and 2) poorly differentiated pancreatic neuroendocrine carcinomas (PanNECs) (Lloyd RV *et al*, 2017). Well-differentiated PanNETs are then graded as G1, G2 and G3, according to Ki67 proliferative index and mitotic count (**Table 1**).

Table 1. *WHO classification for PanNENs (Lloyd RV et al, 2017).*

Definition	Cell morphology	Ki67	Mitotic count
PanNET G1		< 3%	< 2
PanNET G2	Well differentiated	3 – 20%	2 – 20
PanNET G3		> 20%	> 20
PanNEC G3 Small-cell type Large-cell type	Poorly differentiated	> 20%	> 20
MiNEN	Well or poorly differentiated	Variable	Variable

Mitotic rates expressed as the number of mitoses/2 mm^2 in 50 fields of 0.2 mm^2; Ki-67 proliferative index determined by counting ≥ 500 cells in the regions of highest nuclear labelling; the final grade is based on the proliferation index that places the neoplasm in the higher-grade category. *MiNEN*, mixed neuroendocrine-non-neuroendocrine neoplasm.

Tumor staging

The European Neuroendocrine Tumor Society (ENETS) TNM classification and staging system for PanNENs are illustrated in **Table 2** (Rindi *et al*, 2006).

Table 2. *ENETS TNM staging system for PanNENs (Rindi et al, 2006).*

T – Primary tumor

TX	Primary tumor cannot be assessed.
T0	No evidence of primary tumor.
T1	Tumor limited to pancreas < 2 cm.
T2	Tumor limited to pancreas 2-4 cm.
T3	Tumor limited to pancreas > 4 cm or invading duodenum or bile duct.

T4	Tumor invading adjacent organs or the wall of large vessels (celiac axis or superior mesenteric artery).

N – Loco-regional lymph nodes

NX	Loco-regional lymph nodes cannot be assessed.
N0	No loco-regional lymph node metastasis.
N1	≥1 loco-regional lymph node metastasis.

M – Distant metastases

MX	Distant metastasis cannot be assessed.
M0	No distant metastases.
M1	Distant metastases.

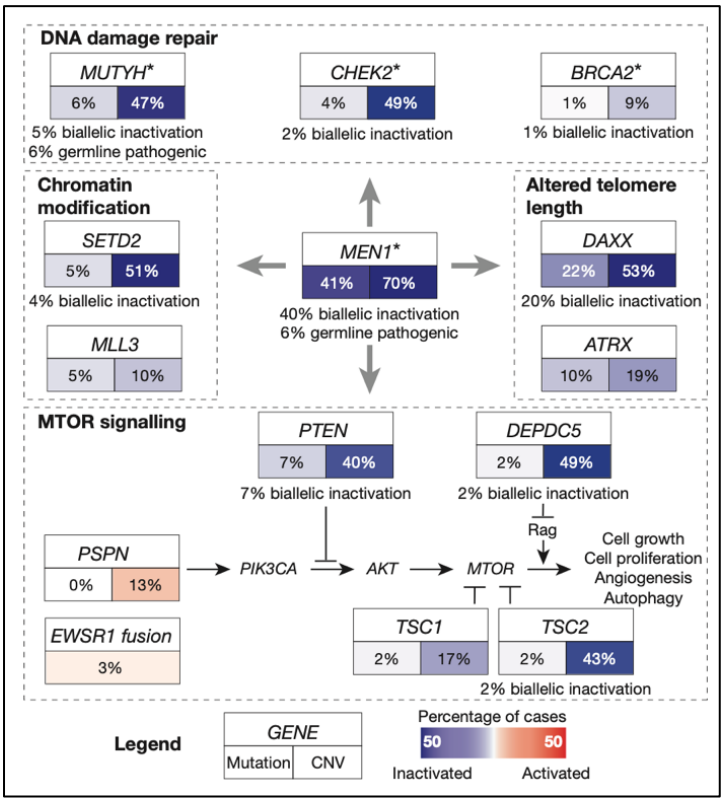
Genomic landscape

The genomic landscape of PanNENs has been comprehensively described, with PanNETs and PanNECs being characterized by different molecular alterations. According to a recent whole-genome sequencing study (Scarpa *et al*, 2017), four pathways are commonly altered in PanNETs (**Figure 1**):

1) DNA damage repair: mutation of *MUTYH*, *CHEK2* and *BRCA2* genes (Scarpa *et al*, 2017);
2) Chromatin remodelling: *MEN1* (mutated in 25-44% of resected PanNETs), *SETD2* and *MLL3* genes are recurrently inactivated and their mutations drive a widespread dysregulation of transcription (Pulvirenti *et al*, 2020);
3) Telomere maintenance: *DAXX* and *ATRX* genes are inactivated in ~30% of PanNETs and their mutation is associated with worse oncological outcomes (Marinoni *et al*, 2014). DAXX and ATRX proteins are involved in chromatin remodelling at telomeric/pericentromeric regions. *DAXX*/*ATRX* mutation is associated with increased telomere length and activation of the alternative lengthening of telomeres pathway, which is a pro-survival mechanism in solid neoplasms.
4) mTOR signaling activation: inactivating mutations in negative regulators of this pathway (*PTEN*, *TSC1* and *TSC2*) are found in approximately 12-15% of patients and represent a potential therapeutic target (Scarpa *et al*, 2017).

Genetic alterations in PanNECs are considerably different from those described in PanNETs. In particular, genes involved in the cell cycle, such as *TP53*, *RB1* and *CDKN2A* (also known as *P16*) are often target of somatic mutations in PanNECs, whereas *MEN1*, *DAXX* and *ATRX* are not (Lloyd RV *et al*, 2017).

Figure 1. *Genetic pathways altered in well differentiated PanNETs.*
The rate of somatic mutations and copy number variations is reported for the most important genes of genetic pathways commonly altered in PanNETs (Scarpa et al, 2017 - Open Access publication).

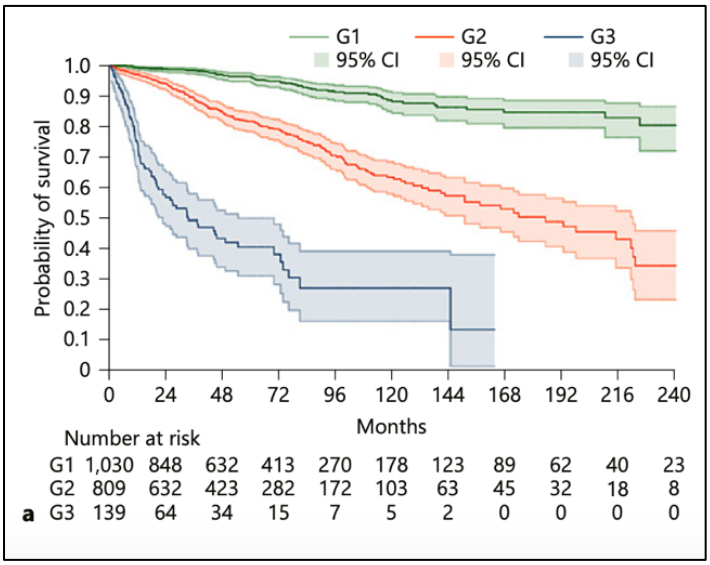


Prognosis

PanNENs are usually slow-growing tumors, with 5-year survival rates ranging between 65% and 86% in patients undergoing surgery for localized well-differentiated tumors (Lloyd RV *et al*, 2017). On the other hand, PanNECs are fast-growing neoplasms showing an aggressive biological behaviour. Patients with PanNECs rarely survive more than one year, mainly due to the small probability of early diagnosis and to the ineffectiveness of radical surgery. Consistently, in this subgroup, the risk of death after radical surgery is between 50- and 180-fold higher compared to that of the general population (Ricci *et al*, 2021).

Tumor grade and tumor stage are the most relevant factors for prognosis. A higher tumor grade is associated with an increased risk of relapse after surgery and with a shorter OS (Genç *et al*, 2018; Rindi *et al*, 2018; Pulvirenti *et al*, 2019a; Zaidi *et al*, 2019; Marchegiani *et al*, 2019). Specifically, G2 PanNETs display a risk of relapse up to 11 times higher compared to G1 PanNETs (Pulvirenti *et al*, 2020), whereas G3 PanNETs are characterized by a significantly worse prognosis compared to both G1 and G2 neoplasms (Rindi *et al*, 2018). Finally, patients with poorly differentiated PanNECs exhibit the worst survival outcomes, with a 5-year survival rate around 16%, compared to 29% in patients with PanNETs G3 (Basturk *et al*, 2015).

Figure 2. *OS stratified according to tumor grade.*
Kaplan-Meier curves showing the OS of patients with G1, G2 and G3 PanNENs who underwent surgical resection (Rindi et al, 2018 - Open Access publication).



Disease stage is another relevant prognostic factor, as both nodal (stage III) and distant metastases (IV) are powerful determinants of survival. Patients with stage I-II disease, especially in the presence of low-grade tumors, display a probability of normal lifespan close to that of the general population. However, this probability progressively decreases with increasing stage of disease, within each tumor grade category (Ricci *et al*, 2021). When distant metastases are present, it becomes unlikely to reach a complete cure. However, tumor progression occurs slowly in most of the cases. Consistently, patients with metastatic PanNETs display a median survival of ~2.3 years (Hamilton *et al*, 2012) and their 5-year survival rate is around 60% (Khan *et al*, 2013b).

Angiogenesis in PanNENs

PanNENs are highly vascularized tumors and angiogenesis is likely to carry out a crucial role in their development. The density of microvessels depends on PanNEN biological behaviour. Differently from other tumor types, a high microvessel density (MVD) is associated with more benign biological behaviour and improved oncological outcomes (Couvelard *et al*, 2005). On the contrary, a low MVD is a marker of disease aggressiveness and correlates with poorer survival outcomes (Marion-Audibert *et al*, 2003). This "reversed" relationship represents the first NET paradox. A possible explanation for this evidence is that the most differentiated tumors retain the capability to induce the formation of a vascular network similar to the one observed in the normal endocrine pancreas (i.e. islets of Langerhans). Consistently with these observations, PanNENs with low MVD more frequently express markers of hypoxia (Couvelard *et al*, 2005), such as carbohydrate antigen 9 (CA-9) and glucose transporter type 1 (GLUT-1). The presence of positive hypoxia markers is also associated with worse prognosis (Couvelard *et al*, 2005; Fujino *et al*, 2016; Kim *et al*, 2018).

The second NET paradox is represented by the fact that signs of angiogenic activity, including increased endothelial cells (ECs) proliferation and altered vessels architecture, are more frequently observed in high-grade compared to low-proliferating PanNENs (Takahashi *et al*, 2007). Therefore, the most aggressive tumors are the less vascularized, but the most angiogenic.

To complicate things further, highly vascularized tumors can sometimes express hypoxia markers. These tumors are defined as "pseudo-hypoxic" as the hypoxia pathway is constitutively activated due to germline *VHL* mutation (hereditary PanNENs), *VHL* deletion or promoter methylation (sporadic PanNENs). These tumors seem to be more aggressive compared with the highly vascularized PanNENs not expressing hypoxia markers (Couvelard *et al*, 2005; Schmitt *et al*, 2009).

The regulation of PanNENs vascular biology reaches a high level of complexity and many players, possibly exerting opposite functions, are likely to be involved. Further investigations are then needed to clarify the mechanisms underlying the peculiar vascular features of PanNENs and to possibly identify new therapeutic targets.

Treatment options and follow-up

The management of NENs is multimodal by definition and remains clinically challenging despite advances in available treatment options and innovations in terms of imaging modalities and diagnostic procedures. NENs treatment depends on several factors, including primary tumor site, disease stage and tumor grade.

Surgical resection represents the mainstay for the curative treatment of localized PanNENs, as it allows the complete removal of the primary tumor (Andreasi *et al*, 2020; Falconi *et al*, 2016; Partelli *et al*, 2017; Howe *et al*, 2020). Surgery can be considered also in well-selected patients with metastatic PanNETs, within the context of a multimodal treatment strategy. On the other hand, the surgical management is usually not recommended for patients with PanNECs and systemic treatment is generally preferred in this setting (Shah *et al*, 2021b; Howe *et al*, 2020; Garcia-Carbonero *et al*, 2016).

The therapeutic options available for patients with advanced/metastatic NENs have considerably increased. Currently, somatostatin analogues (SSAs), peptide receptor radionuclide therapy (PRRT), targeted therapies (i.e. sunitinib and everolimus) and chemotherapy are the most frequently used medical treatments. However, different combination strategies are commonly adopted over the years, with the purpose of delaying local or metastatic disease progression.

The risk of disease relapse after curative surgery ranges between 10% and 30% and it can persist for up to 10 years (Capretti *et al*, 2019; Landoni *et al*, 2019; Partelli *et al*, 2020b). Therefore, prognostic nomograms and predictive models have been developed in order to establish personalized follow-up schedules tailored on the risk features displayed by each patient. However, the optimal timings and modalities of follow-up still represent a debated issue and there is no consensus about which patients should be included in postoperative follow-up programs.

An accurate detection of recurrent or progressive disease is of paramount importance in order to offer a prompt and appropriate treatment. In this setting, PanNEN variable phenotype and heterogeneous biological behaviour stress the need for robust biomarkers to help the assessment of prognosis as well as the evaluation of treatment response. The tools currently available for these purposes include only high-quality imaging modalities, such as magnetic resonance imaging (MRI), computer tomography (CT) and ^{68}Gallium-DOTA positron emission tomography (PET) (Falconi *et al*, 2016; Howe *et al*, 2020). On

the other hand, circulating biomarkers are poorly accurate or still experimental and not available in the clinical practice (Marotta *et al*, 2012; Puliani *et al*, 2021).

Biomarkers in neuroendocrine tumor disease

A National Cancer Institute meeting on GEP-NENs, held in September 2007, identified the lack of reliable biomarkers as a major unmet clinical need in the setting of NENs. The use of biomarkers in the clinical practice has three main aspects: i) to determine the natural history of the neoplasm (type 0 biomarkers), ii) to define the efficacy of treatments (type I biomarkers), and iii) to act as surrogate disease endpoints to predict clinical benefit (type III biomarkers) (Frank & Hargreaves, 2003). Over the years, a number of biomarkers have been investigated for diagnostic, prognostic and follow-up purposes in patients with NENs. The clinical utility of neuroendocrine biomarkers lies in the need for an earlier tumor diagnosis and a better definition of tumor aggressiveness. Also, biomarkers might allow an early detection of recurrence or progression during follow-up. Finally, they can be useful for the definition of surgical radicality and for tumor burden quantification (Oberg *et al*, 2015).

Assessment of tumor response: imaging is not enough

For many solid non-neuroendocrine neoplasms, tumor response to treatment is assessed through radiological imaging techniques. However, NENs often display an indolent biological behaviour and the available treatment options tend to determine a disease stabilization more than an objective tumor response. Therefore, the imaging assessment alone, using the Response Evaluation Criteria in Solid Tumors (RECIST) (Schwartz *et al*, 2016), has relevant and well-documented limitations in this setting (Sundin & Rockall, 2012; Bodei *et al*, 2015). The available imaging modalities might be inadequate to predict aggressive tumor behaviour, to provide an early detection of disease relapse and to monitor the efficacy of treatments. Also, the long-life expectancy that often characterizes these patients should be taken into account, as prolonged exposure to radiations and costs associated with repetitive radiological examinations can be detrimental. Finally, the use of expensive and often toxic treatments imposes that tumor responsiveness is adequately monitored.

Functional imaging with ^{68}Gallium-DOTA PET might also play a role in this setting. Consistently, this technique has been demonstrated to better detect somatostatin receptor

(SSTRs) positive disease compared with other imaging modalities, with consequent utility in monitoring disease status (Srirajaskanthan *et al*, 2010). However, the limited spatial resolution (~ 6-8 mm) constrains the ability to identify small lesions. Also, changes in the standardized uptake value (SUV) have been described as unreliable measures for disease monitoring (Oberg *et al*, 2016). Finally, ^{68}Gallium-DOTA PET is not widely available and its usefulness is reduced in patients with SSTR-negative tumors.

^{18}F-fluorodeoxiglucose (FDG) PET may be useful for a prognostic purpose, but its role for the assessment of tumor responsiveness is limited to aggressive neoplasms presenting a relevant FDG uptake at the time of diagnosis (Rinzivillo *et al*, 2018). Therefore, available imaging modalities, both morphological and functional, are suboptimal for the detection of residual and occult disease. All these factors support the need for accurate circulating biomarkers that could provide a real-time feedback to the clinician.

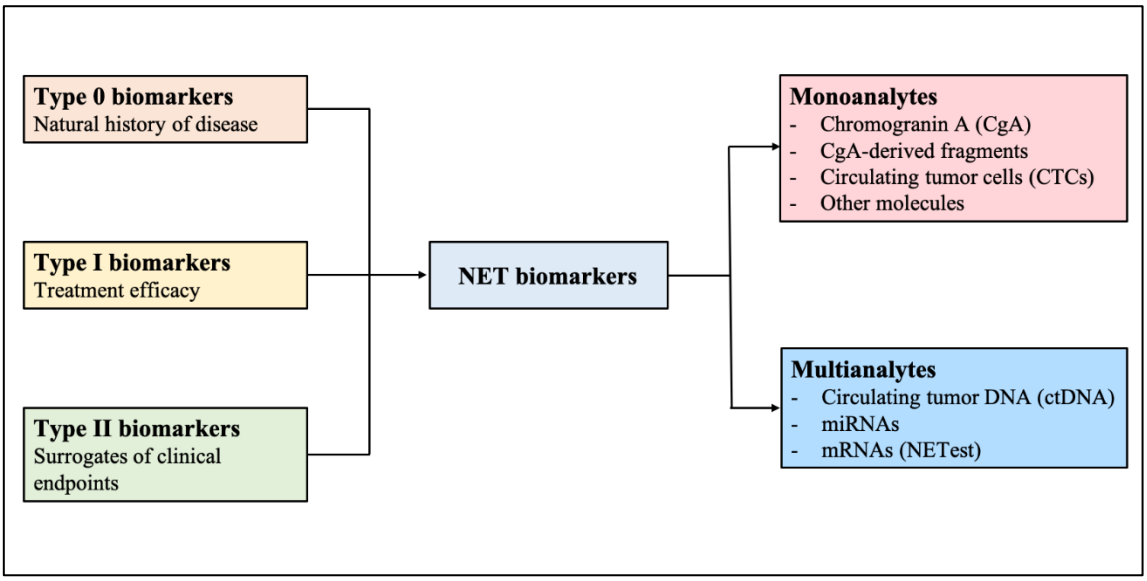
Monoanalyte versus multianalyte biomarkers: pros and cons

Biomarkers have been defined as "cellular, biochemical or molecular alterations that can be measured in biological media such as human tissues, cells or fluids" (Hulka, 1990). In the setting of NENs, the "products" secreted from neuroendocrine tumor cells have been largely investigated as biomarkers, although they have been demonstrated to be ineffective in providing information regarding tumor biology, especially when the neoplasm is non-functioning. Two main classes of biomarkers do exist: the first one is represented by monoanalyte biomarkers, which are commonly measured via immunoassays, whereas the second one comprises multianalyte biomarkers, such mRNA or circulating tumor DNA (Öberg, 2021).

Monoanalyte biomarkers are based on the identification of a single analyte, such as a circulating protein secreted by tumor cells (e.g. chromogranin A), whose level is considered representative of the disease. The main problem is related to the fact that available monoanalyte neuroendocrine biomarkers fail to capture the biological complexity of NENs and display severe limitations in providing both diagnostic and prognostic information (e.g. definition of tumor burden, disease progression and response to treatment) (Modlin *et al*, 2016a; Öberg, 2021). Moreover, the assays commonly used for their measurement are not standardized, thus limiting the proper evaluation of results and the reproducibility at a clinical level (Lim *et al*, 2019) (**Figure 3**).

Multianalyte biomarkers represent the new generation of tumor markers and display the highest sensitivity and specificity for diagnosis, prediction of response to treatment and prognostic evaluation (**Figure 3**). The assessment of multianalytes on tissue samples has several limitations. First, its availability is restricted to a single time point, with consequent failure in capturing tumor evolution with time and treatment. Second, a potential heterogeneity between primary tumor and metastases might be present (Shah *et al*, 2021a). Conversely, multianalyte biomarkers measured on blood samples (i.e. liquid biopsy) provide easily accessible, repeatable and real-time data regarding tumor status and response to treatment, allowing to capture temporal and spatial intratumor heterogeneity (Öberg, 2021). The main limitation related to the use of multianalyte biomarkers lies in the need for specific laboratory facilities. Moreover, complex analytic techniques are required in order to decipher the results. Consequently, the costs associated with their use are expected to be higher compared to monoanalyte biomarkers.

Figure 3. *Available circulating neuroendocrine biomarkers (modified from Oberg et al, 2015).*



Overview of monoanalyte NET biomarkers

NET biomarkers currently available in the clinical practice are mainly secretory proteins produced from neuroendocrine cells (i.e. monoanalytes).

Monoanalyte NET biomarkers are defined as "specific" when the analyte is the secretory product of a functioning PanNEN (i.e. insulin for insulinoma, glucagon for

glucagonoma, gastrin for gastrinoma). Specific biomarkers are effective for diagnosis and detection of recurrence, but functioning tumors represent only a minority of all NENs.

"General" monoanalyte NET biomarkers are commonly measured in patients with NF-PanNENs. In this context, *Chromogranin A* (CgA) represents the most used and best characterized NET biomarker, despite a number of relevant limitations in terms of assay standardization, specificity and sensitivity (Marotta *et al*, 2012) (see paragraph "Chromogranin A"). Over the years, several other molecules, such as CgA-derived fragments (e.g. pancreastatin, vasostatin-1), neuron specific enolase (NSE) and pancreatic polypeptide (PP), have been assessed as NET biomarkers (Sherman *et al*, 2014; Corsello *et al*, 2018; Baudin *et al*, 1998; Walter *et al*, 2012). NSE has poor sensitivity as its plasma levels are increased in less than 50% of patients, especially when neoplasms are poorly differentiated. Moreover, NSE specificity is even lower than that of CgA (Baudin *et al*, 1998; Nobels *et al*, 1997). For these reasons, NSE measurement is no longer performed for NENs management. Similarly, PP seems to have no clinical utility in patients with localized disease, and a very limited role in patients with metastatic tumors (Langstein *et al*, 1990).

General monoanalyte biomarkers comprise also *circulating tumor cells* (CTCs), which represent a form of liquid biopsy. CTCs are released in circulation from primary tumor or metastatic lesions. Several studies demonstrated the potential utility of CTCs in the setting of solid neoplasms, identifying them as an independent prognostic factor and highlighting their potential role in monitoring treatment response (Cristofanilli *et al*, 2004; Huang *et al*, 2015). The epithelial cell adhesion molecule (EpCAM) allows detection and quantification of CTCs in patients with NENs, through a semi-automated immuno-magnetic method, known as *CellSearch* (Khan *et al*, 2011). Although an association between CTCs, prognosis and response to treatment has been reported (Khan *et al*, 2013a, 2016a; Hsieh *et al*, 2019), CTCs can be detected in only 20-50% of patients with PanNENs (Khan *et al*, 2011; Öberg, 2021). Therefore, the low detection rate, the heterogeneity in EpCAM expression and the varying CTCs cut-off values limit the clinical usefulness of CTCs as a biomarker.

Overview of multianalyte NET biomarkers

Multianalyte biomarkers measurable in blood samples include circulating tumor DNA, micro RNAs and circulating mRNA transcripts (Öberg, 2021).

Circulating tumor DNA (ctDNA) is a fragment of circulating free DNA (cfDNA) released from tumor cells into circulation. ctDNA can be useful to determine driver mutations (i.e. genetic profiling of the tumor) and it could represent a tool to guide targeted treatments (Beltran *et al*, 2020; Zakka *et al*, 2020). However, the use of ctDNA as biomarker for patients with NENs is challenging, as these neoplasms display a very low mutational burden and a relative lack of driver mutations (Scarpa *et al*, 2017; Di Domenico *et al*, 2017). Of note, genetic alterations are more commonly found in NECs, due to the higher mutational burden. Moreover, the identification of mutations might vary depending on the technique used for sequencing or due to variable tumor composition. ctDNA requires further validation in the setting of NENs, in order to evaluate its utility in the clinical setting. Future studies should focus on patients with NECs, who are the best candidates for the identification of potential therapeutic targets through ctDNA (Shah *et al*, 2021a).

Micro RNAs (miRNA) are small (19-25 nucleotides) noncoding RNAs that act as post-transcriptional regulators by targeting specific mRNAs (Malczewska *et al*, 2018). miRNA expression can be significantly dysregulated in cancer cells with consequent loss of proliferation control and avoidance of apoptosis (Shah *et al*, 2021a). MicroRNA profiling seems to have a potential role as biomarker, as miRNA are stable in blood and can discriminate different cancer types (Li *et al*, 2013). Consistently, miRNA profiles of PanNENs and small bowel NENs (SB-NENs) are characterized by non-overlapping expression (Roldo *et al*, 2006; Thorns *et al*, 2014). In this context, the main limitation lies in the fact that both up-regulation and down-regulation of miRNA have been detected in PanNENs, thus suggesting that their clinical use could be challenging (Oberg *et al*, 2015). Also, the technology underlying their measurement is difficult and lacks standardization. In conclusion, current evidence is modest as no relevant blood signatures have been detected so far and miRNA clinical application in the setting of NENs remains limited.

Circulating mRNA has been increasingly investigated as neuroendocrine biomarker over the last few years. Abnormal RNA expression is commonly found in cancer and NET transcripts that can be detected in circulation have been recently identified. Based on these transcripts, panels to define tumor gene expression have been developed. In this setting, the NETest has been described as a multianalyte biomarker evaluating neuroendocrine mRNA transcripts detectable in blood and providing a multidimensional

assessment of disease status (Modlin *et al*, 2018). The performance of available biomarkers is summarized in **Table 3**.

Table 3. *Sensitivity and specificity of available NET biomarkers*

Biomarker	Sensitivity	Specificity
Chromogranin A	43-100%	10-96%
Pancreatic polypeptide	31-63%	≤ 67%
Neuron-specific enolase	33%	≤ 100%
Pancreastatin	64%	58-100%
Circulating tumor cells	≤ 50%	95%
NETest	90-98%	Up to 100%

Chromogranin A (CgA) and CgA-derived fragments

Chromogranin A is an acidic glycoprotein taking its name from bovine adrenal medulla chromaffin vesicles containing catecholamines, where this protein was detected for the first time (Banks & Helle, 1965). CgA is the index member of the "granins" family, secretory proteins stored within the electron-dense granules of neuroendocrine cells. Granins potentially play an important role in biogenesis, maturation and exocytosis of secretory vesicles containing biologically active peptides.

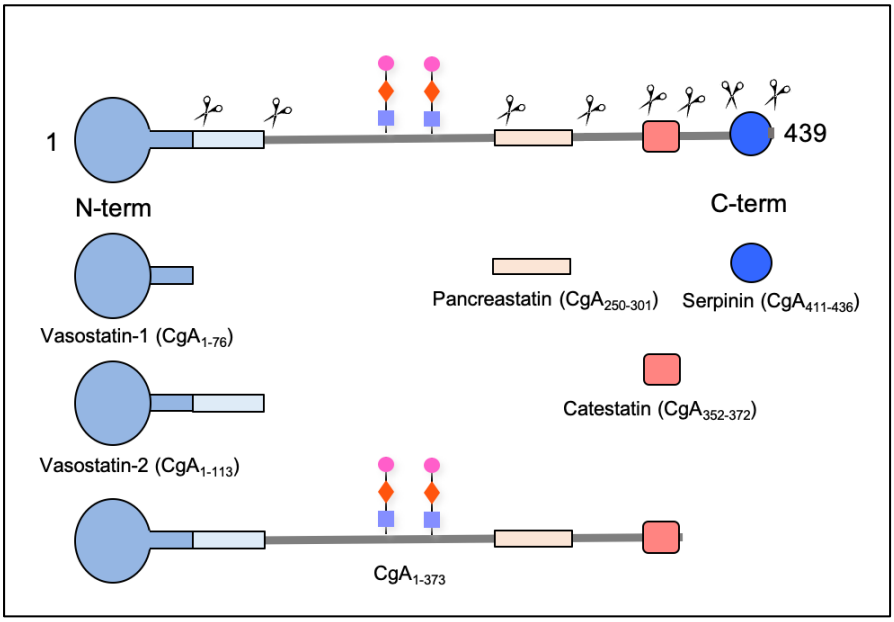
Structure and function

Human CgA is a 439-residue-long glycoprotein (molecular mass 48-52 kDa), encoded by the *HCGA* gene located on chromosome 14q (Taupenot *et al*, 2003). CgA has an intracellular function, as it is involved in the formation of secretory granules, as well as extracellular functions, being precursor of several biologically active peptides (**Figure 4**). CgA undergoes an extensive proteolytic cleavage performed by both intragranular and extragranular proteases, such as prohormone convertases, plasmin and thrombin (Lee *et al*, 2003; Mahata & Corti, 2019). Following this proteolytic processing, several biologically active peptides are generated. CgA-derived fragments are involved in many biological processes, including myocardial contractility and remodelling, regulation of vascular tension, cell adhesion and migration, inflammation, gastrointestinal motility, glucose/lipid/calcium metabolism and angiogenesis (Mahata & Corti, 2019; Corti *et al*, 2018).

The most intensively investigated CgA-derived fragments include (Mahata & Corti, 2019):

- vasostatin-1 (CgA_{1-76}): antiadrenergic, vasodilating and antiangiogenic peptide;
- vasostatin-2 (CgA_{1-113}): this fragment, which comprises the vasostatin-1 and the vasoconstrictive-inhibitory factor (CgA_{79-113}) sequences, has an anti-remodeling, antifibrotic and anti-inflammatory activity;
- pancreastatin ($CgA_{250-301}$): dysglicemic peptide found elevated in diabetic patients, associated with enhanced inflammation and decreased insulin sensitivity;
- catestatin ($CgA_{352-372}$): antiadrenergic, antihypertensive, proangiogenic, anti-inflammatory peptide;
- serpinin ($CgA_{411-436}$): proadrenergic peptide.

***Figure 4**. Schematic representation of full-length CgA and CgA-derived fragments.*



Role of CgA and CgA-derived fragments in the process of angiogenesis

Several studies have shown that CgA-derived fragments may have a role in the regulation of tumor vascular biology, forming a balance of antiangiogenic and proangiogenic factors.

In normal conditions, full-length CgA and vasostatin-1 (VS-1) contribute to maintain the quiescence of the vascular endothelium. Both these peptides are characterized by a powerful antiangiogenic activity, which has been shown in several *in vitro* and *in vivo*

assays (Mahata & Corti, 2019). Consistently, an active antiangiogenic site can be found at the C-terminal region, whereas a latent antiangiogenic site, which requires proteolytic cleavage for activation, lies within the N-terminal region (Crippa *et al*, 2013). At physiological concentrations, CgA_{1-439} and VS-1 modulate the function of the endothelial barrier, preserving its integrity and inhibiting the vascular leakage induced by tumor necrosis factor alpha (TNFα) (Ferrero *et al*, 2004). These fragments also prevent the capillary-like structures formation induced by vascular endothelial growth factor (VEGF) and inhibit the proangiogenic activity of fibroblast growth factor 2 (FGF-2) (Crippa *et al*, 2013). Specifically, VS-1 can inhibit the translocation to the nucleus of the hypoxia inducible factor (HIF)-1α (Belloni *et al*, 2007). Although both VS-1 and CgA exert an antiangiogenic activity, it might be speculated that they play different roles in the spatio-temporal regulation of angiogenesis.

In the presence of damaged tissues, the balance between proangiogenic and antiangiogenic fragments changes completely, and the vascular endothelium is no longer quiescent. In this context, blood coagulation causes an almost complete loss of full-length CgA, with formation of a proangiogenic fragment called CgA_{1-373} (Crippa *et al*, 2013). CgA_{1-373} is able to induce the release of FGF-2 from ECs, thus exerting a proangiogenic effect. CgA cleavage may act as "on/off" switch for tumor angiogenesis, as it has been demonstrated that CgA_{1-439} can inhibit capillary sprouting from endothelial cells spheroids, whereas CgA_{1-373} can stimulate angiogenesis at the same concentrations. Also, a correlation between enhanced CgA C-terminal processing (R_{373}-R_{374}) and MVD has been reported in patients diagnosed with multiple myeloma (Bianco *et al*, 2016b). In particular, CgA cleavage in position R_{373} leads to the exposure of PGPQLR site ($CgA_{368-373}$), which binds the VEGF-binding site of VEGF coreceptor neuropilin-1 (NRP-1) (Dallatomasina *et al*, 2019). Antibodies against this site can inhibit angiogenesis and reduce tumor growth in several *in vivo* models. The proangiogenic activity of CgA_{1-373} depends on NRP-1 binding, for which R_{373} residue is crucial. Therefore, the transition from CgA_{1-373} to CgA_{1-372} may represent an important mechanism to limit the proangiogenic activity in neoplastic or damaged tissues (Dallatomasina *et al*, 2019).

The dose-response curves of CgA and CgA-derived fragments have been shown to be bell-shaped in several angiogenesis assays: as a result, an huge increase in their levels might lead to a lower or even opposite biological effect for reasons that are still unknown

(Crippa *et al*, 2013; Dallatomasina *et al*, 2019; Curnis *et al*, 2016).

The formation of new vascular structures and the alteration of the endothelial barrier are necessary to deliver oxygen and nutrients to cancer cells. Therefore, it is likely that CgA-derived fragments contribute to regulate tumor growth, by regulating tumor vascular biology. In this context, the unbalanced production of proangiogenic and antiangiogenic fragments might lead to altered vasculature morphology, dysregulated angiogenesis, and finally tumor progression. Given these premises and considered the peculiar features of NET vasculature (see paragraph "Angiogenesis in PanNENs"), it might be interesting to study a possible relationship between CgA-derived fragments and vascular biology in PanNENs.

CgA and CgA-derived fragments in normal subjects

CgA is exocytotically released and reaches sub-nanomolar concentrations (0.5-1 nM) in normal subjects (Corti *et al*, 2018). Immunoassays able to distinguish between CgA_{1-439} and CgA-derived fragments have shown that circulating CgA consists of a minor proportion of full-length CgA (0.1 nM) and a larger proportion of peptides lacking part of or the entire C-terminal region (Crippa *et al*, 2013). VS-1 is also present at considerable concentrations (~ 0.3 nM) in the plasma of normal subjects. Therefore, since circulating levels of both full-length CgA and VS-1 are biologically relevant, it is likely that these peptides play a role in the inhibition of angiogenesis in normal conditions. Finally, the presence of other fragments (e.g. catestatin) has also been reported in normal subjects, but the use of different antibodies/assays is responsible for significant discrepancies in terms of concentrations reported by different studies.

CgA as neuroendocrine biomarker: more flaws than strengths?

CgA is the most frequently used biomarker for diagnosis, prognostic stratification and follow-up of patients with PanNENs.

Several studies have shown that CgA plasma levels may correlate with tumor grade, disease stage and burden of liver metastases (Hijioka *et al*, 2014; Massironi *et al*, 2014; Han *et al*, 2015). In particular, higher CgA has been documented in patients with extensive liver disease compared to those with localized tumors or limited liver involvement (Gut *et al*, 2020). A few series suggested that CgA may also have a role as prognostic biomarker as well as in monitoring the response to treatment (Yao *et al*, 2011; Rossi *et al*, 2015; Shanahan *et al*, 2016; Pulvirenti *et al*, 2019b). In this regard, a series

including 38 patients who underwent to surgery for PanNETs reported that both disease-free survival (DFS) and OS were negatively influenced by an increased preoperative CgA plasma level (Shanahan *et al*, 2016). However, all these studies have a retrospective design and include a small number of patients, thus not allowing a survival analysis adjusted for possible confounders.

Despite CgA is the most frequently used neuroendocrine biomarker, relevant concerns about its clinical utility have been raised and several limitations have been highlighted.

First, *CgA sensitivity* as neuroendocrine biomarker is highly variable (60-100%), mainly depending on tumor function and stage of disease (Oberg *et al*, 2016). CgA sensitivity can be considered acceptable for functioning and/or metastatic NENs, but it is extremely low for non-functioning localized tumors (Marotta *et al*, 2012). Consistently, Nehar et al. reported that CgA elevation was present in almost 75% of patients with metastatic NENs compared to less than one third of those with localized disease (Nehar *et al*, 2004). Also, a recent experience showed that increased CgA was found in less than 25% of patients with loco-regional disease, whereas CgA elevation independently predicted the presence of metastatic disease (Pulvirenti *et al*, 2019b). Moreover, the majority of patients with low-grade PanNETs had normal CgA levels, thus corroborating the concern regarding the role of CgA as biomarker for diagnosis and follow-up of indolent NF-PanNETs managed by active surveillance (Pulvirenti *et al*, 2019b). Regarding patients' follow-up after curative surgery, CgA seems to have poor utility, as localized PanNENs display an increased preoperative CgA only in a minority of cases. Therefore, postoperative CgA levels usually do not provide clinically relevant information (Modlin *et al*, 2016b).

CgA sensitivity seems to be sub-optimal also in the setting of advanced disease, since a concordance as low as 40% has been reported between morphological changes at imaging and CgA modifications (Pavel *et al*, 2017). Moreover, a prospective multicenter experience including 239 patients with enteropancreatic NETs recently showed a poor association between changes in CgA levels and modifications in tumor burden, thus suggesting that CgA alone is not adequate to predict disease progression and treatment response (Dam *et al*, 2020).

Second, *CgA specificity* is extremely poor, due to the presence of several conditions that can determine a significant increase of its plasma levels, even in the absence of NENs.

In these patients, CgA reaches levels up to 100-500-fold higher than normal. Oncological diseases, benign conditions and drugs that can be responsible for CgA elevation in patients without NENs are listed in **Table 4**.

Table 4. *Conditions associated with increase of CgA plasma levels (Marotta et al, 2012).*

Gastrointestinal diseases	Chronic atrophic gastritis, chronic hepatitis, liver cirrhosis, inflammatory bowel diseases, pancreatitis, Helicobacter pylori infection
Cardiovascular diseases	Chronic heart failure, hypertension (especially if untreated), acute coronary syndrome, atherosclerosis
Organ dysfunction	Impaired kidney and/or liver function
Other diseases	Rheumatoid arthritis, systemic lupus erythematosus, pulmonary obstructive disease, hyperthyroidism, sepsis
Non-neuroendocrine neoplasms	Colorectal carcinoma, gastric carcinoma, breast carcinoma, ovarian carcinoma, hepatocellular carcinoma and pancreatic carcinoma, non-small cell lung cancer
Drugs	Proton pump inhibitors, histamin 2 receptor antagonists, serotonin reuptake inhibitors

Assumption of proton pump inhibitors (PPI) and chronic atrophic gastritis represent the most common causes of falsely increased CgA plasma levels. In these conditions, the chronic hypo/achlorhydria leads to hypergastrinemia (owing to lack of negative feedback), which stimulates CgA secretion from enterochromaffin cells (Waldum *et al*, 1996). PPI can increase CgA levels up to 5-10 times higher than the upper limit of normal, starting from 5 days after the first intake and persisting for up to two weeks after treatment interruption (Pregun *et al*, 2011; Mosli *et al*, 2012). Also, non-neuroendocrine neoplasms can be associated with increased CgA. A recent study investigating CgA specificity in identifying PanNETs reported comparable CgA plasma levels between patients with PanNETs and those with pancreatic ductal adenocarcinoma (Jun *et al*, 2017).

Third, *standardization of assays* used for CgA measurement is challenging as CgA is a heterogeneous analyte owing to an extensive proteolytic cleavage. Therefore, the use of assays that are specific for different epitopes and recognize different combinations of CgA-derived fragments leads to discrepant results in terms of total-CgA plasma levels. For these reasons, it is important to measure also the levels of CgA_{1-439} and specific CgA-derived fragments (e.g. VS-1, pancreastatin) (Corti *et al*, 2018).

Pancreastatin as neuroendocrine biomarker

Pancreastatin (PST) is 52-residue-long peptide ($CgA_{250-301}$) derived from CgA cleavage. This fragment is involved in the inhibition of glucose-stimulated insulin secretion, insulin-stimulated glucose transport and glycogen synthesis (Mahata & Corti, 2019; Watanabe, 2021). PST also modulates the lipid metabolism by exerting a lipolytic action and has a proinflammatory effect. Globally, PST shows an anti-insulin diabetogenic effect (Mahata & Corti, 2019).

The role of PST as neuroendocrine biomarker has been mainly studied in the setting of SB-NENs. Several series have shown that increased plasma PST is associated with poorer survival outcomes as well as with the presence of liver metastases (Stronge *et al*, 2008; Sherman *et al*, 2014; Khan *et al*, 2016b). PST sensitivity has been reported to be around 85% for the detection of liver metastases in patients with SB-NETs (Khan *et al*, 2016b). A recent study including 300 patients with small intestinal NETs reported that elevated PST plasma levels after surgical cytoreduction were associated with poor prognosis (Woltering *et al*, 2019). Consistently, Strosberg et al. showed that PST measurement can be a useful prognostic indicator for patients submitted to transarterial chemoembolization (TACE) for neuroendocrine liver metastases. In this setting, high pre-treatment levels are associated with worse OS, whereas a significant post-procedural drop correlates with improved survival outcomes. Also, a PST increase after an initial drop can predict a progressive liver disease requiring further treatment (Strosberg *et al*, 2018). PST might be useful also in the setting of postoperative follow-up, as postoperative PST was shown to correlate with disease burden and to provide better discrimination of oncological outcomes compared with CgA, in patients with SB-NENs (Tran *et al*, 2021).

The role of PST as biomarker in the specific setting of PanNENs has been scarcely investigated. Only Sherman et al. reported that elevated preoperative PST was a predictor of poorer oncological outcomes in patients submitted to surgery for localized and metastatic PanNENs (Sherman *et al*, 2014).

PST seems to be less influenced by coexisting conditions and medication use (e.g. PPI) compared with CgA, suggesting that this fragment might be a more accurate neuroendocrine biomarker. Also, a more standardized assay, specific for CgA sequence 286-301, is available for PST measurement (O'Dorisio *et al*, 2010). This assay can detect slight changes in liver burden, and it has been reported to be up to 100-fold more sensitive

and specific than CgA assays (O'Dorisio *et al*, 2010). However, also PST has its flaws: PST circulating levels might be affected by food intake, medications interfering with glucose metabolism and diabetes, due to PST role in this context (Valicherla *et al*, 2013). Moreover, patients with primary hyperparathyroidism might have falsely increased PST plasma levels (Bergenfelz *et al*, 2000). Finally, different PST conformations might render assay interpretation controversial, in addition to the fact that some commercial assays might be less accurate due to the use of antibodies cross-reacting with full-length CgA (O'Dorisio *et al*, 2010).

Vasostatin-1 as neuroendocrine biomarker

In the attempt to face the lack of a reliable biomarker for PanNENs, also other CgA-derived fragments, among which VS-1, have been investigated.

In this regard, our group conducted a study assessing the circulating levels of total-CgA (i.e. full-length CgA plus fragments lacking the C-terminal region but not CgA_{1-76}), CgA_{1-439} (full-length CgA), CgA_{1-373} and CgA_{1-76} (VS-1) in 17 patients with SB-NENs (n = 10) or PanNENs (n = 7), in 10 healthy subjects and 21 normal volunteers before and after treatment with PPI (Corsello *et al*, 2018).

Patients with NENs showed significantly higher levels of both total-CgA and VS-1, but not of full-length CgA and CgA_{1-373}, compared to healthy controls. Moreover, VS-1 elevation in patients with NENs was markedly higher compared to that of total-CgA (9.6-fold *versus* 2.4-fold). Also, VS-1 showed a better capability to distinguish between patients and healthy subjects compared to total-CgA, with the best VS-1 cut-off being able to correctly classify 96% of patients in terms of disease status, compared to 81% of patients for total-CgA (Corsello *et al*, 2018).

VS-1/total-CgA and CgA_{1-373}/total-CgA ratios were also investigated in order to evaluate whether elevated VS-1 plasma levels depended on enhanced CgA N-terminal cleavage or increased CgA secretion. Patients with NENs showed an increased VS-1/total-CgA ratio and a decreased CgA_{1-373}/total-CgA ratio, thus suggesting that CgA proteolytic cleavage is altered in NENs and that VS-1 generation is favored in this setting (Corsello *et al*, 2018).

Regarding VS-1 specificity, an interesting finding was that VS-1 plasma levels were not affected by PPI use, differently from total-CgA levels (Corsello *et al*, 2018). At the time being, Takayasu arteritis and carotid artery stenosis have been identified as

comorbidities associated with VS-1 increase in the absence of a neuroendocrine disease (Bachetti *et al*, 2017; Tombetti *et al*, 2016). Critically ill patients also can display increased VS-1 (Chung *et al*, 2012), with plasma levels approximately 1.4-fold higher than those of healthy subjects (Schneider *et al*, 2012). However, this increase is lower than that displayed by patients with NENs.

Finally, VS-1 measurement might be easily comparable between different laboratories, due to the fact that this fragment does not undergo a further proteolytic processing, differently from CgA.

VS-1 seems a promising neuroendocrine biomarker, easier to standardize and more accurate compared with total-CgA. However, further studies including larger and more selected cohorts are needed to corroborate these preliminary findings and to investigate the role of VS-1 in the specific setting of PanNENs.

NETest: a promising multianalyte biomarker

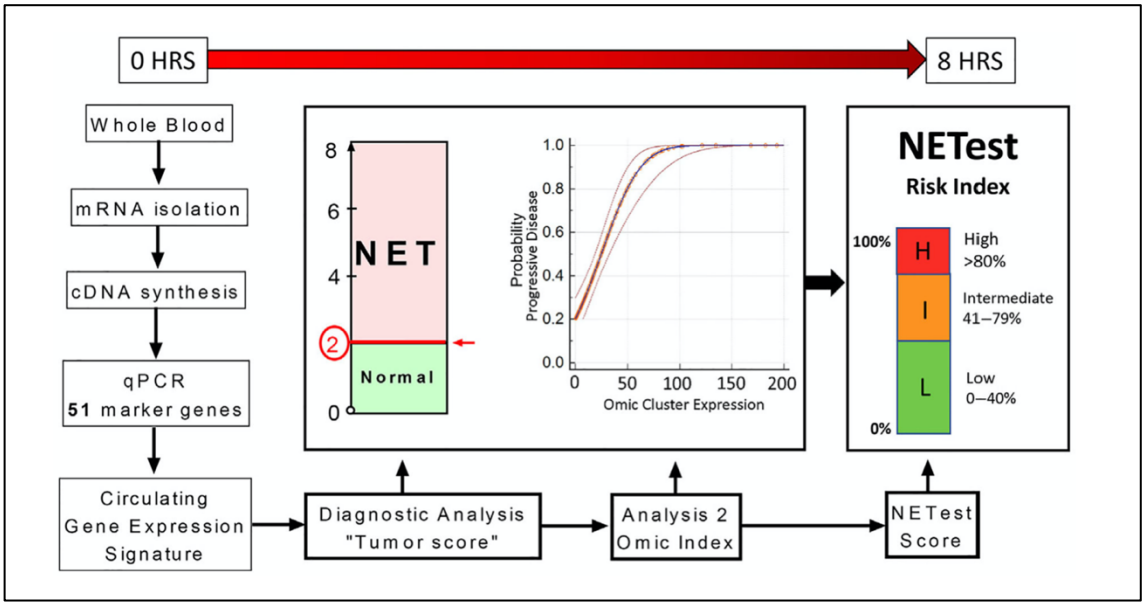
NETest is the first successful multigene molecular biomarker (i.e. liquid biopsy) that can be used for the management of patients with NENs.

NETest is a multianalyte biomarker which measures 51 NET-related gene transcripts that have been identified through transcriptional profiling of tumor tissue. These transcripts are detected in blood and then algorithmically analyzed to build a "biological signature" correlating with tumor tissue expression. The assay comprises mRNA isolation, cDNA production and quantitative polymerase chain reaction (qPCR), which is standardized and reproducible (Öberg, 2021; Puliani *et al*, 2021). After PCR, results are algorithmically analyzed to discriminate healthy controls from patients with NENs, producing a "tumor score" ranging between 0 and 8: samples scored as 0-2 are categorized as normal, whereas those with scores between 3 and 8 are classified as NENs (Modlin *et al*, 2016b). A study analyzing the gene expression profiles of more than 10000 tumors belonging to 32 different types of neoplasia reported that NETest signature was able to accurately identify the NET genotype (Chen *et al*, 2018).

After this step, a second algorithmic analysis is performed to quantify the expression of gene clusters related to proliferation (proliferome), peptide secretion (secretome), metabolism (metabolome), SSTRs expression (SSTRome) and epigenomic changes (epigenome). This second algorithm, incorporated with the first 0-8 tumor score, produces

a clinical activity score ranging between 0% and 100% (NETest score), which is able to distinguish stable from progressive disease (Modlin *et al*, 2018) and provide a multidimensional assessment of disease status and treatment response (Pavel *et al*, 2017; Modlin *et al*, 2018) (**Figure 5**). Based on the findings of validation studies, NETest values ≤ 20% are considered as "normal", values between 21% and 40% indicate low biological activity, values between 41% and 79% indicate intermediate biological activity, whereas values between 80% and 100% correspond to high biological activity (Modlin *et al*, 2018; van Treijen *et al*, 2018; Puliani *et al*, 2021).

Figure 5. *Multistep protocol followed to obtain the NETest score (Modlin et al, 2018 - Open Access publication).*



NETest: clinical utility

Several experiences from independent datasets demonstrated the role of NETest as diagnostic and prognostic marker for patients with gastroenteropancreatic and bronchopulmonary NENs. NETest performance exceeds that of CgA and meets the National Institutes of Health (NIH) criteria to define a biomarker as "effective".

The NETest exhibits high sensitivity (~ 90%) and specificity (~ 97%) and there seem to be no alterations related to food intake, medications, gender, ethnicity or age. NETest shows a high diagnostic accuracy (~ 96%), being robust in discriminating patients with NENs from healthy subjects and being concordant with imaging findings in the majority of cases (Modlin *et al*, 2015; Oberg *et al*, 2020; Puliani *et al*, 2021).

NETest has also been identified as a reliable tool to define disease status, with an accuracy around ~ 85% in distinguishing stable from progressive disease (Malczewska *et al*, 2019b; Oberg *et al*, 2020). Also in this setting, a high (85-95%) concordance between NETest score and morphological/functional imaging findings has been reported (Malczewska *et al*, 2019c; Liu *et al*, 2019). Therefore, NETest might be a guide for treatment choices and, in case of low scores, it may help in reducing the need for radiological examinations.

Apart from its usefulness in diagnosis and disease status assessment, NETest has also a prognostic role and can be employed to improve the quality of follow-up (Öberg, 2021). In this regard, several surgical series showed that patients with disease relapse had higher NETest scores compared to those submitted to R0 resections without recurrence (Modlin *et al*, 2016b; Filosso *et al*, 2018; Genc *et al*, 2018). In particular, a NETest score > 40% was found to be significantly correlated with disease relapse (Genc *et al*, 2018). Also, combining clinico-pathological criteria with NETest seems to be more effective than using clinico-pathological criteria alone to define the presence of disease recurrence.

The NETest can also be useful monitor treatment effectiveness in patients with advanced disease. In this regard, several studies have shown that treatment efficacy can be demonstrated in the presence of NETest score decrease. Consistently, disease progression during treatment with SSAs was associated in more than 90% of cases with NETest score elevation, whereas stable or responding disease correlated with no changes or reduction in NETest score (Cwikla *et al*, 2015). Similarly, NETest is an accurate surrogate marker to evaluate response to PRRT, showing high concordance with image-based response assessment (Bodei *et al*, 2020).

Based on these findings, one might argue that the time for monoanalytes is over and that the future is in the hands of multianalyte molecular biomarkers. Nevertheless, biomarkers accessibility and cost-effectiveness are crucial, especially in patients with NENs, given their usually long life-expectancy. In this regard, the main problem related to the use of NETest in the everyday clinical practice is represented by the need for a dedicated laboratory and a specialized analysis, in order to obtain and interpret the results.

Pancreatic ductal adenocarcinoma

Pancreatic ductal adenocarcinoma (PDAC) in an epithelial tumor arising from cells of pancreatic ducts. PDAC is the most frequent pancreatic neoplasm, accounting for >90%

of all pancreatic malignant neoplasms (Kleeff *et al*, 2016). It currently represents the fourth most frequent cause of cancer-related death, with 5-year OS rates lower than 8% (Siegel *et al*, 2021). The incidence of PDAC is progressively growing worldwide, mainly due to ageing of population, obesity and type 2 diabetes, which are clearly implicated in the pathogenesis of this cancer (Calle *et al*, 2003).

Despite the increasing incidence, PDAC prognosis remains poor and little progress has been made in terms of available treatment options. Surgical resection associated with neoadjuvant/adjuvant chemotherapy represents the only potentially curative treatment and it can be proposed only to patients presenting with localized and resectable tumors (10-20%) (Neoptolemos *et al*, 2004; Birrer *et al*, 2021). However, even after surgery, the 5-year survival rate is lower than 15% and a consistent proportion of patients die within the first year due to early recurrence.

The vast majority of patients diagnosed with PDAC has a locally advanced or metastatic disease than cannot be managed by surgery, at the time of diagnosis. In this setting, systemic chemotherapy is the gold-standard treatment, although it achieves only marginal improvements in survival outcomes. The best treatment option for metastatic patients with good performance status is currently represented by a regimen based on folinic acid, 5-fluorouracil, irinotecan and oxaliplatin (FOLFIRINOX), which has been associated with a survival advantage in metastatic patients compared to gemcitabine alone (Conroy *et al*, 2011).

In this setting, studies investigating the mechanisms underlying PDAC growth as well as those assessing new prognostic markers and therapeutic targets might be highly relevant from both an experimental and clinical standpoint.

Premises for investigating CgA and CgA-derived fragments in PDAC

The role of CgA and CgA-derived peptides in the process of angiogenesis has been previously demonstrated by our group (see paragraph “Role of CgA and CgA-derived fragments in the regulation of angiogenesis”). In the setting of cancer, an altered production of antiangiogenic and proangiogenic factors can be responsible for altered vascular morphology, uncontrolled angiogenesis and tumor growth. In particular, disease progression seems to be associated with increased CgA fragmentation in several murine models of solid tumors (Dallatomasina *et al*, 2019). For example, the fragmented CgA/full-length CgA ratio progressively increased during tumor progression in mice

implanted with fibrosarcoma cells, thus suggesting a tumor-dependent CgA cleavage (Dallatomasina *et al*, 2019). On the other hand, CgA_{1-439} and its N-terminal fragment (VS-1) have been shown to control tumor cell trafficking and decrease tissue infiltration in mouse models of chronic lymphocytic leukemia (Bianco *et al*, 2016a). Also, the full-length CgA, but not of CgA-derived peptides lacking the C-terminal region, was able to reduce tumor progression in several murine models (Curnis *et al*, 2016). Therefore, uncleaved CgA (CgA_{1-439}) seems to inhibit tumor progression, whereas C-terminal CgA cleavage promotes angiogenesis and tumor development.

Data regarding the role of CgA in the specific setting of PDAC are extremely poor. CgA elevation can be found in different types of non-neuroendocrine neoplasms, such as colorectal, breast and pancreatic cancer (Wu *et al*, 2000; Syversen *et al*, 2004). Moreover, it has been suggested that increased CgA levels in patients with PDAC might be associated with an advanced stage of disease (Malaguarnera *et al*, 2009). A recent retrospective experience analyzed CgA plasma levels in 350 patients with PDAC, reporting that high CgA values might predict worse prognosis in these patients, especially in the presence of metastatic disease (Lee *et al*, 2019). Regarding the possible role of neuroendocrine cells in this context, a study assessing the molecular profile of PDAC found that the neuroendocrine gene signature was enriched in PDAC squamous subtype, which is the most aggressive one (Bailey *et al*, 2016). However, it is unclear whether CgA plasma levels might reflect the degree of neuroendocrine differentiation in PDAC. Also, proteases released by tumor cells might undertake cleavage of normally circulating CgA, thus leading to an increase of CgA-derived fragments.

However, current findings regarding the role of CgA in the context of PDAC are pretty vague as CgA comprises both the full-length protein and the isoforms derived from its proteolytic processing, which have been demonstrated to have specific biological activities. Therefore, given the ominous prognosis of this neoplasm, the need to find new therapeutic targets and the role of CgA-derived fragments in tumor biology, we decided to investigate CgA proteolytic cleavage in patients with PDAC and to assess its prognostic value in this setting.

Aims

Biomarkers in PanNENs

1. To evaluate VS-1, compared with total-CgA, as biomarker for patients submitted to surgery for localized NF-PanNETs, by assessing the association with pathological features of aggressiveness and with survival outcomes.

2. To evaluate the ability of VS-1, compared with total-CgA, to assess the effectiveness of surgical resection in patients with NF-PanNETs.

3. To investigate PST and vasostatin-2 (VS-2) as potential biomarkers for NF-PanNETs.

4. To investigate NETest as biomarker for patients undergoing surgery for PanNETs by assessing its effectiveness in defining the extent and efficacy of surgical resection and in predicting disease recurrence.

Biological role of CgA and CgA-derived fragments in PanNENs

5. To investigate the biological role of CgA and CgA-derived fragments in PanNENs, by assessing the site of production and cleavage using *in vitro* models and evaluating the relationship between their tissue expression, MVD and other immunohistochemical markers.

CgA and CgA-derived fragments as PDAC biomarkers

6. To investigate CgA and CgA-derived fragments as biomarkers in patients with PDAC, by correlating their plasma levels with survival outcomes.

Aim 1 - To evaluate VS-1, compared with total-CgA, as biomarker for patients submitted to surgery for localized NF-PanNETs, by assessing the association with pathological features of aggressiveness and with survival outcomes.

[Part of following data have been published in Andreasi V, Partelli S, et al. Association between preoperative Vasostatin-1 and pathological features of aggressiveness in localized nonfunctioning pancreatic neuroendocrine tumors (NF-PanNET). Pancreatology 2019].

Results

Study population

Overall, 50 patients who underwent surgical resection for sporadic non-metastatic well-differentiated NF-PanNETs were included. Demographic features, clinical characteristics and pathological findings are summarized in **Table 5** and **Table 6**.

Table 5. *Demographic and preoperative features of 50 patients diagnosed with NF-PanNETs.*

Variable	***n 50 (%)***
Gender	
Female	24 (48)
Male	26 (52)
Age, years*	58 (49-64)
Abdominal pain	
No	37 (74)
Yes	13 (26)
BMI, kg/m^2*	24.5 (22-28)
PPI assumption	
No	39 (78)
Yes	11 (22)
Total-CgA, nM*	0.66 (0.49-1.61)
VS-1, nM*	0.34 (0.31-0.45)

*Expressed as median with interquartile range (IQR)
BMI, body mass index; *CgA*, chromogranin A; *PPI*, proton pump inhibitors; *VS-1*, vasostatin-1.

Table 6. *Pathological features of patients who underwent surgery for NF-PanNETs.*

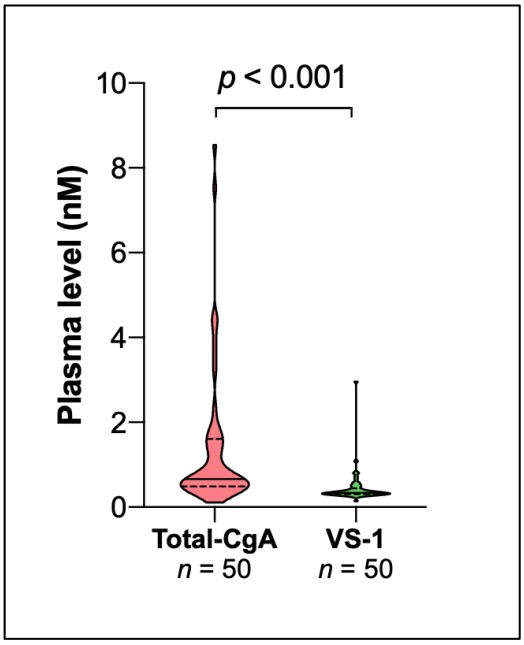
Variable	***n 50 (%)***
Histological diameter, mm*	25 (18-37)
Ki67 proliferative index, %*	3 (1-6.5)
Grade†	
PanNET G1	20 (40)
PanNET G2	28 (56)
PanNET G3	2 (4)
T stage°	
T1	16 (32)
T2	23 (46)
T3	11 (22)
N stage°	
N0	31 (62)
N+	19 (38)
Disease stage°	
I	14 (28)
II	17 (34)
III	19 (38)
Status of resection margins	
R0	45 (90)
R1	4 (8)
R2	1 (2)
Perineural invasion	
Absent	39 (78)
Present	11 (22)
Microvascular invasion	
Absent	28 (56)
Present	22 (44)
Necrosis	
Absent	46 (92)
Present	4 (8)

*Expressed as median with interquartile range (IQR)
†According to 2017 WHO classification (Lloyd, RV et al, 2017)
°According to ENETS TNM staging system (Rindi *et al*, 2006)
PanNET, pancreatic neuroendocrine tumors.

The majority of patients was diagnosed with G1 (n = 20, 40%) or G2 (n = 28, 56%) PanNETs, whereas only 4% (n = 2) of the study population had a high-grade well-differentiated PanNET G3. All the patients but one underwent a surgical resection with curative intent (n = 45 R0, n = 4 R1). In all the cases, at least one lymph node was resected and examined, with 40% (n = 19) of study cohort showing nodal involvement.

Total-CgA and VS-1 were measured preoperatively in all the patients. Total-CgA plasma levels were significantly higher as compared with VS-1 plasma levels [median 0.66 nM (IQR 0.49-1.61 nM) *versus* median 0.34 nM (IQR 0.31-0.45 nM), $p < 0.001$)], as depicted in **Figure 6**.

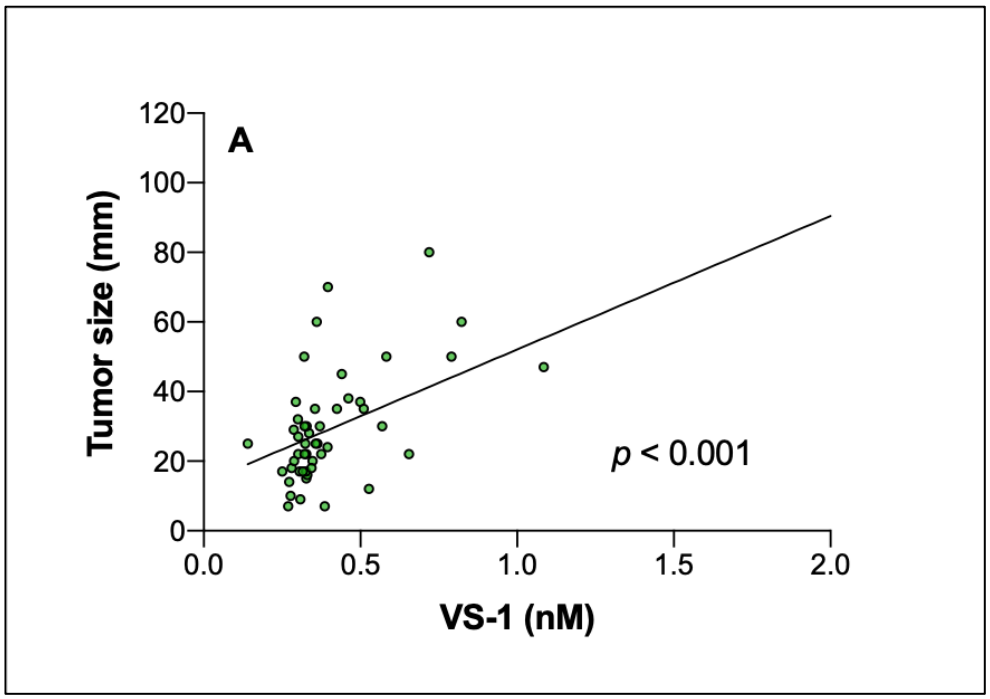
Figure 6. *Matched comparison between preoperative plasma levels of total-CgA and VS-1. Violin plots with median (solid line), 1st quartile (bottom dashed line) and 3rd quartile (top dashed line).*

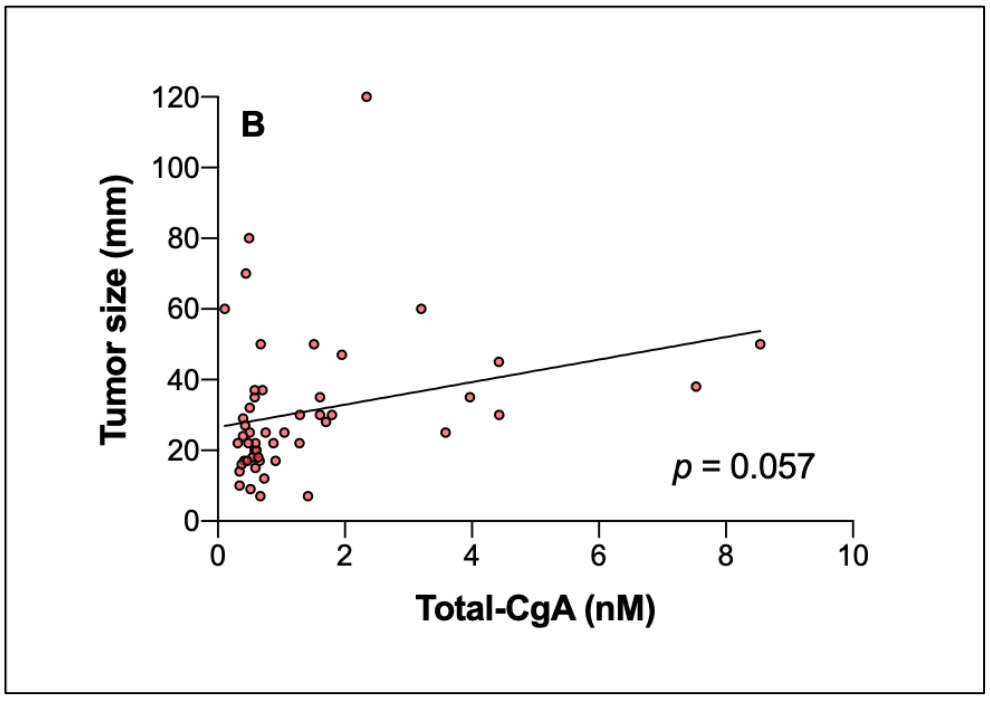


Correlation of VS-1 and total-CgA with pathological features of aggressiveness

The relationship between preoperatively retrievable factors and tumor size was assessed by linear regression analysis. VS-1 plasma levels were the only preoperatively retrievable factor that significantly correlated with tumor size [B = 38.336, 95% Confidence Interval (CI): 28.492-48.179, $p < 0.001$] (**Figure 7A**). No significant correlation between total-CgA plasma levels and tumor diameter was found (B = 3.188, 95% CI: – 0.096-6.471, p = 0.057) (**Figure 7B**).

Figure 7. *Linear regression analysis showing the correlation between VS-1 (A) or total-CgA (B) and tumor size.*





Receiver operating characteristic (ROC) curves were performed in order to assess the accuracy of VS-1 and total-CgA as predictors of tumor diameter, using different cut-offs (**Table 7**).

Table 7. *ROC curve analysis assessing VS-1 and total-CgA plasma levels as predictors of tumor size.*

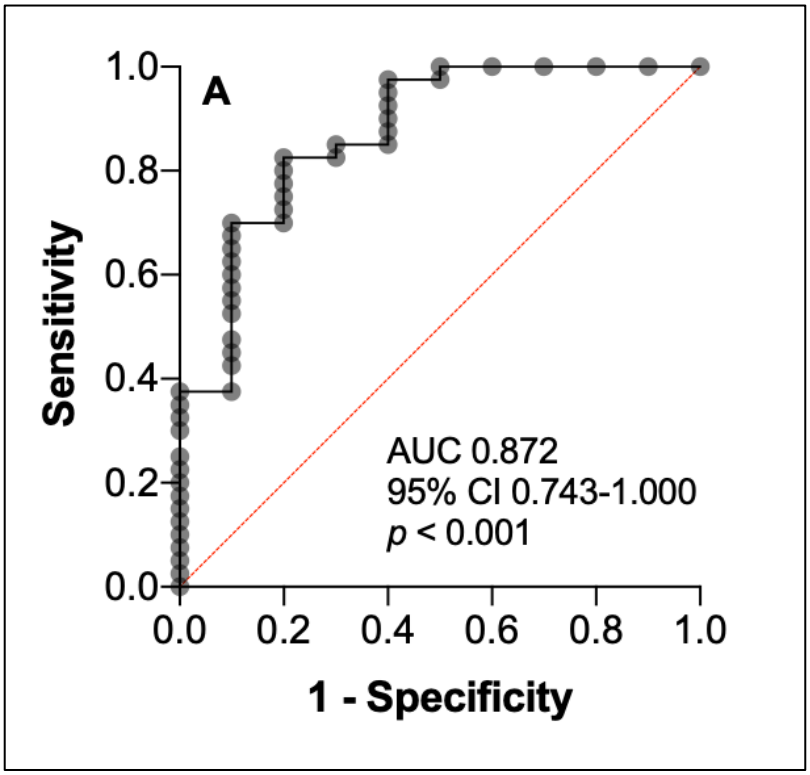
VS-1					
Tumor size cut-off	**AUC**	***p***	**VS-1 level (nM)**	**Sensitivity (%)**	**Specificity (%)**
> 2 cm	0.764	0.003	0.32	82	56
> 4 cm	0.872	<0.001	0.39	80	80
Total-CgA					
Tumor size cut-off	**AUC**	***p***	**CgA level (nM)**	**Sensitivity (%)**	**Specificity (%)**
> 2 cm	0.670	0.025	0.59	65	56
> 4 cm	0.648	0.152	-	-	-

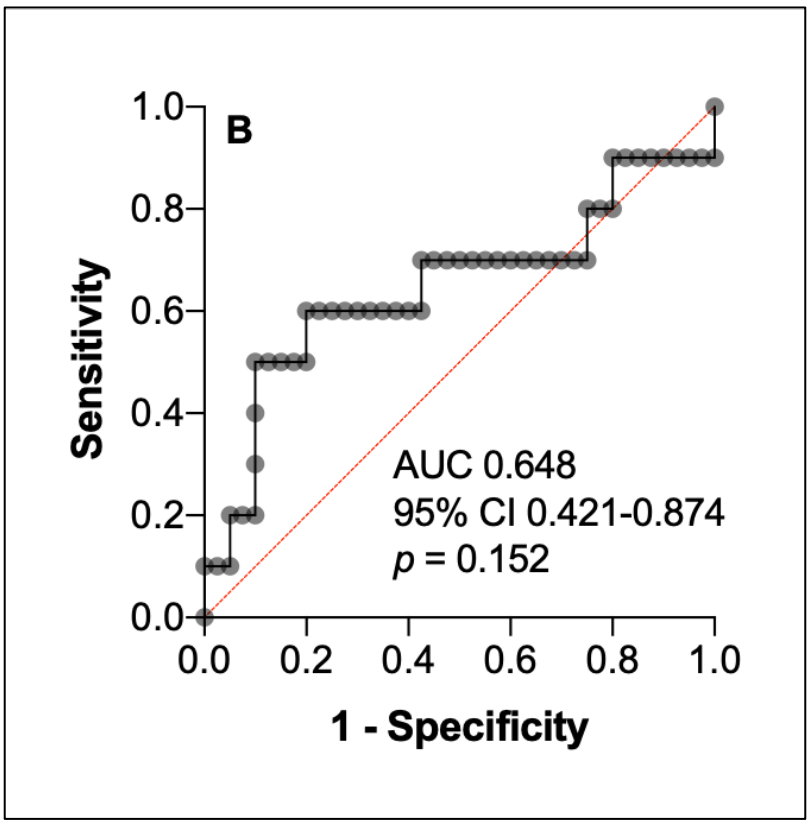
CgA, chromogranin A; *VS-1*, vasostatin-1

The global performance of VS-1, expressed as area under the curve (AUC), was 0.872 (95% CI 0.743-1.000, $p < 0.001$) using a 4 cm cut-off (**Figure 8A**) compared with 0.764 (95% CI 0.627-0.901, $p = 0.003$) when a 2 cm cut-off was used. The best VS-1 cut-off to identify patients with NF-PanNETs > 4 cm was 0.39 nM (sensitivity 80%, specificity 80%).

The correlation between total-CgA plasma levels and tumor size was statistically significant only when a 2 cm cut-off was used (AUC 0.699, 95% CI 0.556-0.841, $p = 0.025$), whereas it did not reach the statistical significance when a 4 cm cut-off was considered (AUC 0.648, 95% CI 0.421-0.874, $p = 0.152$) (**Figure 8B**).

Figure 8. *Receiver operating characteristics curve of VS-1 (A) and total-CgA (B) as determinants of tumor size (using a 4 cm cut-off).*





The study population was then categorized using the VS-1 cut-off previously identified (0.39 nM). Patients with VS-1 plasma ≤ 0.39 nM (low VS-1) and VS-1 > 0.39 nM (high VS-1) were then compared, as shown in **Table 8**.

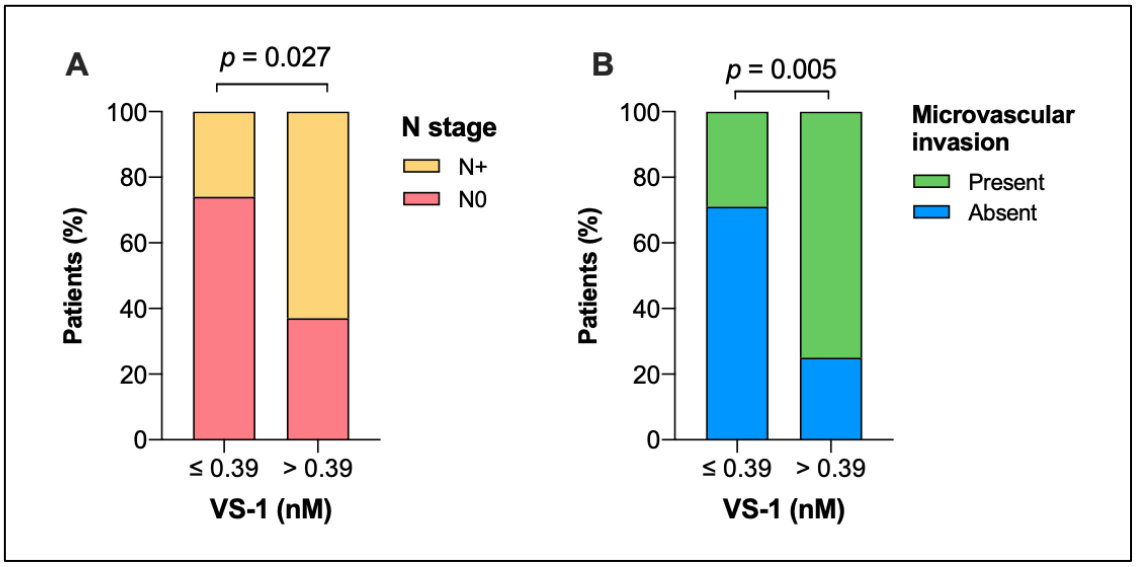
Table 8. *Comparison of clinico-pathological characteristics between patients with low VS-1 plasma levels (≤ 0.39 nM) (n = 34) and those with high preoperative VS-1 (> 0.39 nM) (n = 16).*

Variable	**VS-1 ≤ 0.39 nM** ***n = 34*** **(%)**	**VS-1 > 0.39 nM** ***n = 16*** **(%)**	***p***
Gender			0.227
Female	14 (41)	10 (63)	
Male	20 (59)	6 (37)	
Age			1.000
≤ 60 years	15 (44)	7 (44)	
> 60 years	19 (56)	9 (56)	
Abdominal pain			0.731
No	26 (76)	11 (69)	
Yes	8 (24)	5 (31)	
BMI			0.225
≤ 25 kg/m^2	18 (53)	5 (31)	
> 25 kg/m^2	16 (47)	11 (69)	
PPI assumption			0.297
No	28 (82)	11 (69)	
Yes	6 (18)	5 (31)	
Tumor Grade*			0.074
PanNET G1	17 (50)	5 (19)	
PanNET G2	16 (47)	12 (75)	
PanNET G3	1 (3)	1 (6)	
N category†			**0.027**
N0	25 (74)	6 (37)	
N+	9 (26)	10 (63)	
Microvascular invasion			**0.005**
Absent	24 (71)	4 (25)	
Present	10 (29)	12 (75)	
Perineural invasion			0.728
Absent	27 (79)	12 (75)	
Present	7 (21)	4 (25)	
Necrosis			0.584
Absent	32 (94)	14 (88)	
Present	2 (6)	2 (12)	

BMI, body mass index; *PPI*, proton pump inhibitors
*According to 2017 WHO classification (Lloyd, RV et al, 2017)
†According to ENETS TNM staging system (Rindi *et al*, 2006)

The two groups were comparable for age, gender, PPI assumption, tumor grade, presence of perineural invasion and tumor necrosis. Patients with high VS-1 had a significantly increased rate of nodal involvement (p = 0.027) (**Figure 9A**) and microvascular invasion (p = 0.005) (**Figure 9B**) compared to those with low VS-1 plasma levels.

Figure 9. *Comparison of the rate of nodal metastases and microvascular invasion between patients with low preoperative VS-1 and those with high preoperative VS-1.*



ROC curves were performed to evaluate the accuracy of VS-1, compared with total-CgA, in predicting the presence of pathological features of aggressiveness (i.e. nodal metastases and microvascular invasion).

The global performances of VS-1, expressed as AUCs, were 0.712 (95% CI 0.564-0.861, p = 0.012) for predicting nodal metastases (**Figure 10A**) and 0.763 (95% CI 0.651-0.902, p = 0.002) (**Figure 11A**) for identifying the presence of microvascular invasion.

The global performances of total-CgA, expressed as AUCs, were 0.545 (95% CI 0.358-0.732, p = 0.596) (**Figure 10B**) and 0.594 (95% CI 0.423-0.765, p = 0.257) (**Figure 11B**) for predicting the presence of nodal involvement and microvascular invasion, respectively.

Figure 10. *ROC curves of VS-1 (A) and total-CgA (B) as predictors of nodal involvement.*

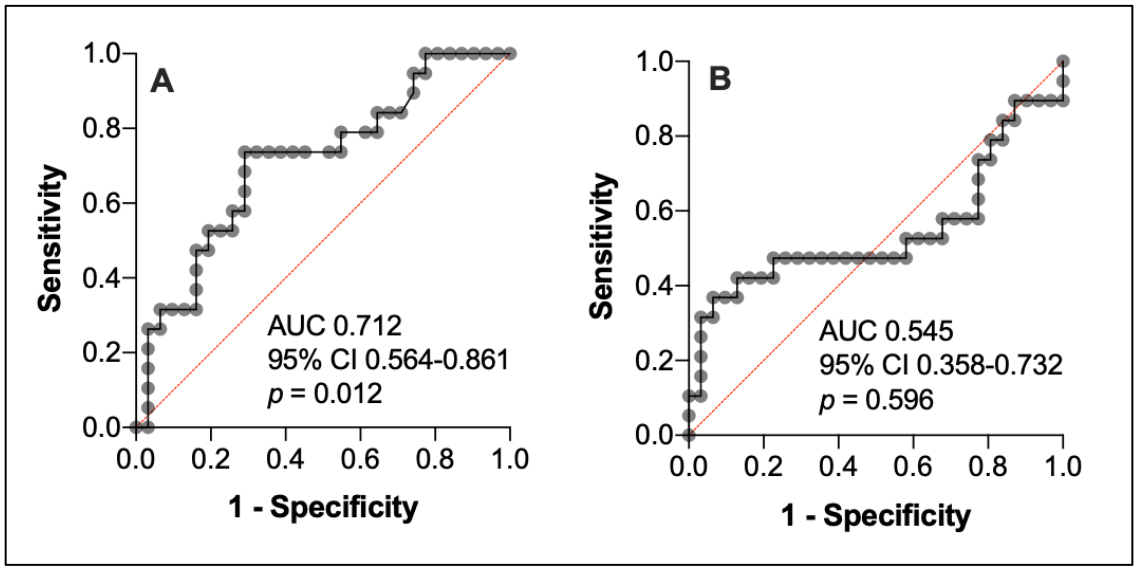
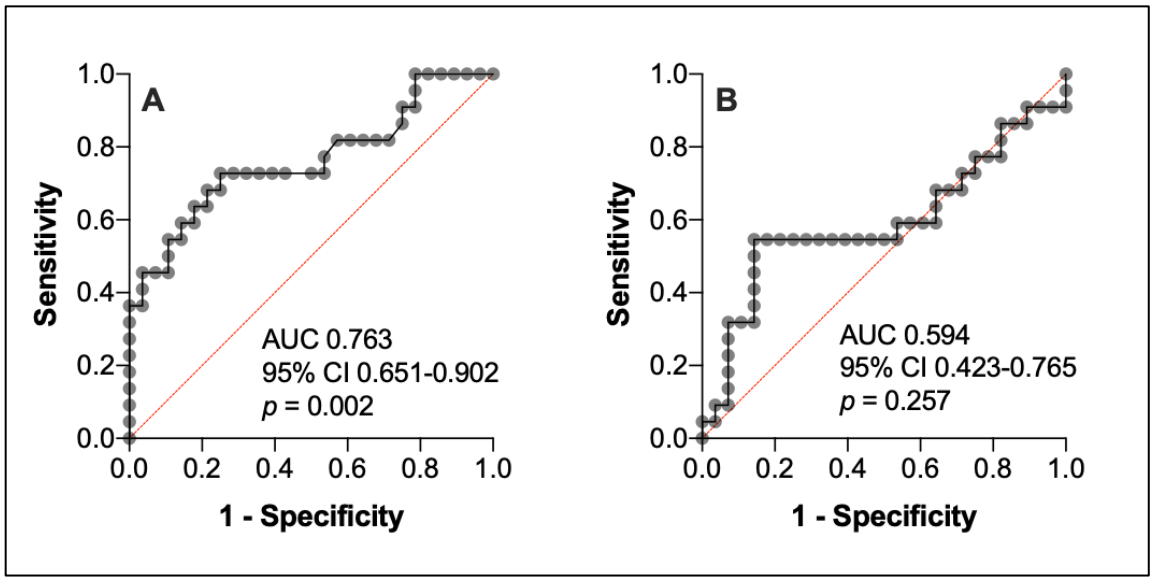


Figure 11. *ROC curves of VS-1 (A) and total-CgA (B) as predictors of microvascular invasion.*



Median VS-1 values were significantly increased in patients with nodal metastases [0.395 nM (IQR 0.324 - 0.655) *versus* 0.327 nM (IQR 0.294 - 0.375), $p = 0.012$] and microvascular invasion [0.411 nM (IQR 0.324 - 0.671) *versus* 0.326 nM (IQR 0.296 - 0.355), $p = 0.001$] (**Figure 12 and 13**). No statistically significant differences were observed in terms of total-CgA plasma levels.

***Figure 12**. Plasma levels of VS-1 (A) and total-CgA (B) in patients with and without nodal involvement.*

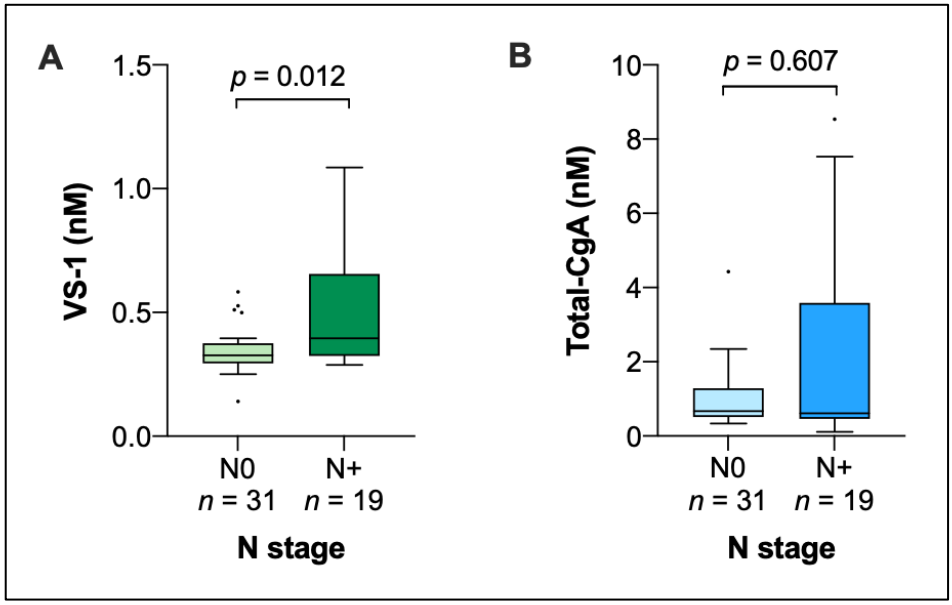
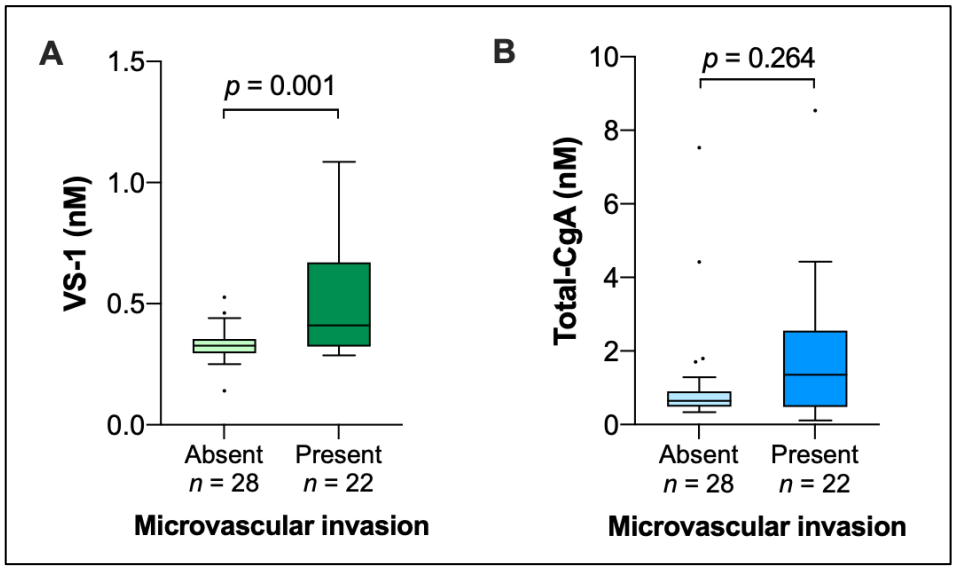
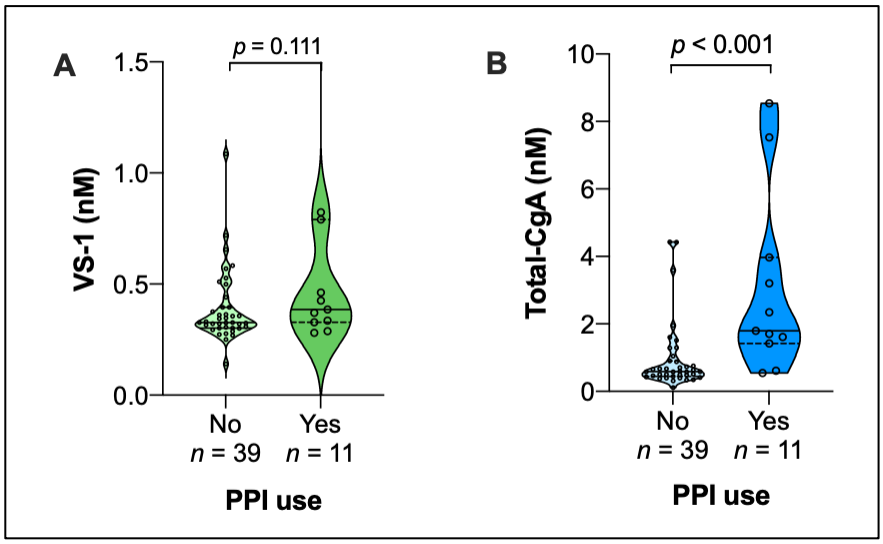


***Figure 13**. Plasma levels of VS-1 (A) and total-CgA (B) according to the presence or absence of microvascular invasion.*



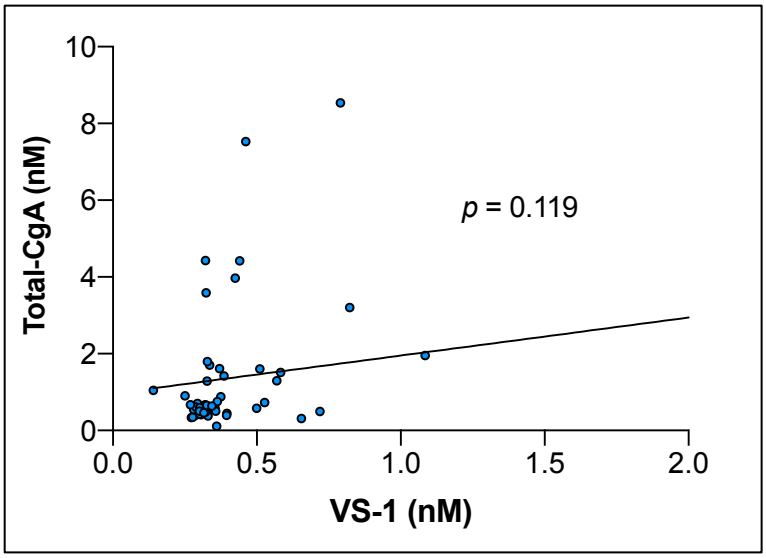
Patients treated with PPI showed significantly higher total-CgA plasma levels as compared to the remaining study cohort [1.799 nM (IQR 1.417 - 3.968) *versus* 0.591 nM (0.443 - 0.908); $p < 0.001$]. On the other hand, VS-1 values were comparable between these two groups [0.386 nM (IQR 0.328 - 0.791) *versus* 0.327 nM (0.302 - 0.396), $p = 0.111$] (**Figure 14**).

Figure 14. *Comparison of VS-1 and total-CgA plasma levels according to PPI use. Violin plots with median (solid line), 1st quartile (bottom dashed line) and 3rd quartile (top dashed line).*



No significant correlation was observed between preoperative plasma levels of VS-1 and total-CgA ($R^2 = 0.052$, $p = 0.119$), as depicted in **Figure 15.**

Figure 15. *Bivariate correlation between preoperative plasma levels of VS-1 and total-CgA.*

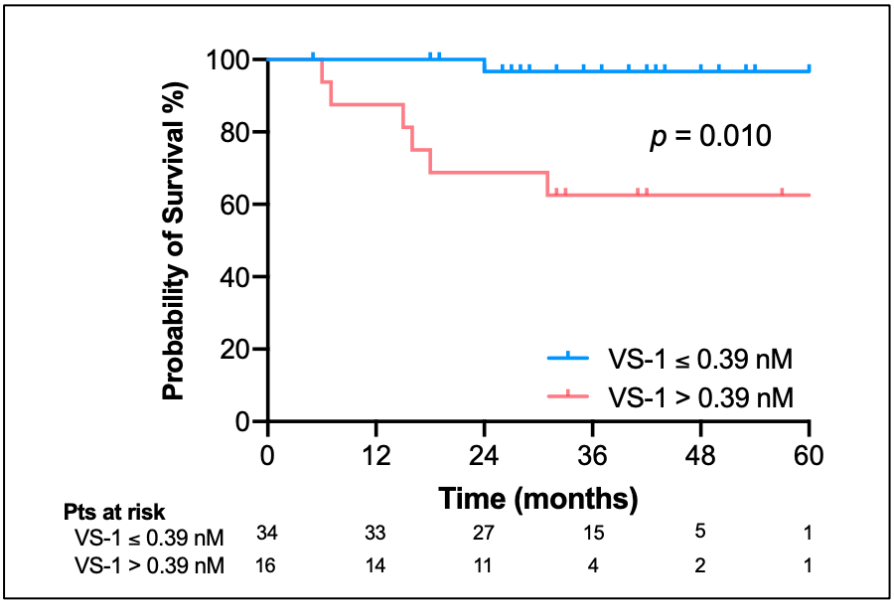


Survival analysis

After a median follow up of 35 months (IQR 29-44 months), 8 patients (16%) experienced disease recurrence and one patient died due to postoperative complications. There were no disease-related deaths. The 2-year DFS rate for the whole study cohort was 88%.

Patients with VS-1 plasma levels > 0.39 nM (n = 34) had a 2-year DFS rate of 97% compared with 69% in patients with VS-1 plasma levels ≤ 0.39 nM (n = 16) (p = 0.010) (**Figure 16**).

Figure 16. *Comparison of disease-free survival between patients with low preoperative VS-1 plasma levels (n = 34) and patients with high VS-1 plasma levels (n = 16).*



Discussion

The present experience showed that preoperative VS-1 plasma levels are significantly correlated with tumor size, nodal metastases and microvascular invasion in patients who underwent surgery for localized NF-PanNETs. On the other hand, no significant correlation between preoperative total-CgA plasma levels, tumor size and features of tumor aggressiveness was observed in this study.

Neuroendocrine biomarkers have been scarcely studied in a well-selected cohort of patients diagnosed with non-metastatic, well-differentiated, resectable NF-PanNETs. Regarding CgA, Jilesen et al. (Jilesen *et al*, 2014) selected patients with localized, G1-

G2 NF-PanNETs and observed that an increase in preoperative CgA plasma levels could be observed in only one third of them. On the other hand, several series assessed the clinical usefulness of CgA in study populations that were quite heterogeneous in terms of disease stage and tumor function (Nolting *et al*, 2012; Walter *et al*, 2012; Paik *et al*, 2013; Modlin *et al*, 2015). Nolting and coworkers (Nolting *et al*, 2012) demonstrated that CgA plasma levels were significantly increased in patients with liver metastatic disease as compared to those with localized neoplasms. Also, another recent experience reported that elevated CgA could be detected in less than 25% of patients with loco-regional disease, whereas CgA increase independently predicted the presence of distant metastases. Moreover, the majority of patients with low-grade PanNETs had normal CgA levels, thus corroborating the concern regarding the role of CgA as biomarker for localized neoplasms (Pulvirenti *et al*, 2019b). Similar results were confirmed by two other series (Paik *et al*, 2013; Hijioka *et al*, 2014). Overall, surgical experiences suggest that CgA accuracy is decreased when PanNETs are localized, with sensitivity ranging between 25% and 50% (Jilesen *et al*, 2014; Shanahan *et al*, 2016; Jun *et al*, 2017).

The evidence of distant metastatic disease does not represent the only feature associated with an increased CgA value. In this regard, tumor function and a small bowel origin are two factors strictly related with elevated CgA plasma levels. Previous experiences showed that SB-NETs, in particular if functioning, are associated with increased CgA plasma levels as compared to PanNETs (Modlin *et al*, 2010; Nolting *et al*, 2012). Also, Nehar et al. (Nehar *et al*, 2004) reported that CgA levels were significantly higher in patients with secreting tumors as compared to those with non-functioning neoplasms. Therefore, in the presence of non-metastatic NF-PanNETs, preoperative CgA is considered poorly accurate and its routine measurement should not be recommended (Nolting *et al*, 2012; Walter *et al*, 2012; Paik *et al*, 2013; Modlin *et al*, 2015; Jilesen *et al*, 2014; Pulvirenti *et al*, 2019b).

Nodal involvement and tumor size are relevant factors for prognosis in patients with PanNENs. It has been previously reported that the risk of recurrence after surgical resection in patients diagnosed with PanNETs with nodal involvement is significantly increased compared patients without nodal metastases (Partelli *et al*, 2013, 2018; Guarneri *et al*, 2021). These findings were consistent with those from a previous study published by Hashim et al. (Hashim *et al*, 2014) who reported poorer survival rates in

patients with nodal involvement compared to those without. Of note, it is difficult to preoperatively detect the presence of metastatic loco-regional nodes. In this study, increased preoperative VS-1 values were associated with the evidence of nodal involvement. This result might be useful from a clinical perspective if validated in a larger cohort, as being able to preoperatively predict nodal involvement would be helpful in choosing the most proper resection and in better defining the extent of lymphadenectomy.

Furthermore, NF-PanNETs with larger tumor size are more likely to display pathological features of aggressiveness and higher risk of relapse after surgical resection (Bettini *et al*, 2011; Partelli *et al*, 2013; Zaidi *et al*, 2019). In patients with localized tumors, the largest tumor diameter is surrogate for disease burden. In the present experience, VS-1 plasma levels were significantly associated with tumor diameter, displaying the highest accuracy in the identification of NF-PanNETs greater than 4 cm. This finding suggests that the higher is the tumor burden, the higher is the tumor production/secretion of VS-1. Among all the neuroendocrine biomarkers evaluated so far, a correlation between tumor diameter and plasma values has only been evaluated for CgA. Consistently with the present results, Jilesen et al. (Jilesen *et al*, 2014) did not found any correlation between CgA plasma levels measured preoperatively and tumor size in patients diagnosed with NF-PanNETs that could be managed by surgery. Similar findings have been reported also by two additional experiences comprising more heterogeneous cohorts (Paik *et al*, 2013; Fuksiewicz *et al*, 2018). On the contrary, Jun et al. (Jun *et al*, 2017) reported a significant correlation between PanNENs size and CgA plasma level. Nevertheless, it should be noted that all the patients treated with PPI or with a history of renal/cardiac insufficiency or malignant tumor had been excluded from this study.

Disease relapse after curative surgery occurs in approximately 10-30% of patients and several clinico-pathological features have been identified as prognostic factors (Singh *et al*, 2018b, 2018a; Pulvirenti *et al*, 2020). Nowadays, there is no consensus regarding the role of CgA as prognostic marker in patients with PanNETs. Several retrospective series reported a correlation between baseline CgA and survival outcomes (Han *et al*, 2015; Pulvirenti *et al*, 2019b). However, these studies had small sample size with a limited number of recurrence events, thus preventing a survival analysis adjusted for confounders. On the contrary, a recent prospective multicentre experience showed that CgA is poorly accurate also in the detection of disease progression in the setting of

advanced disease, as only a slight association between changes in CgA levels and modifications in tumor burden was identified (Dam *et al*, 2020). Therefore, CgA measurement as part of the follow-up schedule might not provide clinically useful information (Modlin *et al*, 2016b). The present experience showed that higher preoperative VS-1 plasma levels are significantly associated with disease relapse during postoperative follow-up. This finding sets the stage for a possible role of VS-1 as prognostic biomarker, that should be further investigated in a prospective setting, accounting also for possible confounding factors.

PPI treatment represents one of the main determinants of CgA elevation in the absence of a neuroendocrine disease (Hijioka *et al*, 2014). Interestingly, the present experience showed that total-CgA plasma levels were significantly increased by the administration of PPI, whereas VS-1 values remained stable. These findings strengthen those previously reported by Corsello et al. regarding the role of VS-1 as novel NET biomarker (Corsello *et al*, 2018). Differently from previous observations (Corsello *et al*, 2018), no significant correlation between preoperative plasma levels of total-CgA and VS-1 was reported in the present experience. These divergent data might be explained considering that patients included in the previous series displayed variable disease stage and site of origin. This difference might also be responsible for the lower total-CgA and VS-1 plasma levels measured in this study compared with those previously described (Corsello *et al*, 2018).

Considering other biomarkers, NETest has recently gained wide acceptance as NET biomarker (Modlin *et al*, 2015; Öberg, 2021). NETest is a blood-based NET gene signature assessing the expression of 51 genes, by using four prediction algorithms. The measurement is then reported as tumor activity score ranging from 0 to 100 (Pavel *et al*, 2017). Since recent findings support the role of multianalytes for diagnosis, prediction of relapse and assessment of treatment response, it might be hypothesized that additional studies on novel monoanalyte biomarkers are of scarce utility. However, VS-1 may have the advantage of being easily reproducible, cost-effective and readily available. This is particularly relevant in patients with localized PanNETs, due to the usually long survival and extended follow-up periods.

This experience has several limitations that should be taken into account. First of all, the clinical implications of this study are limited. Although increased VS-1 values were found to be associated with tumor features of aggressiveness (i.e. nodal metastases and

microvascular invasion), this finding might be a consequence of the strong relationship existing between VS-1 and tumor size. Second, the small sample size did not allow to perform a multivariate analysis evaluating the effect of possible confounders. Third, VS-1 and total-CgA were measured only before surgery. Therefore, it was not possible to determine whether VS-1 was able to predict surgical efficacy and possible residual disease. Finally, the low number of recurrence events did not to allow to perform a multivariate survival analysis assessing the role of VS-1 as independent predictor of postoperative disease relapse. On the other hand, the present experience provides interesting preliminary findings, which support the role of VS-1 as a promising biomarker for PanNENs. Moreover, the inclusion criteria were precisely defined, allowing to select a homogeneous study population, thus significantly limiting the risk of bias.

In conclusion, VS-1 is strongly associated with tumor size, nodal involvement and presence of microvascular invasion in patients with localized NF-PanNETs. Also, patients with high VS-1 values show a high risk of disease relapse after surgical resection. Finally, VS-1 value is not altered by PPI treatment. The present experience supports the hypothesis that VS-1 might be promising novel neuroendocrine biomarker, which requires further evaluation in prospective trials.

Materials and methods

Study design

This study was reported following to the "Standards for Reporting Diagnostic accuracy studies" guidelines (STARD 2015) (Bossuyt *et al*, 2015).

Participants

Preoperative plasma samples of patients with PanNENs who underwent surgery at IRCCS San Raffaele Scientific Institute were prospectively collected starting from May 2015. A written informed consent was obtained from all the patients and the study was approved by the San Raffaele Ethics Committee (protocol NETBANK001). All the patients with asymptomatic well-differentiated NF-PanNETs > 2 cm underwent surgery, whereas those with asymptomatic well-differentiated NF-PanNETs ≤ 2 cm without preoperative signs of disease aggressiveness (i.e. evidence of nodal involvement, dilation of bile duct or Wirsung duct) were managed conservatively through an active surveillance strategy. NF-PanNETs were defined as unresectable in the presence of involvement of

the superior mesenteric artery and/or in the presence of a portal vein/superior mesenteric vein infiltration greater than 180°. For the purpose of this study, only patients who underwent surgery between May 2015 and May 2017 for sporadic, NF, well-differentiated PanNETs were included. Patients diagnosed with functioning (e.g. insulinoma) or metastatic tumors were excluded, as well as those with poorly differentiated neoplasms classified as PanNECs G3 (Lloyd RV *et al*, 2017).

Test methods

VS-1 was considered as the index test and total-CgA was established as reference standard test. VS-1 and total-CgA were measured in plasma samples using two sandwich Enzyme-Linked ImmunoSorbent Assays (ELISAs) (*76-ELISA and total-CgA-ELISA, respectively) (Corsello *et al*, 2018; Chung *et al*, 2012).

*76-ELISA is able to selectively detect VS-1 (CgA_{1-76}), whereas total-CgA-ELISA can identify full-length CgA plus fragments containing the N-terminal and all or part of the central and C-terminal regions (but not VS-1) (Crippa *et al*, 2013). The *76-ELISA is based on the use of the mouse monoclonal antibody (mAb) 5A8 (against CgA_{53-57}) and rabbit polyclonal antibody α76 (against CgA_{71-76}) as capturing and detecting antibodies, respectively. The total-CgA-ELISA is based on the use of the mAb B4E11 (against CgA_{68-71}) and the rabbit polyclonal αCgA (FRs), as capturing and detecting antibodies, respectively. The polyclonal antisera α76 was raised in rabbit by immunization with CgA_{71-76}, whereas the polyclonal antisera αCgA was raised in rabbit by immunization with recombinant human CgA. Different monoclonal capturing Ab (5A8 and B4E11) were used in the two assays because mAb B4E11 and α76 cannot form molecular sandwiches owing to steric hindrance.

Results of the index test (VS-1) were accessible to the performers of the reference standard test (total-CgA) and viceversa. Clinical information was not available to performers and readers of both index and reference standard tests.

Samples and data collection

Blood was collected in ethylenediaminetetraacetic acid (EDTA)-containing tubes and plasma was obtained after centrifugation (1600g for 10 minutes, + 4°C). Plasma samples were frozen slowly (-1°C per minute), stored in a -80°C refrigerator for 24-72 hours, and finally transferred into liquid nitrogen.

Clinical and pathological data were retrieved from prospectively collected database. Preoperative variables that were considered included: gender, age, presence of clinical manifestation, PPI assumption, body mass index (BMI), preoperative VS-1 and total-CgA levels. Tumor size was defined as the largest diameter as measured in the pathological specimen. T and N stages were classified according to the ENETS staging system (Rindi *et al*, 2006). Immunostaining routinely included neuroendocrine markers (CgA and synaptophysin), and Ki67 proliferative index, assessed by MIB1 staining and expressed as the % of cells with positive nuclear staining in 2000 cells counted in the area of highest nuclear labelling (Lloyd RV *et al*, 2017). Tumor grade was classified according to the latest WHO classification as G1 (Ki67 < 3%), G2 (Ki67 3-20%) and G3 (Ki67 > 20%) (Lloyd RV *et al*, 2017). Surgical margins status was defined as R0 (no residual tumor), R1 (microscopic residual tumor) or R2 (macroscopic residual tumor). The presence of perineural invasion, microvascular invasion and necrosis was also reported.

All the patients included in the study were followed up regularly after surgery. Generally, a follow-up schedule, including at least one high-quality imaging procedure (CT or MRI) every 6 months was proposed to all the patients for the first 2 years and yearly thereafter for at least 5 years. Information regarding general health status and disease relapse were collected during outpatient visits or by phone interviews.

Statistical analysis

Continuous variables were reported as median and interquartile range (IQR). For categorical data, numbers and percentages (%) were displayed. Continuous variables were compared between groups using the Student's t test or the Mann-Whitney U test, based on variables distribution. Categorical data were compared using the Chi square test or the Fisher exact test, based on the expected counts. VS-1 and total-CgA level were compared using the Wilcoxon signed-rank test. The correlation between continuous variables was assessed by linear regression analysis. The relationship with tumor size was evaluated in order to find a VS-1 cut-off to stratify the study population and compare pathological data in patients with different VS-1 levels. ROC analysis was performed to evaluate VS-1 and total-CgA as predictors of tumor size, nodal metastases and microvascular invasion. DFS was defined as the time from diagnosis to first evidence of disease relapse at imaging and it was censored at the last follow-up if no events had occurred. Survival probability was estimated according to the Kaplan-Meier method. DFS

was compared between patients with different VS-1 plasma levels using the log-rank test. Statistical analysis was performed in SPSS 25.0 for Mac software (SPSS Inc, Chicago, Illinois, USA). *P* values were considered significant when less than or equal to 0.05. There were no indeterminate or missing data.

Aims 2 and 3 - To evaluate the ability of VS-1, compared with total-CgA, to assess the effectiveness of surgical resection in patients with NF-PanNETs. To investigate PST and vasostatin-2 (VS-2) as potential biomarkers for NF-PanNETs.

Results

Study population

Overall, 35 patients who underwent surgery for sporadic NF-PanNETs were included in the study. Demographic, clinical and pathological characteristics are reported in **Table 9** and **Table 10**.

Table 9. *Demographic and perioperative features of patients submitted to surgery for NF-PanNETs.*

Variable	Study population *n 35* (%)
Gender	
Male	20 (57)
Female	15 (43)
Age, years*	58 (46-66)
BMI, Kg/m^2*	24.5 (21-26)
Incidental diagnosis	
No	13 (37)
Yes	22 (63)
Preoperative PPI assumption	
No	28 (80)
Yes	7 (20)
Maximum radiological diameter, mm*	35 (24-65)
^{68}Gallium PET	
Not performed	1 (3)
Negative	1 (3)
Positive	33 (94)
^{18}F-FDG PET	
Not performed	18 (52)
Negative	5 (14)
Positive	12 (34)

Surgical procedure	
Pancreaticoduodenectomy	11 (31)
Distal pancreatectomy**	18 (51)
Total pancreatectomy	3 (9)
Enucleation	1 (3)
Middle pancreatectomy	2 (6)
Postoperative complications°	
Clavien-Dindo 0-I	17 (49)
Clavien-Dindo II	12 (34)
Clavien-Dindo III	6 (17)

*Values are expressed as median (interquartile range); †*n*=4 distal pancreatectomy with liver resection, *n*=1 distal pancreatectomy with radiofrequency ablation of liver metastases.
°According to (Dindo *et al*, 2004)
BMI, body mass index; *FDG*, fluorodeoxyglucose; *PET*, positron emission tomography; *PPI*, proton pump inhibitors.

Table 10. *Pathological details of patients submitted to surgery for NF-PanNETs.*

Variable	**Study population *n 35* (%)**
Tumor site	
Pancreatic head	14 (40)
Pancreatic body	10 (29)
Pancreatic tail	11 (31)
Ki67 proliferative index, %*	2 (1-5)
Tumor grade†	
PanNET G1	19 (54)
PanNET G2	15 (43)
PanNET G3	1 (3)
Tumor diameter, mm	30 (25-65)
T stage°	
T1-T2	21 (60)
T3-T4	14 (40)
N stage°	
Nx	1 (3)
N0	16 (46)
N+	18 (51)
M stage°	
M0	29 (83)
M1	6 (17)
Resection margins	
R0	28 (80)
R1	3 (9)
R2	4 (11)

Microvascular invasion	
Absent	19 (54)
Present	16 (46)
Perineural invasion	
Absent	22 (63)
Present	13 (37)
Necrosis	
Absent	32 (91)
Present	3 (9)

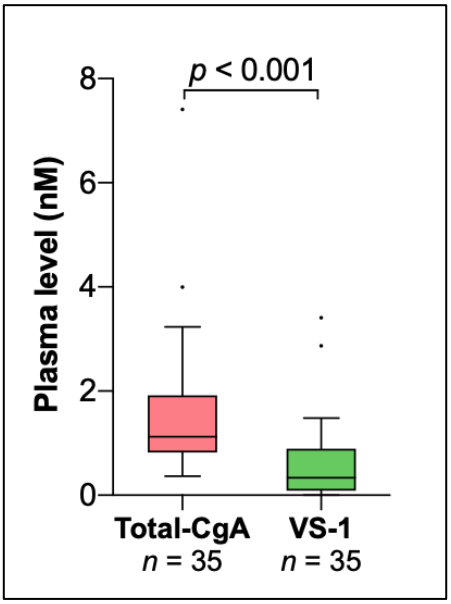
*Values are expressed as median (interquartile range).
†According to 2017 WHO classification (Lloyd, RV et al, 2017)
°According to ENETS TNM staging system (Rindi *et al*, 2006)

Most of patients were diagnosed with G1 (*n* = 19, 54%) or G2 (*n* = 15, 42%) NF-PanNETs, whereas only one subject had a high-grade well-differentiated PanNET G3. Overall, 89% of the study cohort underwent a surgical resection with curative intent (*n* = 28 R0, *n* = 3 R1), whereas 4 patients underwent debulking surgery (R2). The tumor was localized 83% of cases (*n* = 29), while distant metastases were present in 6 patients.

AIM 2 - Test results: total-CgA and VS-1

Total-CgA and VS-1 were measured preoperatively and postoperatively in all the patients (*n* = 35). Preoperative total-CgA plasma levels were significantly higher as compared with preoperative VS-1 plasma levels [median 1.123 nM (IQR 0.824-1.918) *versus* median 0.338 nM (IQR 0.088-0.893 nM), $p < 0.001$], as depicted in **Figure 17**.

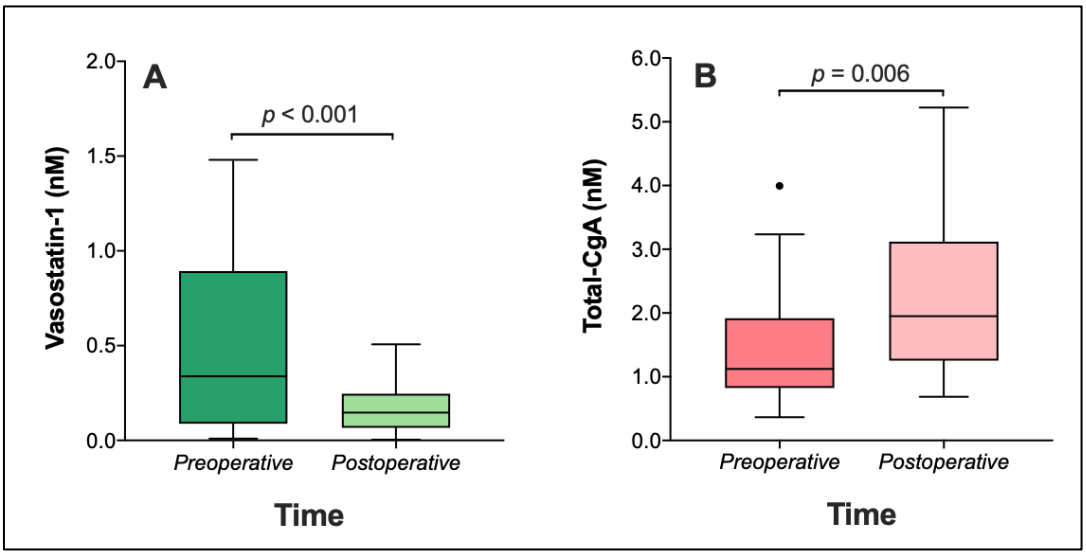
Figure 17. *Matched comparison between preoperative total-CgA and VS-1 plasma levels.*



Patients assuming PPI preoperatively (n = 7) had significantly higher preoperative total-CgA plasma levels as compared to patients not assuming PPI (n = 28) [median 2.327 nM (IQR 0.913-7.410) *versus* median 1.058 nM (IQR 0.796-1.653), p = 0.039)]. No statistically significant differences were observed in terms of VS-1 plasma levels between patients assuming or not PPI preoperatively (p = 0.384).

Median VS-1 plasma levels significantly decreased after surgery [0.338 nM (IQR 0.088-0.893 nM) *versus* 0.147 nM (IQR 0.066-0.246 nM), $p < 0.001$] (**Figure 18A**), whereas total-CgA values increased significantly after surgical resection [1.123 nM (IQR 0.824-1.918) *versus* 1.949 nM (IQR 1.252-3.120 nM), p = 0.006] (**Figure 18B**).

Figure 18. *Comparison between preoperative and postoperative VS-1 (A) and total-CgA (B).*

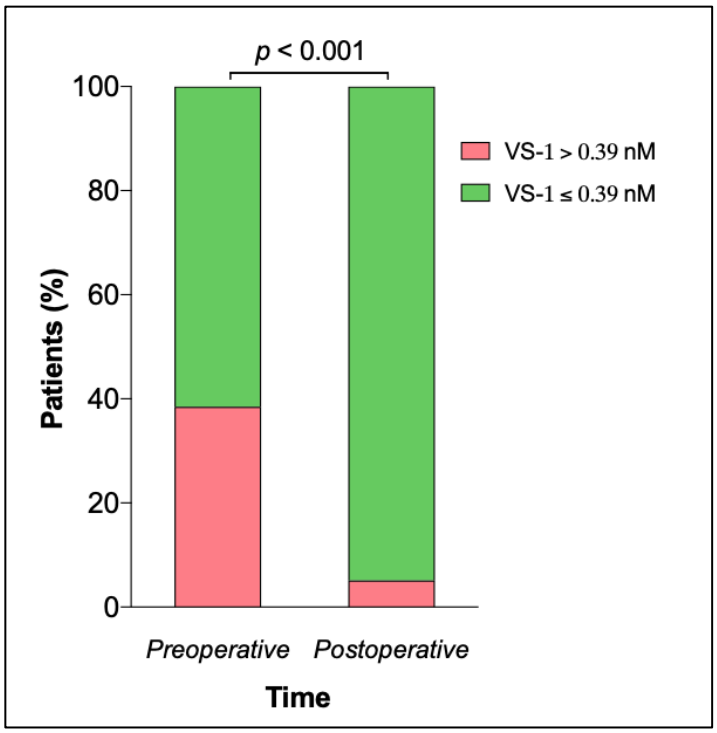


Postoperative VS-1 plasma levels were similar between patients with low-grade (Clavien-Dindo 0-I-II, n = 29) and high-grade (Clavien-Dindo III, n = 6) postoperative complications (p = 0.379).

The percentage of patients with VS-1 > 0.390 nM (cut-off defined in the previous study) significantly decreased from preoperative time (n = 15, 43%) to postoperative day (POD) 5 (n = 2, 6%) ($p < 0.001$), as depicted in **Figure 19**. All the patients with preoperative VS-1 values ≤ 0.390 (n = 20) still had a VS-1 level below this cut-off postoperatively. Postoperative VS-1 was > 0.390 nM in 2 patients. The first one had a G2 PanNET with microvascular invasion and extensive nodal involvement and experienced a nodal relapse 13 months after surgery. The other one had a G1 PanNET pT2 pN0

associated to the presence of at least 2 pancreatic neuroendocrine microadenomas (in the absence of a known familial syndrome).

Figure 19. *Percentage of patients with VS-1 higher than the predefined cut-off (0.39 nM) preoperatively and postoperatively.*



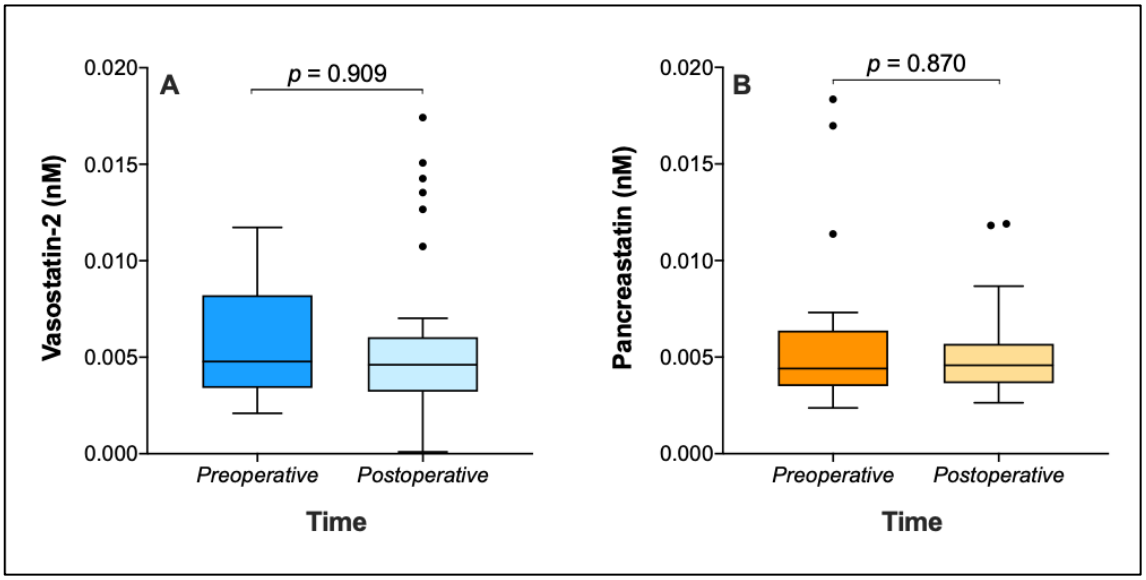
Overall, four patients underwent surgery with palliative intent (R2) due to the evidence of liver metastases: in 3 of these cases, VS-1 decreased after primary tumor resection, whereas the remaining patient had no postoperative VS-1 reduction. This latter patient was diagnosed with a 28 mm G1 PanNET with nodal and distant metastases and experienced a disease progression in the liver 15 months after surgery.

Three patients underwent R1 resection (i.e. microscopic residual tumor) and two of them did not show any postoperative decrease in VS-1 plasma levels. The median percentage decrease in VS-1 plasma levels was 44% (IQR 16-83%) in patients who underwent R0 resections (n = 28) and 58% (IQR 0-88%) in patients who underwent R1-R2 resections (n = 7) (p = 0.920).

AIM 3 - Test results: VS-2 and PST

Median preoperative VS-2 and PST plasma levels were 0.005 nM (IQR 0.003-0.008 nM) and 0.004 nM (IQR 0.003-0.006 nM), respectively. No statistically significant differences were detected between preoperative [0.005 nM (IQR 0.003-0.008 nM)] and postoperative VS-2 [0.005 nM (IQR 0.003-0.006 nM)] (p = 0.909) (**Figure 20A**). PST plasma levels were similar preoperatively [0.004 nM (IQR 0.003-0.006 nM)] and postoperatively [0.004 nM (IQR 0.003-0.005 nM)] (p = 0.870) (**Figure 20B**).

Figure 20. *Comparison between preoperative and postoperative plasma levels of vasostatin-2 (A) and pancreastatin (B).*



Determinants of high (> 0.390 nM) preoperative VS-1

By univariate logistic regression analysis (**Table 11**), higher T stage (T3-T4, OR 8.00, 95% CI 1.73-37.09, $p = 0.008$) and microvascular invasion (OR 4.67, 95% CI 1.11-19.65, $p = 0.036$) were the only variables significantly associated with preoperative VS-1 plasma levels greater than 0.390 nM.

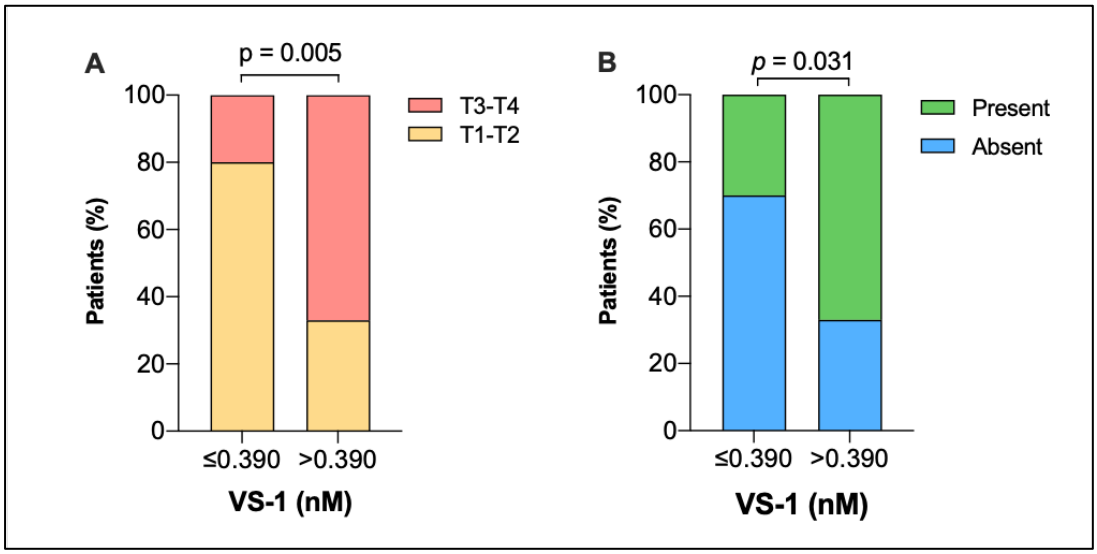
Table 11. *Univariate logistic regression analysis evaluating demographic, clinical, and pathological determinants of "high" (>0.390 nM) preoperative VS-1.*

Variable	Odds Ratio (OR)	95% CI	*p*
Gender			0.694
Male	1	–	
Female	1.31	0.34-5.08	
Age			0.699
< 70 years	1	–	
≥ 70 years	1.42	0.24-8.26	
Tumor grade*			0.435
PanNET G1	1	–	
PanNET G2-G3	1.71	0.44–6.63	
T stage†			**0.008**
T1-T2	1	–	
T3-T4	8.00	1.73-37.09	
N stage†			0.557
N0	1	–	
N+	1.50	0.39-5.81	
M stage†			0.210
M0	1	–	
M1	3.27	0.51–20.93	
Microvascular invasion			**0.036**
No	1	–	
Yes	4.67	1.11–19.65	
Perineural invasion			0.762
No	1	–	
Yes	1.24	0.31–4.93	
Necrosis			0.401
No	1	–	
Yes	2.92	0.24–35.68	

*According to 2017 WHO classification (Lloyd, RV et al, 2017)
†According to ENETS TNM staging system (Rindi *et al*, 2006)

Patients with high (> 0.390 nM) preoperative VS-1 had a significantly increased rate of T3-T4 neoplasms [n = 10/15 (67%) *versus* n = 4/20 (20%), p = 0.005] and microvascular invasion [n = 10/15 (67%) *versus* n = 6/20 (30%), p = 0.031] as compared to patients with low (≤ 0.390 nM) preoperative VS-1 (**Figure 21**).

Figure 21. *Comparison of the rate of nodal metastases and microvascular invasion between patients with low VS-1 (≤ 0.390 nM) and those with high VS-1 (> 0.390 nM).*

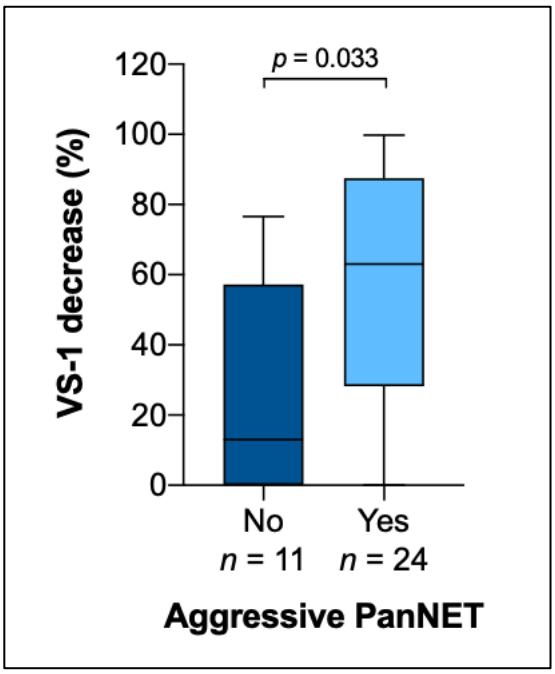


VS-1 postoperative decrease in patients with and without features of aggressiveness

Overall, 24 out of 35 patients (69%) presented at least one feature of tumor aggressiveness (i.e. T3-T4 tumor, nodal and/or distant metastases, Ki67 proliferative index >5%, microvascular invasion, perineural invasion, necrosis).

In patients with at least one pathological feature of aggressiveness, median VS-1 plasma levels decreased significantly after surgery [0.380 nM (IQR 0.093-1.082) *versus* 0.101 nM (IQR 0.061-0.235 nM), p = 0.001]. On the other hand, the decrease was not statistically significant in patients without aggressiveness features (p = 0.423). The median VS-1 percentage decrease was 63% (IQR 28-88%) in patients with aggressive tumors, compared to 13% (IQR 0-57%) in the remaining subjects (p = 0.033) (**Figure 22**).

Figure 22. *Comparison of VS-1 percentage decrease between patients with and without aggressive NF-PanNETs (features of aggressiveness: T3-T4 tumors, nodal/distant metastases, Ki67 >5%, microvascular/perineural invasion, necrosis).*



Discussion

The lack of reliable monoanalyte biomarkers represents a relevant unmet clinical need in the field of NF-PanNENs. The limitations related to the use of CgA as neuroendocrine biomarker have been extensively reported, but no better and easily retrievable alternatives have been introduced so far in the routine clinical practice (Marotta *et al*, 2012; Oberg, 2011; Öberg, 2021). Over the last few decades, a variety of circulating analytes have been investigated, but none of them has been demonstrated to display adequate sensitivity and specificity to meet the NIH criteria to define a reliable biomarker. For these reasons, CgA still represents the most frequently used biomarker in clinical practice (Oberg *et al*, 2015).

Recently, the circulating levels of peptides derived from the proteolytic processing of CgA (i.e. CgA-derived fragments) have been investigated as potential biomarkers in patients diagnosed with GEP-NETs (Corsello *et al*, 2018; Andreasi *et al*, 2019; Tran *et al*, 2021; Woltering *et al*, 2019). In particular, the N-terminal fragment, which is known as VS-1, has shown interesting and promising results, with higher plasma values being associated to the presence of nodal metastases and microvascular invasion in patients who underwent surgical resection for localized NF-PanNETs (Andreasi *et al*, 2019). However,

no data are currently available regarding the ability of VS-1 to assess the efficacy of neuroendocrine tumors surgical management.

The present experience showed that VS-1, but not total-CgA, seems able to assess the effectiveness of surgical treatment, as its plasma levels decrease significantly after surgery in patients with NF-PanNETs. On the other hand, a postoperative rise of total-CgA plasma levels was reported. This increase in postoperative CgA might be explained by the routine administration of PPI after surgery (Giusti *et al*, 2004; Pregun *et al*, 2011).

The present data also confirm that VS-1 values are not altered by the assumption of PPI (Corsello *et al*, 2018; Andreasi *et al*, 2019). A possible explanation for this finding is that enterochromaffin-like cells, which are considered as the principle responsible for CgA increase induced by PPI, do not produce the proteases involved in CgA processing at the N-terminal region. Therefore, only total-CgA, but not its N-terminal fragment VS-1, are increased in patients assuming PPI. On the other hand, NENs are likely to produce these proteases, thus leading to CgA processing at its N-terminal region and to a consequent increase in VS-1 plasma levels (Corsello *et al*, 2018). Moreover, we also observed that the occurrence of major postoperative complications did not alter significantly VS-1 plasma levels measured on POD 5.

The limited role of CgA in PanNETs diagnosis and evaluation of surgical effectiveness has been previously reported (Pulvirenti *et al*, 2019b; Tseng *et al*, 2018; Baekdal *et al*, 2020; Qiu *et al*, 2016). Consistently with the present results, Qiu et al. reported that CgA values did not change significantly following surgical resection in patients affected by PanNETs in the context of MEN-1 (Qiu *et al*, 2016). Similarly, our group previously observed that CgA values did not vary significantly between preoperative and postoperative time in a cohort of patients submitted to surgery for PanNETs (Partelli *et al*, 2020a). Therefore, CgA does not seem able to provide clinically useful information regarding the effectiveness of surgical resection in patients with PanNENs.

This is the first series evaluating preoperative and postoperative VS-1 plasma levels in patients who underwent surgery for NF-PanNETs. Preoperatively, almost half of patients had a VS-1 value higher than a previously defined cut-off (0.390 nM) associated with features of tumor malignancy (Andreasi *et al*, 2019). Postoperatively, VS-1 levels decreased significantly, especially in patients with neoplasms defined as aggressive. The only data currently available in the literature suggest a potential role of VS-1 in the

assessment of treatment efficacy. Specifically, Corsello et al. measured VS-1 plasma levels in 14 patients with pancreatic and small intestinal NETs. The Authors of this previous experience reported a relevant VS-1 decrease in the majority of patients after treatment with SSAs (Corsello *et al*, 2018).

Apart from the evaluation of surgical efficacy, VS-1 might have a role also in the detection of disease relapse during post-surgical follow-up. The present experience did not assess the long-term predictive role of VS-1, but it was clearly shown that VS-1 postoperative drop is significantly greater for patients with aggressive neoplasms, as compared to those with more indolent tumors. This finding suggests a possible role of VS-1 in monitoring patients at high risk of relapse after resection of NF-PanNETs. However, this hypothesis needs to be further confirmed in future studies. The presence of a circulating biomarker able to detect disease recurrence would be of paramount importance from a clinical standpoint, as CgA accuracy has been clearly demonstrated to be poor. In this regard, Jilesen et al. found that CgA plasma values after curative surgery performed for NF-PanNETs were falsely increased in approximately 50% of cases (Jilesen *et al*, 2014). More recently, a prospective study including patients with advanced GEP-NETs identified only a slight association between changes in CgA values and modifications in tumor burden, thus questioning the utility of CgA also in predicting tumor progression in the setting of metastatic disease (Dam *et al*, 2020).

The present series investigated also two additional CgA-derived peptides, VS-2 and PST. Plasma levels of both VS-2 and PST did not change significantly between preoperative and postoperative time. These results are partially in contrast with those previously reported by several experiences investigating PST as biomarker for patients with metastatic SB-NETs. These studies reported that PST performed better than CgA in detecting disease progression and in predicting survival outcomes (Sherman *et al*, 2014; Strosberg *et al*, 2018; Woltering *et al*, 2019, 2016). In particular, a high PST plasma level after curative resection or cytoreduction of small intestinal NETs was found to be associated with poorer oncological prognosis (Tran *et al*, 2021; Woltering *et al*, 2019). Regarding VS-2, a previous experience described a higher expression of this fragment in metastases from SB-NETs as compared to primary tumors (Giovinazzo *et al*, 2013). However, the different biological behaviour of PanNETs compared to SB-NETs and the

relatively low disease burden of patients included in the present study might explain these conflicting findings regarding PST and VS-2.

CgA and peptides derived from its proteolytic cleavage are not the only biomarkers that have been investigated in patients with PanNETs. One of the most promising biomarkers is NETest, a multianalyte biomarker assessing the expression of 51 neuroendocrine gene transcripts, that has been validated through the use of independent datasets (Pavel *et al*, 2017; Modlin *et al*, 2021a, 2021b). NETest has been previously demonstrated as an accurate tool for detecting residual disease and for assessing postoperative disease status in patients who underwent surgery for GEP-NENs (Partelli *et al*, 2020a; Laskaratos *et al*, 2020; Modlin *et al*, 2021b). Also, several series have reported that the efficacy of medical therapies is associated with a decrease in NETest scores. On the other hand, it has been observed that a persistent or a subsequent increase in NET transcript levels is strongly associated with the presence of a progressive or recurrent neuroendocrine disease (Modlin *et al*, 2021c; Oberg *et al*, 2016). Based on this evidence, it might be argued that the time for monoanalyte circulating biomarkers is over. However, a small peptide like VS-1 may provide some benefit, being more easily reproducible, accessible, and cost-effective as compared to NETest. Cost-effectiveness should always be taken into account given the long life-expectancy and the consequently long follow-up of patients with NETs.

The present experience has several limitations that should be considered. First, VS-1 and total-CgA postoperative measurement was performed only in the early postoperative period (on POD 5) and CgA values have been altered by the administration of PPI. Therefore, it was not possible to compare these biomarkers at different time points after surgery by analyzing their usefulness in the long-term. Second, the small sample size did not allow to perform a multivariate analysis evaluating the impact of possible confounders on VS-1 levels.

In conclusion, VS-1 is confirmed as a promising novel biomarker, which can provide an early assessment of surgical effectiveness in patients with NF-PanNETs, especially in those with aggressive tumors. On the other hand, total-CgA, VS-2 and PST seem to have no clinical utility in this context. Further studies are now required to evaluate the accuracy of VS-1 in predicting tumor recurrence and disease progression during follow-up.

Materials and Methods

Study design

The present study was reported following the "Standards for Reporting Diagnostic accuracy studies" (STARD 2015) guidelines (Bossuyt *et al*, 2015).

Participants

Patients who underwent surgery for sporadic, NF-PanNETs at San Raffaele Hospital, between 2018 and 2019, were included. Patients diagnosed with neoplasms classified as PanNECs G3 as well as those with functioning tumors were excluded from this study. Preoperative plasma samples of patients with PanNETs were collected prospectively from May 2015. Postoperative plasma samples were collected prospectively on POD 5 starting from May 2018. Written informed consent was obtained from all participants. The study was approved by the San Raffaele Scientific Institute Ethics Committee (protocol NETBANK001).

Test methods

VS-1 was defined as the index test. Total-CgA (i.e. mixture of full-length and fragmented CgA) was considered as the reference standard test (Falconi *et al*, 2016; Oberg, 2011).

VS-1 and total-CgA plasma levels were detected using two sandwich ELISAs. The assay for VS-1 (*76-ELISA) selectively detects the N-terminal fragment of CgA (VS-1), whereas the assay for total-CgA (total-CgA-ELISA) can detect both CgA_{1-439} and peptides containing the N-terminal region and all or part of the central and C-terminal regions, but not VS-1 (Crippa *et al*, 2013). For *76-ELISA, the mAb 5A8 (against CgA_{53-57}) and the rabbit polyclonal Ab α76 (against CgA_{71-76}) were used as capturing and detecting antibodies, respectively. For total-CgA ELISA, the mAb B4E11 (against CgA_{68-71}) and the rabbit polyclonal Ab αCgA were used as capturing and detecting antibodies, respectively. Two different capturing mAbs were used in the two assays as mAbs B4E11 and α76 are not able form molecular sandwiches.

Two additional CgA-derived fragments, VS-2 and PST, were investigated as NET biomarkers. VS-2 (CgA_{1-113}) was measured using a human VS-2 ELISA kit developed by AvisceraBioscience® (Aviscera Bioscience Inc, Santa Clara, CA, USA). PST ($CgA_{250-301}$)

was measured using a human pancreastatin ELISA kit developed by Cusabio® (Cusabio Technology LLC, Houston, TX, USA).

No test positivity cut-off was set for total-CgA, due to the significant variability existing between the different available assays. No predefined cut-offs defining test positivity were available for the investigated CgA-derived fragments, as their measurement is not part of routine clinical practice. Regarding VS-1, a previously identified cut-off (0.390 nM) associated with pathological features of tumor aggressiveness was used to stratify the study cohort (Andreasi *et al*, 2019).

All the plasma samples were deidentified to the laboratory group. Results of the reference standard test (total-CgA) and index tests (VS-1, PST and VS-2) were available to test performers. The clinical study group had access to clinical information, which was provided to performers and readers of the tests only after results finalization.

Samples and data collection

Full blood samples were collected in 6 mL EDTA tubes, before surgery and after surgery on POD 5. Plasma was obtained after full blood centrifugation for 10 minutes (1600xg, room temperature). Plasma samples were stored for 24-72 hours in a -80°C refrigerator and then transferred into liquid nitrogen tanks.

Clinico-pathological characteristics were also collected. The initial diagnostic work-up included at least one high-quality imaging examination (MRI or CT) and it was always completed with ^{68}Ga-DOTA PET/CT or with ultrasound endoscopy with fine-needle aspirate. ^{18}F-FDG PET/CT was not routinely performed. Postoperative complications were graded based on the Dindo-Clavien classification of surgical complications (Dindo *et al*, 2004). All the patients included in this study were postoperatively treated with PPI for at least one month.

TNM staging was defined according to ENETS classification (Rindi *et al*, 2006). Ki67 proliferative index was assessed by MIB1 antibody staining in 2000 cells counted in the area of highest nuclear labelling. Tumor grade was defined according to the latest WHO classification into G1 (Ki67 < 3%), G2 (Ki67 3-20%) and G3 (Ki67 > 20%) (Lloyd RV *et al*, 2017). The status of resection margins was categorized as R0 (no residual tumor), R1 (microscopic margin involvement) and R2 (macroscopic residual tumor). The presence of microvascular invasion, perineural invasion and necrosis was also assessed. Tumor aggressiveness was defined in the presence of at least one of the following

pathological features: T3-T4 stage, nodal involvement, distant metastases, Ki67 proliferative index > 5%, microvascular invasion, perineural invasion and necrosis.

Statistical analysis

Continuous variables were expressed as median with IQR. Categorical data were described with numbers and proportions (%). The Wilcoxon signed-rank test was used to compare plasma levels of CgA and CgA-derived fragments before and after surgery. Qualitative variables were compared using the Chi square test or the Fisher exact test, when necessary. The Mann-Whitney U test was used to compare continuous variables between two groups. The McNemar test was employed to compare the proportion of patients with VS-1 plasma level higher than the pre-specified cut-off, before and after surgical resection. Univariate logistic regression analysis was performed to investigate variables associated with preoperative VS-1 higher than the pre-specified cut-off. OR with 95% CI were reported. Statistical analyses were performed using SPSS 25.0 for Mac software (SPSS Inc, Chicago, IL, USA). *P* values were considered significant when equal to or lower than 0.05.

Aim 4 - To investigate NETest as biomarker for patients undergoing surgery for PanNETs by assessing its effectiveness in defining the extent and efficacy of surgical resection and in predicting disease recurrence.

[The following data have been published in Partelli S, Andreasi V, et al. Circulating Neuroendocrine Gene Transcripts (NETest): A Postoperative Strategy for Early Identification of the Efficacy of Radical Surgery for Pancreatic Neuroendocrine Tumors. Ann Surg Oncol 2020].

Results

Study cohort

Overall, 40 patients preoperatively diagnosed with GEP-NET and subsequently submitted to surgery were enrolled. Of these, 30 patients had a PanNET at the final pathological examination and were finally included in the study. Demographic, clinical and pathological features are reported in **Tables 12** and **13**.

Table 12. *Demographic and perioperative features of 30 patients with histologically confirmed PanNETs.*

Variable	Study cohort *n 30* (%)
Gender	
Male	11 (37)
Female	19 (63)
Age, years*	54 (± 13.4)
BMI, Kg/m^2*	25.3 (± 4.3)
Tumor function	
Non-functioning	22 (73)
Functioning†	8 (27)
Type of diagnosis	
Symptoms	21 (70)
Incidental	9 (30)
Pain	
Absent	24 (80)
Present	6 (20)
Jaundice	
Absent	28 (93)
Present	2 (7)
Radiological tumour diameter, mm*	25 (± 11.7)

^{68}Gallium PET	
Not performed	9 (30)
Negative	1 (3)
Positive	20 (67)
^{18}F-FDG PET	
Not performed	12 (40)
Negative	6 (20)
Positive	12 (40)
Surgical procedure	
Distal Pancreatectomy°	17 (57)
Pancreaticoduodenectomy	7 (23)
Enucleation	4 (13)
Middle Pancreatectomy	1 (3.5)
Total Pancreatectomy°	1 (3.5)
Postoperative Complications‡	
None	10 (33)
Grade I-II	16 (54)
Grade III-IV	3 (10)
Grade V	1 (3)

*Expressed as mean [± standard deviation (SD)]
†*n* = 7 insulinoma, *n* = 1 ACTHoma
°*n* = 1 distal pancreatectomy + liver wedge resection, *n* = 1 total pancreatectomy + liver wedge resection
‡According to (Dindo *et al*, 2004)

Table 13. *Pathological features of patients who underwent surgery for PanNETs.*

Variable	**Study cohort *n 30* (%)**
Tumor site	
Pancreatic head	11 (37)
Pancreatic body	10 (33)
Pancreatic tail	9 (30)
Ki67 proliferative index, %*	6 (± 7.3)
Tumour grade†	
PanNET G1	12 (40)
PanNET G2	17 (57)
PanNET G3	1 (3)
Histological tumor size, mm*	23 (± 13.5)
T stage°	
T1	13 (43)
T2	11 (37)
T3	6 (20)

N stage°	
N0	15 (50)
N1	12 (40)
Nx	3 (10)
M stage°	
M0	26 (87)
M1	4 (13)
Stage°	
I	11 (37)
II	5 (17)
III	10 (33)
IV	4 (13)
Resection margin status	
R0	26 (87)
R1	2 (6.5)
R2	2 (6.5)
Microvascular invasion	
Absent	15 (50)
Present	15 (50)
Perineural invasion	
Absent	23 (77)
Present	7 (23)
Necrosis	
Absent	27 (90)
Present	3 (10)

*Expressed as mean (± standard deviation)
†According to 2017 WHO classification (Lloyd, RV et al, 2017)
°According to ENETS TNM staging system (Rindi *et al*, 2006)

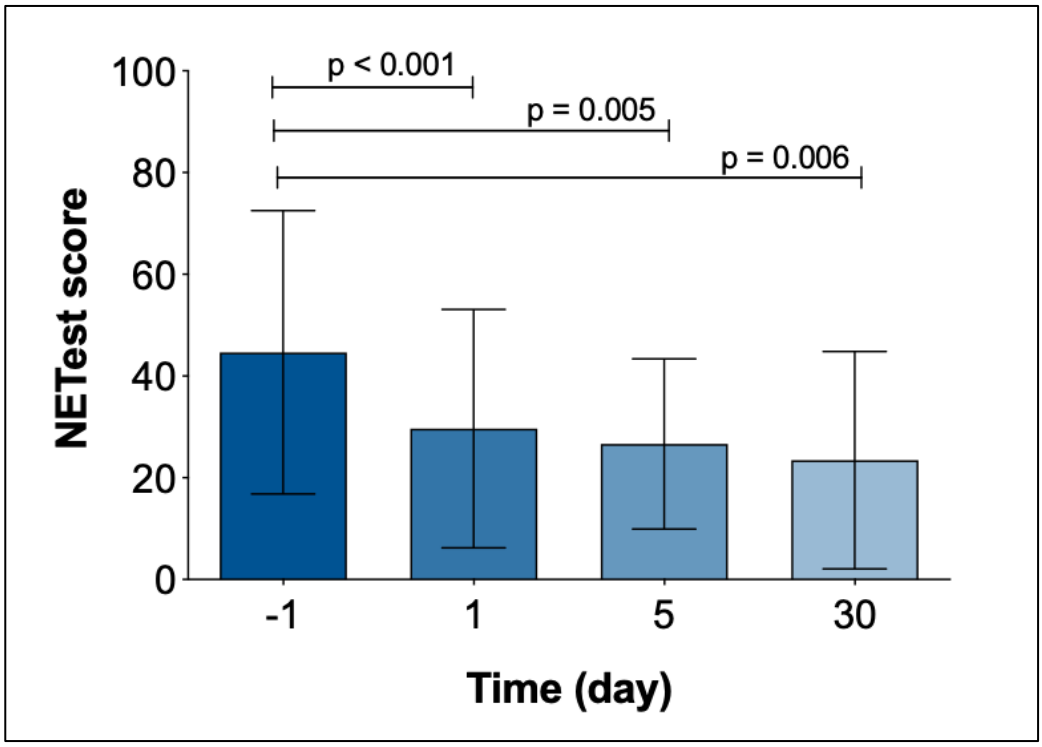
The majority of patients had NF-PanNETs, whereas 7 patients were affected by insulinoma and one patient by a functioning PanNET secreting ACTH. Most of patients had G1 (*n* = 12, 40%) or G2 (*n* = 17, 57%) PanNETs, whereas only one patient was diagnosed with a high-grade well-differentiated G3 PanNET. Overall, 93.5% of the study population underwent curative surgery (*n* = 26 R0, *n* = 2 R1), whereas 2 patients were submitted to palliative surgical resection (R2). The tumor was localized in 87% of cases (*n* = 26), whereas distant metastases were present in 4 patients.

Test results: NETest

NETest score was preoperatively elevated in all the patients, showing a mean value of 44.7 (SD ± 23). Overall, 9 patients had NETest score > 40, which corresponds to high disease activity.

Preoperative NETest score was significantly higher as compared to NETest score measured on postoperative on POD 1, POD 5 and POD 30 [preoperative: 44.7 (SD ± 23) *versus* POD 1: 27.3 (SD ± 23) $p = 0.001$, *versus* POD 5: 25.7 (SD ± 19.6) $p = 0.005$, *versus* POD 30: 24.7 (SD ± 24) $p = 0.006$], as shown in **Figure 23**).

Figure 23. *Relationship between NETest score and surgical resection.*
NETest was measured at four different time points: preoperatively, POD 1, POD 5 and POD 30. Bars represent mean (middle line) and standard deviation (top and bottom whiskers).

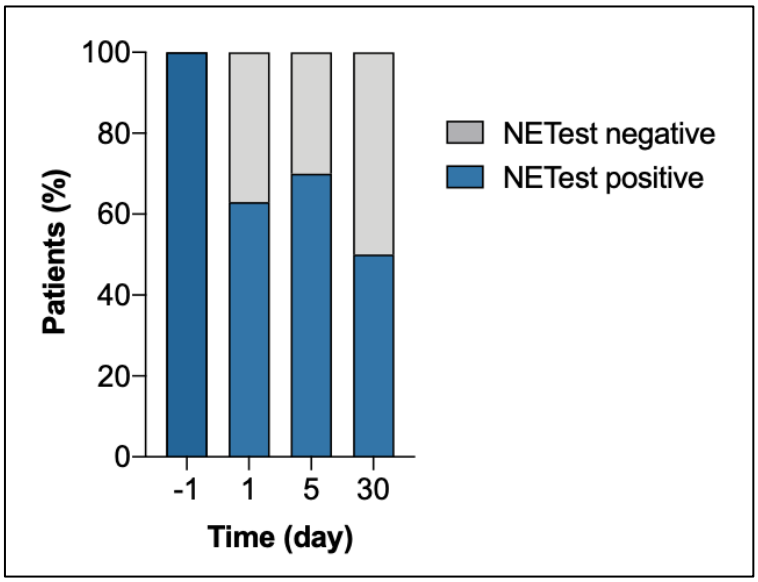


The NETest levels decrease remained stable after surgery and no statistically significant differences were observed between the three post-surgical measurements (POD 1 *versus* POD 5 $p = 1.000$, POD 5 *versus* POD 30 $p = 0.930$, POD 1 versus POD 30 $p = 0.630$).

The percentage of patients with elevated NETest decreased significantly from preoperative time ($n = 30/30$, 100%) to POD 30 ($n = 15/30$, 50%) ($p < 0.001$), as depicted in **Figure 24**. Overall, 15 patients still had increased NETest levels at POD 30. The majority of them ($n = 12/15$) showed slightly increased scores ranging between 26.7 and 33.3, whereas 3 patients had POD 30 NETest scores ≥ 40. These 3 patients had the following characteristics: patient #1 underwent a palliative R2 resection and had a POD 30 NETest score of 40; patient #2 underwent a R1 resection and had a POD 30 NETest

score of 93; patient #3 underwent a R0 resection and showed a POD 30 NETest score of 80. Patient #3 was diagnosed with a G2 PanNET (Ki67 18%) with large nodal metastases. Therefore, the elevated POD 30 NETest levels were consistent with the presence of residual disease in this patient. The increased POD 30 NETest scores of patients #1 and #2 (40 and 93) were also associated with known residual disease (R2 and R1 resections, respectively).

Figure 24. *NETest score changes and surgical resection.*
Percentage of patients that were NETest positive versus NETest negative at four different time points: preoperative, POD 1, POD 5 and POD 30. Bars represent the percentage of patients with a positive/negative NETest score. NETest positivity is defined for scores > 20.



A subanalysis of patients submitted to R0 resection provided interesting information. Overall, 13 (50%) out of 26 patients who underwent R0 surgery showed a positive NETest score at POD 30 [31.2 (SD ± 14.7)]. These blood transcript data might suggest the presence of residual disease, although complete resection was confirmed by both surgical and histological assessments.

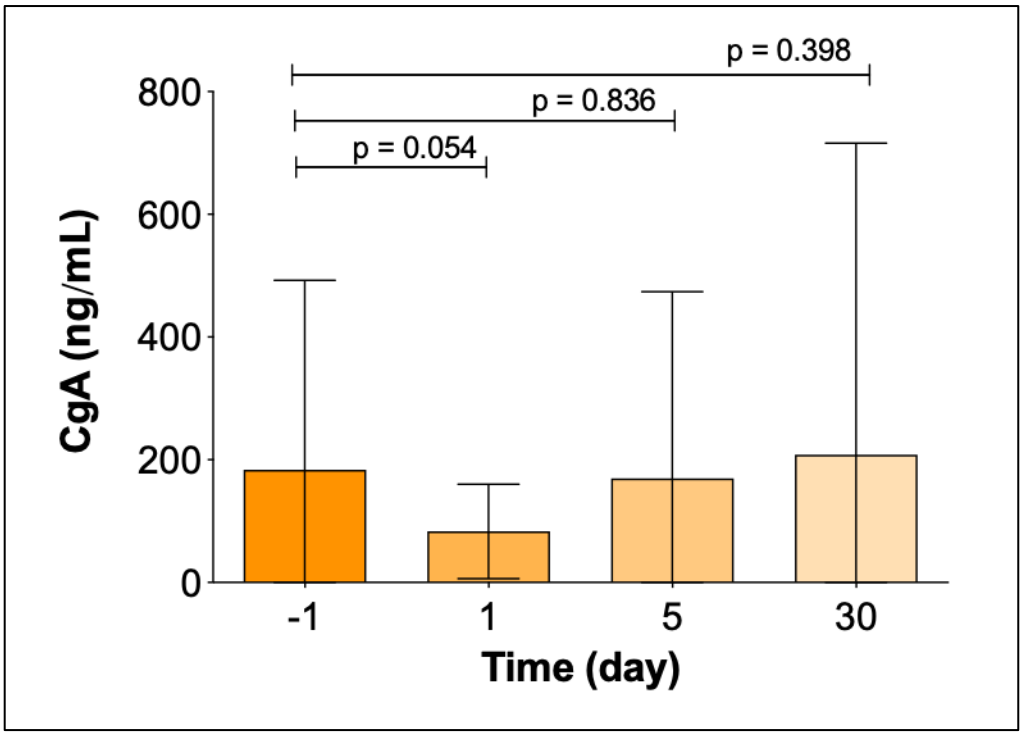
Regarding preoperative staging, 9 patients (30%) did not undergo ^{68}Gallium PET: six of them had an insulinoma, whereas the remaining three were diagnosed with NF-PanNETs (n = 2) and ACTHoma (n = 1). All the patients without ^{68}Gallium PET (n = 9) had increased NETest scores [61.5 (SD ± 32)] preoperatively. Four of them, all diagnosed with insulinomas, had a slightly elevated NETest score at POD 30 [28 (SD ± 3.3)],

whereas the other 5 patients (n = 2 insulinoma, n = 2 NF-PanNET, n = 1 ACTHoma,) who did not undergo ^{68}Gallium PET had normal NETest scores on POD 30.

Test results: CgA

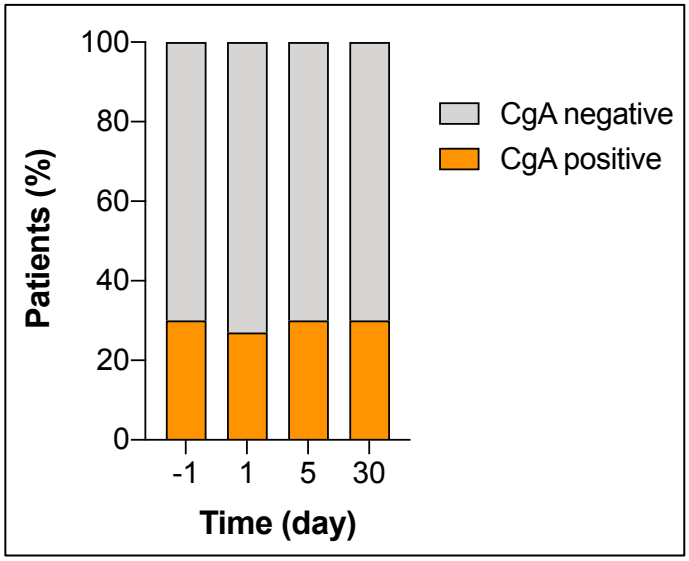
Preoperative CgA was increased in 9 patients (30%). CgA plasma levels did not change significantly between preoperative and postoperative time [184 ng/mL (SD ± 360 ng/mL) *versus* POD 1: 93 ng/mL (SD ± 87.5 ng/mL) p = 0.054, *versus* POD 5: 170 ng/mL (SD ± 335.3 ng/mL) p = 0.836, *versus* POD 30: 260 ng/mL (SD ± 589 ng/mL) p = 0.398)] (**Figure 25**).

Figure 25. *Relationship between CgA plasma levels and surgical resection.*
CgA was measured at four different time points: preoperatively, POD 1, POD 5 and POD 30. Bars represent mean (middle line) and standard deviation (top and bottom whiskers).



The percentage of patients with increased CgA did not change significantly from preoperative time (n = 9/30) to POD 30 (n = 9/30) (p = 1.000), as shown in **Figure 26**. Moreover, no differences were observed in CgA decrease between patients who underwent curative surgery and those who were submitted to palliative surgical resection (R2). In the R0 group, 7 patients (27%) had increased CgA on POD 30.

Figure 26. *CgA changes and surgical resection.*
Percentage of patients with elevated (CgA positive) versus normal (CgA negative) CgA plasma levels at four different time points: preoperatively, POD 1, POD 5 and POD 30. Bars represent the percentage of patients with increased CgA.



Determinants of preoperative NETest scores

At univariate linear regression analysis, the presence of a functioning tumor was the only factor significantly correlated with NETest score (B = 27.727, 95% CI: 6.289-49.165, p = 0.013) (**Table 14**). No correlation with M stage was observed probably due to the low number of metastatic patients included in the study (n = 4).

Table 14. *Univariate linear regression analysis assessing the determinants of preoperative NETest score.*

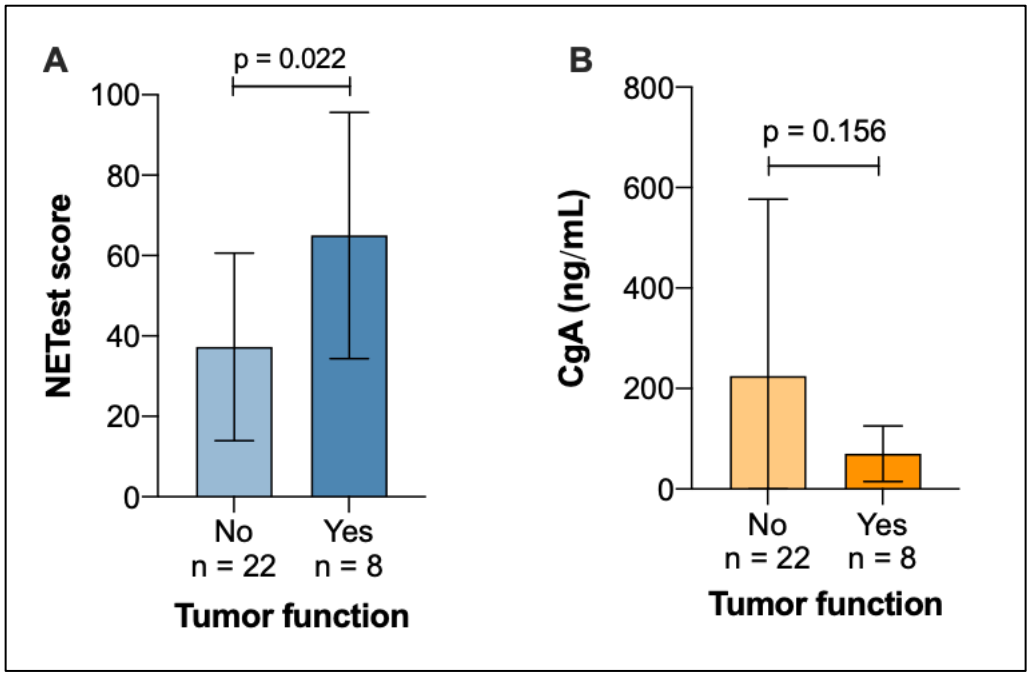
Variable	B value	95% CI	*p*
Gender			
Male	1	-	
Female	7.368	-14.447-29.183	0.495
Age	-0.093	-0.895-0.710	0.815
Function			
No	1	-	
Yes	27.727	6.289-49.165	**0.013**
Tumor size	-0.321	-1.112-0.470	0.412
Ki67 proliferative index	-0.510	-1.922-0.901	0.458
N stage*			
N0	1	-	
N1	5.111	-17.061-27.283	0.639

M stage*			
M0	1	-	
M1	-11.154	-42.042-19.734	0.466
Perineural invasion			
Absent	1	-	
Present	-8.571	-33.418-16.275	0.486
Microvascular invasion			
Absent	1	-	
Present	-8.444	-29.395-12.506	0.416
Necrosis			
Absent	1	-	
Present	-24.938	-58.934-9.058	0.144

*According to ENETS TNM staging system (Rindi *et al*, 2006)

The NETest score was significantly higher in patients with functioning tumors [65 (SD ± 31) *versus* 37 (SD ± 23], $p = 0.022$)] compared to patients with NF-PanNETs (**Figure 27A**). CgA plasma levels were similar between patients with functioning [70 ng/mL (SD ± 55 ng/mL)] or NF [225 ng/mL (SD ± 351 ng/mL)] neoplasms (**Figure 27B**).

Figure 27. *Comparison of preoperative NETest score (A) and CgA plasma levels between patients with functioning (n = 8) and non-functioning (n = 22) PanNETs.*



By univariate linear regression analysis, tumor function ($B = 37.460$, 95% CI: 3.488-71.433, $p = 0.032$) was the only variable significantly correlated with NETest change (preoperative – 30 days after surgery).

Discussion

Surgical management represents the only potentially curative option for PanNETs. Disease relapse during postoperative follow-up is key issue that affects significantly patients' outcome (Genç *et al*, 2018; Zaidi *et al*, 2019). The tools currently available for early identification of recurrent or residual disease are limited to high-quality imaging examinations or specific biomarkers in patients with functioning neoplasms (Falconi *et al*, 2016; Howe *et al*, 2020). However, morphological imaging has a limited discriminative power mainly related to the effects of tissue healing and possible fibrosis after surgery. Similarly, functional imaging (^{68}Gallium-DOTA PET/CT) has variable accuracy due to the presence of inflammatory cells expressing SSTRs (Bodei *et al*, 2017). For patients with functioning PanNETs, specific blood biomarkers are available (i.e. insulin) and an increase or decrease in their plasma levels is helpful in assessing the presence of residual/recurrent disease (Falconi *et al*, 2016). However, functioning tumors represent a small fraction of all PanNETs. Therefore, a general NET biomarker able to identify also the presence of non-functioning neoplasms is required (Öberg, 2021; Oberg *et al*, 2016).

In the precision medicine era, new attention has been drawn to the use of molecular tools such as liquid biopsies, in order to improve the management of cancer (Siravegna *et al*, 2017). Currently available biomarkers for NENs are monoanalytes (i.e. serotonin, gastrin, insulin, CgA) derived from tumors secretion.

Recently, a NET transcriptomic analysis (NETest) has been investigated as liquid biopsy for NETs (Modlin *et al*, 2013). NETest is a multianalyte biomarker assessing the expression of 51 NET gene transcripts. These transcripts are detected in blood samples and then algorithmically analyzed to obtain a signature which reflects the different biological aspects of the tumor. Therefore, the NETest, differently from CgA, is a multianalyte molecular signature encoding biological information which affect the disease course. The applications of this novel biomarkers have been documented in different settings, including diagnosis, identification of residual disease after surgical resection, assessment of disease status and treatment efficacy (Modlin *et al*, 2018; Frilling *et al*, 2021; Pavel *et al*, 2017). Previous studies have reported high accuracy, sensitivity and specificity of this biomarker for NET diagnosis (Filosso *et al*, 2018; Malczewska *et al*, 2019c). These metrics meet the NIH criteria to define an optimal diagnostic biomarker

(Oberg *et al*, 2015). Also, a correlation between NETest scores and evidence of neuroendocrine disease at imaging techniques has been reported (Modlin *et al*, 2014, 2021a). In this setting, a positive NETest might allow the early detection of disease recurrence, possibly preceding disease detection obtained through standard imaging modalities (Pavel *et al*, 2017). An independent validation of NETest in the setting of patients with surgically resected PanNETs is required. Therefore, we aimed at validating NETest as a diagnostic and disease status marker for patients who underwent surgery for PanNETs.

CgA represents the current default biomarker, despite having a limited role in the evaluation of surgical efficacy (Oberg *et al*, 2015). In the present experience, CgA did not correlate with disease status as it was preoperatively increased in less than one third of patients. After surgical resection, CgA plasma levels did not change significantly. Therefore, this biomarker did not provide any clinically relevant information for the assessment of surgical efficacy. On the other hand, NETest correlated with disease status as it was preoperatively positive in 100% of patients. Moreover, after surgical resection NETest scores significantly decreased. The postoperative fall of NETest scores is consistent with the primary tumor being the source of NET transcripts.

Consistently with the present findings, a previous experience investigating the use of NETest in patients undergoing surgery for GEP-NETs showed that NETest levels decreased after surgery and that the lack of NETest normalization was associated with radiological evidence of persistent or recurrent disease (Modlin *et al*, 2016b). Similar outcomes were reported also in a series evaluating the role of NETest after surgical resection of bronchopulmonary NETs (Filosso *et al*, 2018). The NETest increase was sometime evident prior to recurrent disease demonstration at imaging modalities (Modlin *et al*, 2016b). In some instances, NET relapse was histologically demonstrated when repeated imaging resulted negative despite repeated NETest elevation (Malczewska *et al*, 2019a).

In the present study, PanNET resection was associated with a relevant decrease of NETest scores in the majority of patients. In half of the study cohort, NETest scores returned to normal. Among the remaining half, twelve patients had a mildly increased POD 30 NETest level (mean 27), which might be an unspecific finding or indicate the presence of residual disease. However, three patients had a NETest score ≥ 40 on POD

30. Of these, one patient underwent a R2 resection (macroscopic residual disease) for a PanNET with nodal involvement and liver disease. This patient subsequently underwent adjuvant therapy with PRRT. The second patient had previously undergone neoadjuvant PRRT and was then submitted to R1 resection for a G1 PanNET staged as T1N0 at the final pathological examination. The third patient had a G2 tumor (Ki67 18%) with large nodal metastases. It is therefore likely that these patients either have residual disease or will experience disease recurrence during postoperative follow-up. Also, since two out of three underwent R1 and R2 resections, it can be hypothesized that NETest correctly identifies the presence of persisting disease.

The possible relevance of increased NETest in patients with negative imaging needs to be taken into account. It has been previously shown that NETest can identify the presence of neuroendocrine disease several months before radiological confirmation (Pavel *et al*, 2017). A series including 111 patients found that increased NETest levels had a high concordance with imaging findings (Malczewska *et al*, 2019c). Therefore, it might be speculated that elevated NETest scores at POD 30 could represent an early detection of a disease burden that is too small to be identified by imaging. Consistently, a previous report including 11 patients with metastatic NETs showed that half of histologically diagnosed neuroendocrine liver metastases were undetectable at preoperative imaging (Elias *et al*, 2010).

Overall, the present study indicates that the measurement of circulating NET transcript levels might improve the early detection of residual or recurrent disease (Modlin *et al*, 2016b). An early identification of disease relapse could facilitate personalized treatment schedules and allow to manage patients when the disease burden is lowest (Tie *et al*, 2016; Chaudhuri *et al*, 2017). Also, the postoperative follow-up schedule could be tailored considered also NETest scores. In this setting, it would be interesting to evaluate whether starting treatment at an earlier stage may be of benefit in terms of response and survival in patients with recurrent NETs.

Overall, the present data suggest that a blood-based multianalyte biomarker is accurate and provides data concordant with the intraoperative assessment of surgical efficacy. However, a prospective study with larger sample size and long-term follow-up is required to define the effectiveness of NETest in identifying relapse or progression after surgery.

Alterations in NETest levels do not correlate necessarily with the extent of resected disease, when examined as an aggregate. This reflects the fact that NETest measures a number of "omic indices" in each neoplasm. Different tumors show different levels of "omic clusters". Thus, in the present series functional neoplasms had an overall higher NETest as compared to non-functional lesions because genes involved in secretion regulation are significantly elevated in the functional group as compared to the non-functional one.

The present experience has several limitations that should be recognized. First, the study period was limited as only the first month after surgery was considered. Therefore, a further extension is now required in order to assess the relationship between increased postoperative NETest levels and disease recurrence as detected by imaging modalities. Second, it was not possible to assess the independent determinants of increased preoperative/postoperative NETest scores, due to the low number of patients included. Third, although NETest seems a promising biomarker for NETs, the main problem related to its applicability in the everyday clinical practice is represented by the need for a dedicated laboratory and a specialized statistical analysis in order to derive the scores and interpret them.

In conclusion, the present study shows that an effective surgical resection is followed by a decrease in NETest blood levels. Therefore, NETest seems able to provide a proper assessment of the early postoperative disease status in setting of PanNETs. An early detection of residual or recurrent disease might then be helpful for patients' treatment and increase the likelihood of obtaining a significant response. A multianalyte blood marker combined with imaging may therefore be employed as a clinical tool to improve the management of PanNETs, especially in terms of early identification of residual or recurrent disease.

Materials and Methods

Study Design

The present prospective monocentric study was reported according to the 2015 "Standards for Reporting Diagnostic accuracy studies" (STARD) guidelines (Bossuyt *et al*, 2015). The study was approved by the San Raffaele Hospital Ethical Committee (ClinicalTrials.gov ID: NCT03012789).

Patients

Between November 2017 and April 2018, patients diagnosed with functioning or non-functioning GEP-NETs who were candidates for surgical resection were enrolled if they met the following inclusion criteria: age > 18 years, pathologically confirmed diagnosis of GEP-NET, disease documentation in least one high-quality imaging technique, WHO status ≤ 2. Both treatment-naïve patients as well as those who underwent neoadjuvant therapies were included. Patients with history of HIV seropositivity were excluded. All the patients signed an informed consent. For the purpose of this study, only patients with a histological confirmation of PanNET were considered.

Test Methods

NETest was considered as the index test. CgA was considered as reference standard test as it is currently represents the best-described neuroendocrine biomarker (Falconi *et al*, 2016).

Regarding NETest, a 2-step protocol comprising RNA isolation, cDNA production and PCR was followed. Real-time PCR was performed (384-well plate, HT-7900 machine) with 200 ng/µl of cDNA and 16 µl of reagents per well (Fast Universal PCR master mix, Applied Biosystems®). All primers were exon spanning and were < 150 bprs. PCR values were normalized to house-keeping genes and expression was quantified against a control population (calibrator sample) (Modlin *et al*, 2013). Thereafter, multianalyte algorithm analyses were performed. The final gene expression results were reported as an activity index score ranging from 0 to 100 (Kidd *et al*, 2015), based on the integration of the majority vote and summated expression of five gene clusters including epigenome, growth factor signalome, proliferome and genes involved in pluripotency (Kidd *et al*, 2015). A normal NETest score was defined for values ≤ 20 (van Treijen *et al*, 2018), as clinical assessment demonstrated that any value > 20 represents neuroendocrine disease. Values between 20-40 define low activity disease. Values > 40 represent progressive disease. Values > 80 correspond to highly progressive disease (Liu *et al*, 2019; Pavel *et al*, 2017). CgA was measured using the NEOLISA assay (Eurodiagnostica®). The upper limit of normal was 108 ng/mL.

All blood samples were deidentified to the laboratory group. Results of the index test (NETest) and those of the reference standard test (CgA) were available to the laboratory group (Wren Laboratories®), whereas clinical information was available only to the

clinical study group and not to performers and readers of both index and reference standard tests.

Samples and data collection

Venous whole blood samples were collected in 5 mL EDTA tubes. Two 5 mL blood samples were obtained at the same time before surgery, on POD 1, POD 5 and POD 30. After collection of blood samples, one EDTA tube (whole blood for NETest) was frozen in -80°C refrigerator, whereas the second EDTA tube was spun for 10 minutes and then plasma was frozen in the -80°C refrigerator. All samples were deidentified and then sent by courier on dry ice, for measurement, to Wren Laboratories LLC®.

A prospectively collected database was queried for all clinical and pathological characteristics. The initial diagnostic workup always included at least one high-quality imaging examination (CT or MRI) and it was always completed either with ^{68}Gallium-DOTA PET/CT or with endoscopic ultrasound with fine needle aspirate. ^{18}F-FDG PET/CT was not routinely performed as is it not recommended in patients with well-differentiated NETs. All the patients were treated with PPI for at least 30 days after surgery.

Preoperative variables that were considered include: gender, age, abdominal pain, jaundice, BMI, type of diagnosis, tumor function, radiological tumor diameter and ^{68}Gallium and ^{18}F-FDG PET/CT findings. The surgical procedure was planned according to site and size of the neoplasm. Postoperative surgical complications were graded according to the Dindo-Clavien classification of surgical complications (Dindo *et al*, 2004). Tumor size was defined as the maximum tumor diameter as measured in the pathological specimen. T, N, M stages were classified according to the current ENETS classification (Rindi *et al*, 2006). Immunostaining routinely included synaptophysin, CgA and Ki67 proliferative index, which was assessed by MIB1 antibody staining and expressed as % of cells with positive nuclear staining in 2000 cells counted in the area of highest nuclear labelling (Lloyd RV *et al*, 2017). Tumor grade was classified according to the 2017 WHO classification as G1 (Ki67 < 3%) and G2 (Ki67 3-20%) (Lloyd RV *et al*, 2017). Surgical margins status was defined as: R0 (no residual tumour), R1 (microscopic residual tumour), R2 (macroscopic residual tumour). The presence of necrosis, microvascular invasion and perineural invasion was also assessed.

Statistical Analysis

Continuous variables were reported as mean and standard deviation (± SD). For categorical variables, number and proportion (%) were displayed. The comparison of continuous variables between groups was performed using Student's t test, or Mann-Whitney U test, as appropriate based on variables distribution. Paired t-test or Wilcoxon signed-rank test were employed to compare preoperative and postoperative test methods measurements before and after surgery. Qualitative data were compared by Chi square test or Fisher exact test, as appropriate based on expected cell counts. The relationship between continuous variables was assessed by univariate linear regression analysis. Statistical analyses were performed using SPSS 25.0 for Mac software (SPSS Inc, Chicago, IL, USA). *P* values were considered significant when less or equal than 0.05.

Aim 5 – To investigate the biological role of CgA and CgA-derived fragments in PanNENs, by assessing the site of production and cleavage using *in vitro* models and evaluating the relationship between their tissue expression, MVD and other immunohistochemical markers.

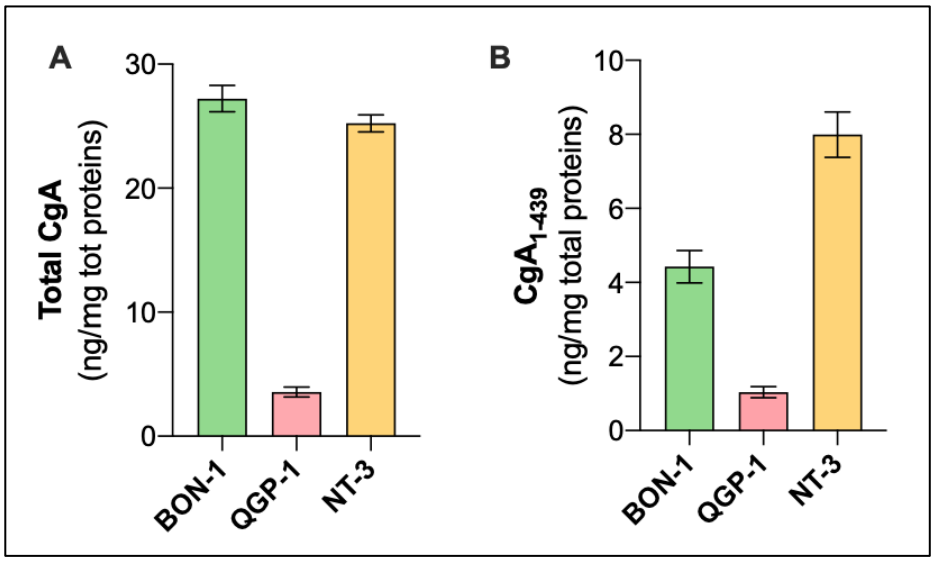
Results

PanNEN cell lines and patient-derived islet-like tumoroids produce and secrete CgA and CgA-derived fragments

The site of production and secretion of CgA and CgA-derived fragments was investigated using PanNEN cell lines (BON-1, QGP-1, NT-3) and patient-derived islet-like tumoroids (n = 18).

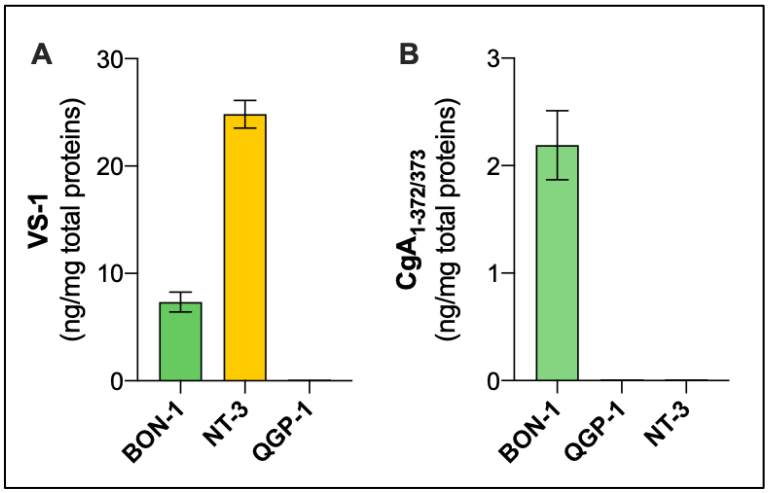
Total-CgA, full-length CgA ($CgA_{1\text{-}439}$), VS-1 ($CgA_{1\text{-}76}$) and $CgA_{1\text{-}372/373}$ were measured in the cell lysate of PanNEN cell lines using specific immunoassays (ELISAs). The mean amount of total-CgA measured in QGP-1 cell lysate was 3.2 (± 0.4) ng/mg of total proteins, compared with 27.2 (± 1.1) ng/mg of total proteins in BON-1 and 25.3 (± 0.7) ng/mg of total proteins in NT-3 cell lysates (**Figure 28A**). Similarly, the amount of full-length CgA was higher in BON-1 and NT-3 cell lysates as compared with QGP-1 lysate (**Figure 28B**).

Figure 28. *Total-CgA and full-length CgA measurement in cell lysate from BON-1, QGP-1 and NT-3. Concentrations are normalized to the amount of total proteins measured in each cell lysate sample.*



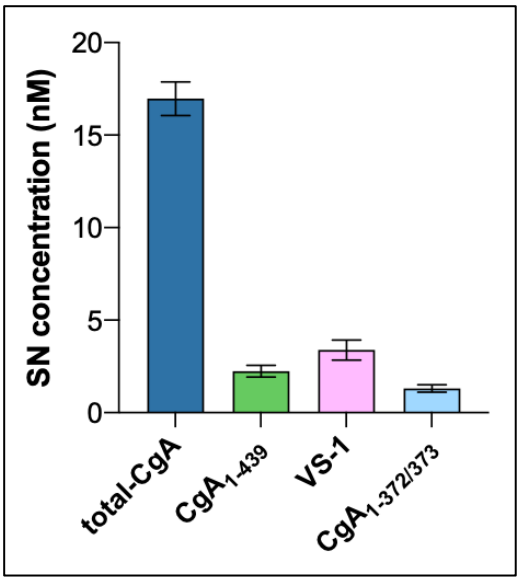
NT-3 was identified as the PanNEN cell line with the highest amount of VS-1 in the lysate (24.8 ± 1.3 ng/mg total proteins) (**Figure 29A**). On the other hand, BON-1 was the only cell line with a detectable, even if low, quantity of $CgA_{1\text{-}372/373}$ in the cell lysate (2.2 ± 0.3 ng/mg total proteins) (**Figure 29B**).

Figure 29. *VS-1 and $CgA_{1\text{-}372/373}$ measurement in cell lysate from BON-1, QGP-1 and NT-3. Concentrations are normalized to the amount of total proteins measured in each cell lysate sample.*



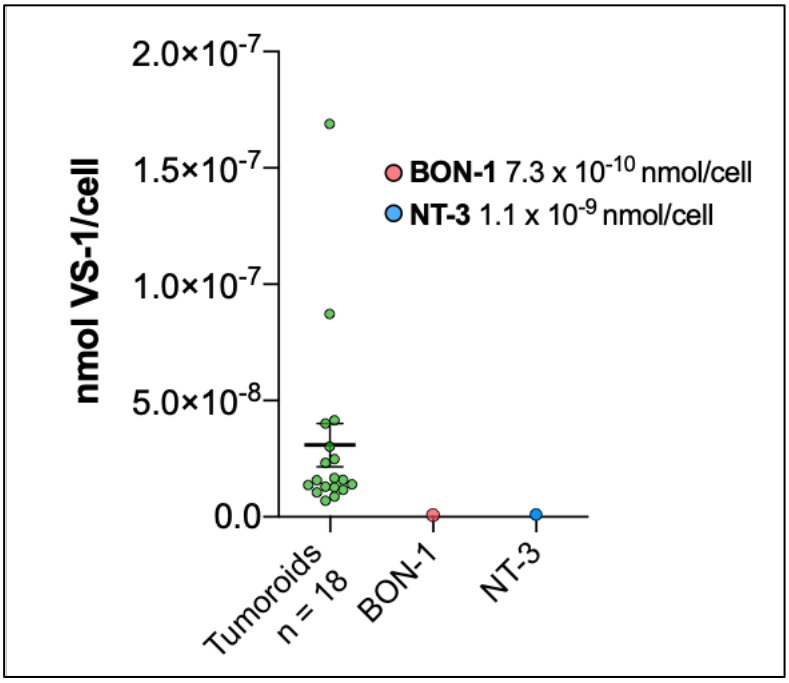
Similar findings were obtained when CgA and CgA-derived fragments were measured in the supernatant (SN) of PanNEN cell lines. CgA-derived fragments were undetectable in QGP-1 SN. VS-1 was measurable in BON-1 and NT-3 SNs, whereas $CgA_{1\text{-}373}$ could be measured in BON-1 SN only (**Figure 30**).

Figure 30. *CgA and CgA-derived fragments measurement in BON-1 supernatant.*



Finally, VS-1 was measured in the SN of patient-derived islet-like tumoroids. VS-1 could be detected in all the samples (n = 18), with concentrations that were approximately 1 and 2 orders of magnitude higher than those measured in NT-3 and BON-1 SN, respectively (**Figure 31**).

Figure 31. *VS-1 measurement in tumoroids, BON-1 and NT-3 supernatant (normalized to the number of plated cells)*



These findings demonstrate that CgA-derived fragments (i.e. VS-1, $CgA_{1\text{-}372/373}$) are produced and secreted from neuroendocrine tumor cells.

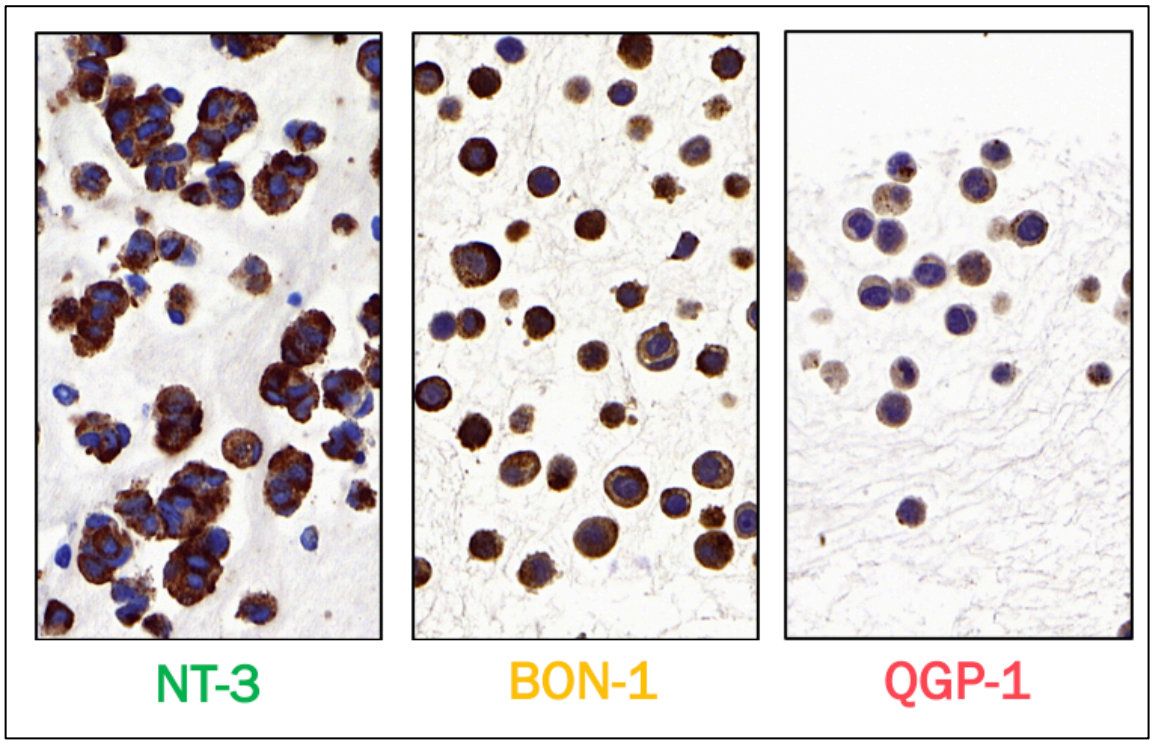
Immunohistochemistry set-up and scoring for CgA and CgA-derived fragments

Based on the observations that PanNEN cell lines produce different amounts of CgA/CgA-derived fragments and that CgA cleavage occurs within neuroendocrine tumor cells, we decided to set-up immunohistochemistry (IHC) for these peptides. In particular, we mainly focused on VS-1 given its promising role as biomarker in the clinical practice.

We established IHC for CgA and CgA-derived fragments using the antibodies previously used for ELISAs (i.e. anti-VS-1, anti-$CgA_{1\text{-}372/373}$, anti-total-CgA and anti-$CgA_{1\text{-}439}$). To do so, we first stained a tissue microarray (TMA) including on BON-1, NT-3 and QGP-1 cell blocks. Consistently with previous observations obtained on cell lysates, different levels of staining positivity were observed between the three cell lines.

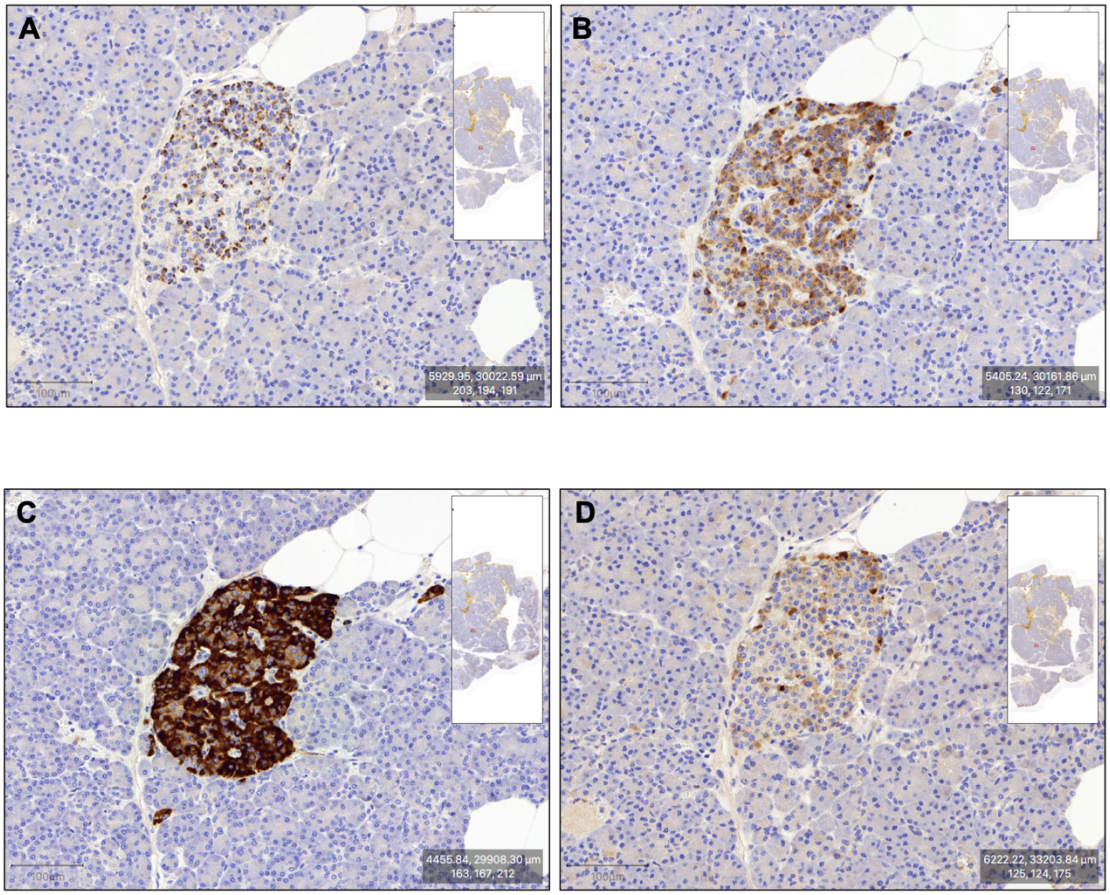
An example of VS-1 IHC staining on NT-3, BON-1 and QGP-1 cell blocks is shown in **Figure 32**.

Figure 32. *VS-1 staining of NT-3, BON-1 and QGP-1 cell blocks.*



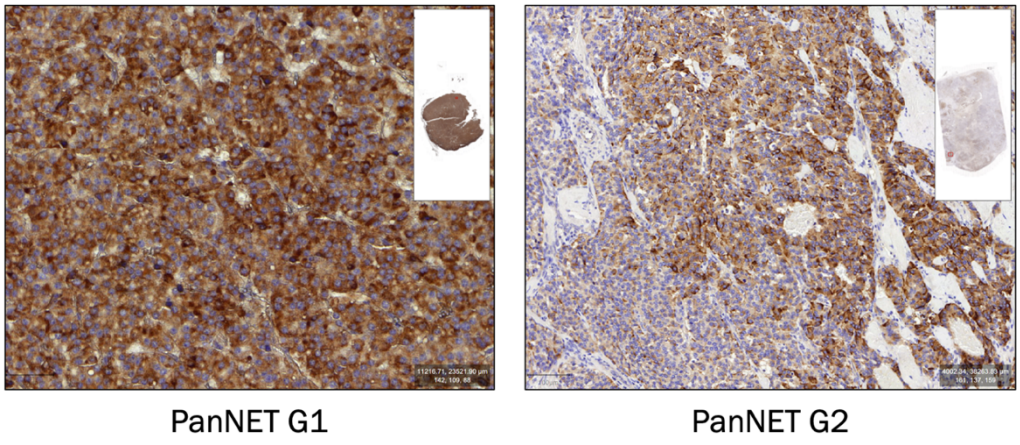
Additionally, we tested the antibodies for CgA and CgA-derived fragments on normal pancreatic tissue (obtained from patients who underwent surgery for other than PanNET diagnosis). We observed that the pancreatic endocrine component, represented by the islets of Langerhans, was selectively stained and no staining positivity was detected in the remaining pancreatic parenchyma. These data indicate that these antibodies are specific for the detection of neuroendocrine cells, thus suggesting specificity for their target (i.e. CgA and CgA-derived fragments). Based on the staining of cell blocks and normal pancreatic tissue, total-CgA and VS-1 were identified as the most abundant CgA isoforms. Consistently, previous data have demonstrated that CgA circulating pool in normal subjects is heterogeneous and mainly consists of fragments lacking part of or the entire C-terminal region (which are comprised in total-CgA). Also, VS-1 can be measured in the normal plasma at a biologically relevant level. On the other hand, full-length CgA and $CgA_{1\text{-}372/373}$ were identified as the least represent isoforms in normal plasma as well as in the IHC of cell blocks and normal pancreatic tissue.

***Figure 33**. Stainings for full-length CgA (A), total-CgA (B), VS-1 (C) and $CgA_{1\text{-}372/373}$ on normal islets.*



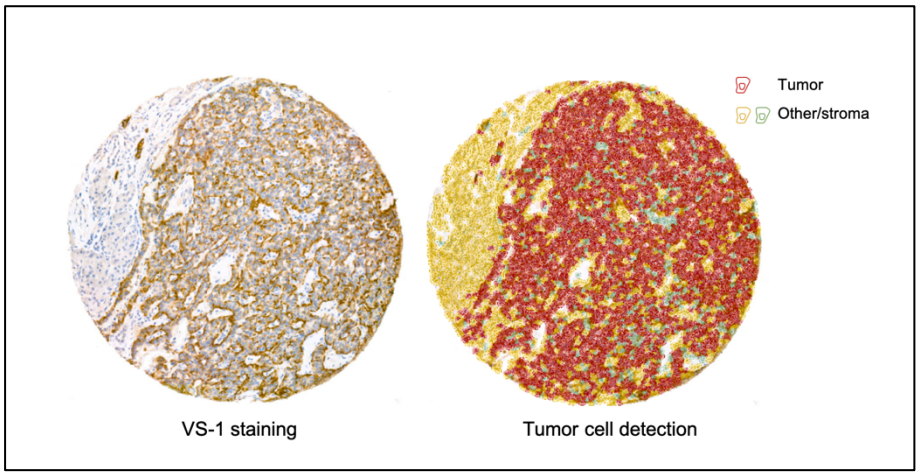
Finally, we tested the antibodies on PanNET samples. Two PanNET samples (G1 and G2) were used for this pilot staining and showed different levels of IHC positivity (**Figure 34**), thus suggesting that tissue expression of CgA and CgA-derived fragments might vary according to the biology of the tumor.

Figure 34. *VS-1 staining of two PanNET samples showing different levels of positivity.*



Once we have established the IHC, the expression of the different CgA isoforms was assessed on 62 PanNET samples (included in TMAs) from patients who underwent surgery for sporadic NF-PanNETs. The stainings were scored using QuPath software (open source software for digital pathology image analysis) (Bankhead *et al*, 2017). First, neuroendocrine tumor cells were detected through a detection classifier created by annotating examples of each detection (i.e. tumor cells, stroma, other) (**Figure 35**).

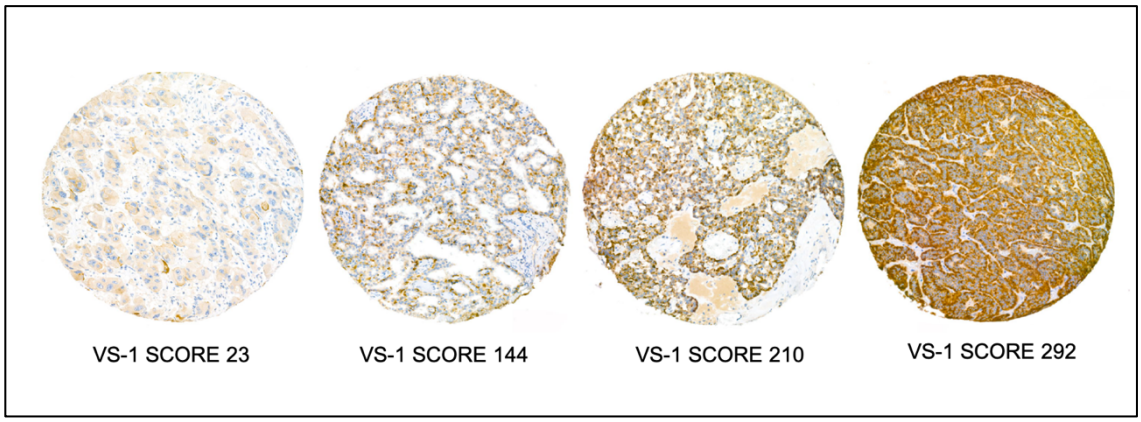
Figure 35. *Example of tumor cell detection using a digital pathology software.*



Finally, the intensity of the staining was classified by using the maximum cytoplasm optical density, with three thresholds to define negative (0), weakly positive (1+), moderately positive (2+) and strongly positive (3+) tumor cells.

The scoring for VS-1 (and other CgA-derived fragments) was then calculated as follows: (0 * % negative tumor cells + 1 * % weakly positive tumor cells + 2 * % moderately positive tumor cells + 3 * % strongly positive tumor cells). This score ranges between 0 (all tumor cells are negative) and 300 (all tumor cells are strongly positive). Examples of increasing VS-1 scores are depicted in **Figure 36**.

Figure 36. *PanNET samples showing increasing VS-1 histological scores.*



Correlation between pathological features and histological scores

Overall, 62 patients submitted to surgery for NF-PanNETs were considered. Clinico-pathological features of these patients are reported in **Table 15**.

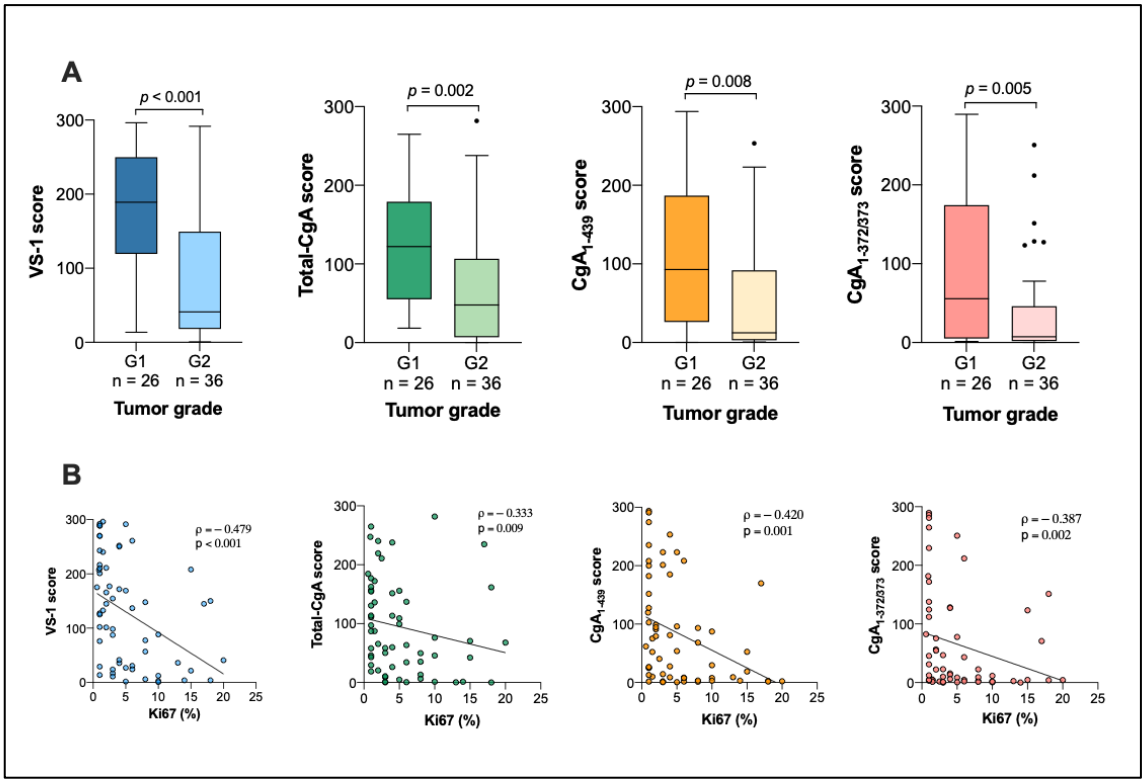
Table 15. *Clinico-pathological features of 62 patients who underwent surgical resection for NF-PanNETs.*

Variable	***n 62 (%)***
Gender	
Male	25 (40)
Female	37 (60)
Age, years*	57 (49-64)
Tumor size, mm*	30 (22-39)
T stage†	
T1-T2	43 (69)
T3-T4	19 (31)
N stage†	
N0	37 (60)
N1	23 (37)
Nx	2 (3)
M stage†	
M0	57 (92)
M1	5 (8)
Ki67 proliferative index, %*	3.5 (1-8)
Tumor grade°	
G1	26 (42)
G2	36 (58)
DAXX/ATRX status	
Preserved	42 (68)
Lost	20 (32)
MVD, n/mm^2*	161 (105-288)
CA-9	
Negative	50 (81)
Positive	12 (19)

*Expressed as median (interquartile range)
†According to ENETS TNM staging system (Rindi *et al*, 2006)
°According to 2017 WHO classification (Lloyd, RV et al, 2017)

Patients with G2 PanNETs showed lower VS-1, total-CgA, full-length CgA and $CgA_{1-372/373}$ histological scores as compared to patients with G1 PanNETs, as reported in **Figure 37A**. Also, negative correlations between CgA/CgA-derived fragments histological scores and Ki67 proliferative index were found, as shown in **Figure 37B**.

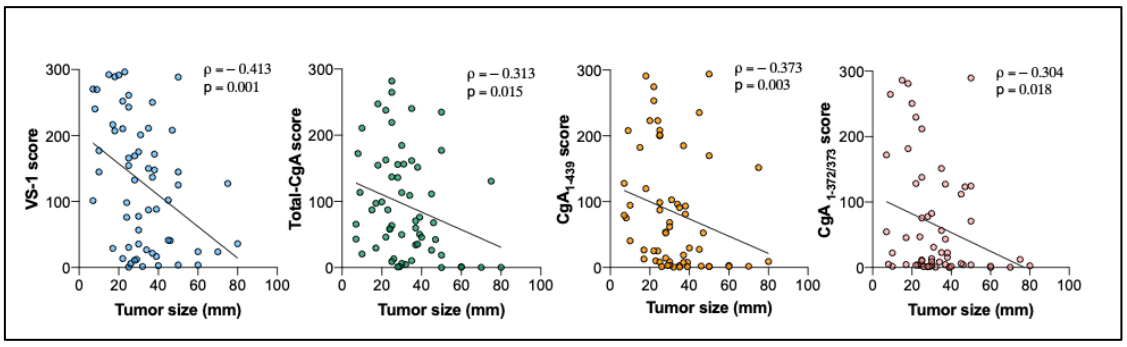
Figure 37. *A) Comparison of CgA and CgA-derived fragments histological scores according to tumor grade. B) Spearman correlation between histological scores and Ki67 proliferative index.*



VS-1 histological score showed the strongest negative correlation with Ki67 proliferative index ($\rho = -0.479$, $p < 0.001$).

CgA and CgA-derived fragments histological scores were negatively correlated also with tumor size (**Figure 38**). VS-1 histological score showed the strongest negative correlation with histological tumor diameter ($\rho = -0.413$, $p = 0.001$).

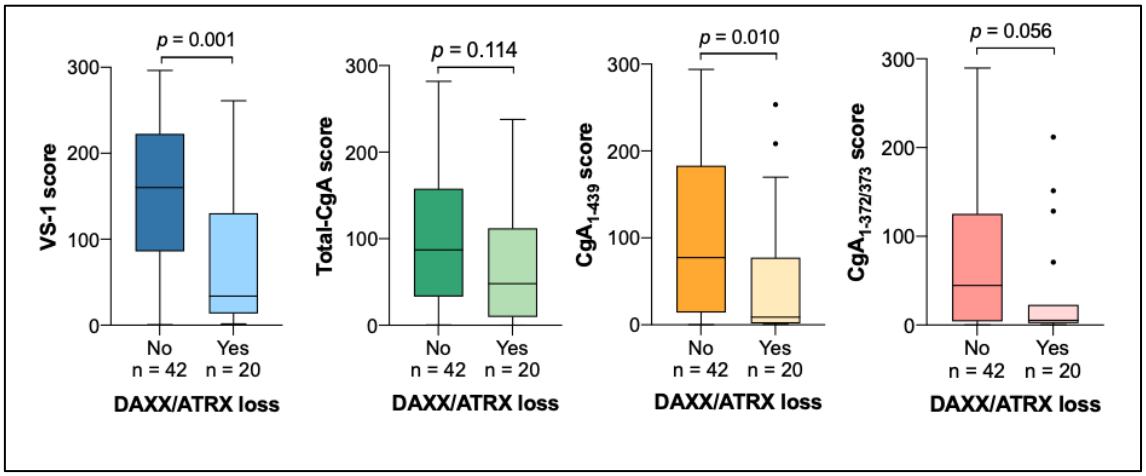
Figure 38. *Spearman correlation between histological scores and tumor size.*



Finally, VS-1 ($p = 0.001$) and full-length CgA ($p = 0.010$) histological scores were significantly lower in patients with DAXX and/or ATRX loss as compared to the

remaining subjects (**Figure 39**). No statistically significant differences were observed for total-CgA and $CgA_{1\text{-}372/373}$ histological scores according to DAXX/ATRX status.

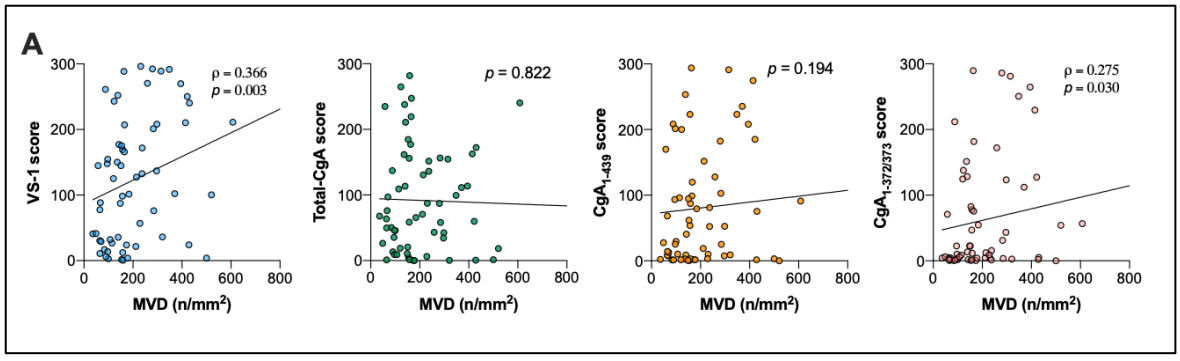
Figure 39. *Comparison of CgA and CgA-derived fragments histological scores according to DAXX/ATRX status.*

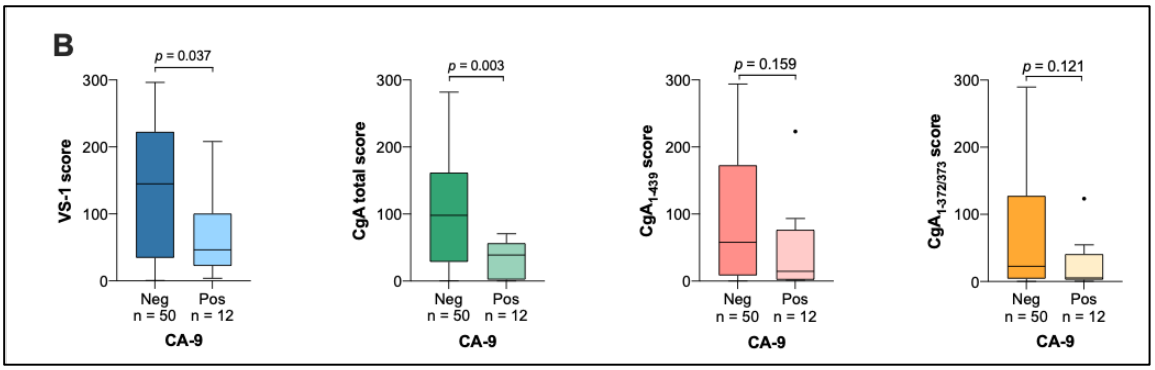


Correlation with MVD and hypoxia marker CA-9

Given the role of CgA and CgA-derived fragments in the process of angiogenesis, the relationship between their tissue expression in PanNETs, MVD and hypoxia marker CA-9 was assessed. A positive correlation between MVD and increasing VS-1 histological score was observed ($\rho = 0.366$, $p = 0.003$). A weaker, but significant, positive correlation was found also between MVD and $CgA_{1\text{-}372/373}$ score ($\rho = 0.275$, $p = 0.030$). Total-CgA and full-length CgA histological scores showed a trend toward a positive correlation with MVD but it was not statistically significant (**Figure 40A**). Consistently with these findings, patients with hypoxic tumors (CA-9 +) showed lower CgA and CgA-derived fragments histological scores (**Figure 40B**).

Figure 40. *Correlation between CgA and CgA-derived fragments histological scores, MVD (A) and hypoxia marker CA-9 (B).*

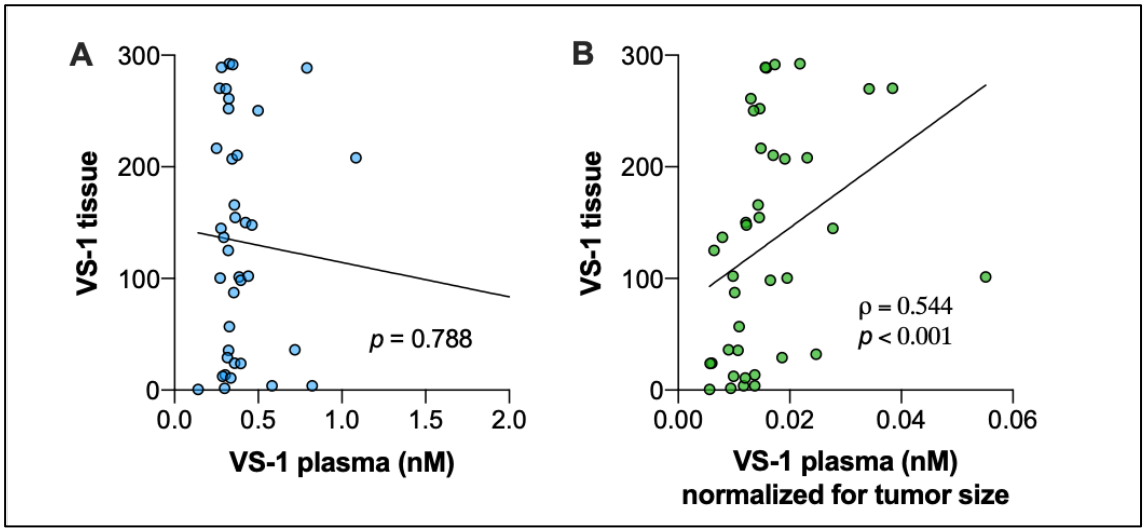




Correlation between plasma and tissue levels of VS-1

Overall, 39 patients had available plasma and tissue levels of VS-1. No statistically significant correlation was found between plasma and tissue levels of VS-1 ($p = 0.788$). However, when VS-1 plasma levels were corrected for tumor size, a statistically significant positive correlation between plasma and tissue levels was observed (**Figure 41**). Therefore, it seems that circulating VS-1 values are strictly dependent on tumor burden, rather than on other features of disease aggressiveness.

Figure 41. *Correlation between VS-1 plasma and tissue levels, before (A) and after (B) normalization of VS-1 plasma levels for tumor size.*



Determinants of VS-1 tissue score and plasma levels

By multivariate linear regression analysis, tumor size ($B = –1.29$, 95% CI –2.38;–0.09, $p = 0.035$), Ki67 proliferative index ($B = –6.55$, 95% CI –11.43;–1.68, $p = 0.009$) and MVD ($B = 0.17$, 95% CI 0.04;0.29, $p = 0.009$) were identified as independent determinants of VS-1 histological scores. Specifically, larger tumors with higher Ki67

proliferative index show lower VS-1 tissue expression. On the other hand, well-differentiated tumors with high MVD display a higher VS-1 tissue score (**Table 16**).

Table 16. *Univariate and multivariate analysis investigating determinants of VS-1 histological scores.*

	Univariate analysis			Multivariate analysis		
Variables	**B**	**95% CI**	***p***	**B**	**95% CI**	***p***
Gender (female *vs.* male)	-14.79	-65.15;34.57	0.559			
Age, years	-0.54	-1.30;2.37	0.560			
Tumor size, mm	-1.60	-2.81;-0.40	**0.010**	-1.29	-2.38;-0.09	**0.035**
Ki67, %	-6.84	-11.44;-2.23	**0.004**	-6.55	-11.43;-1.68	**0.009**
N stage (N1 *vs.* N0)	-33.23	-85.50;-19.04	0.208			
M stage (M1 *vs.* M0)	-69.02	-159.30;21.25	0.131			
DAXX/ATRX loss	-94.65	-145.07;44.23	**<0.001**	–	–	–
MVD, n/mm^2	0.18	0.05;0.32	**0.010**	0.17	0.04;0.29	**0.009**
CA-9 (pos *vs.* neg)	-71.27	-130.94;-1.60	**0.024**	–	–	–

On the other hand, tumor size was identified as the only independent determinant of circulating VS-1 plasma levels (B = 0.015, 95% CI 0.011-0.020, $p < 0.001$) (**Table 17**).

Table 17. *Univariate and multivariate analysis investigating determinants of VS-1 histological scores.*

	Univariate analysis			Multivariate analysis		
Variables	**B**	**95% CI**	***p***	**B**	**95% CI**	***p***
Gender (female *vs.* male)	0.125	-0.167;-0.416	0.391			
Age, years	0.02	-0.010;0.015	0.715			
Tumor size, mm	0.015	0.011;0.020	**<0.001**	0.015	0.011;0.020	**<0.001**
Ki67, %	0.016	-0.014;0.046	0.285			
N stage (N1 *vs.* N0)	0.058	-0.244;-0.360	0.699			
DAXX/ATRX loss	0.270	-0.055;0.594	0.101			
MVD, n/mm^2	0.000	-0.001;0.001	0.593			
CA-9 (pos *vs.* neg)	0.450	0.134;0.765	**0.006**	–	–	–

Therefore, VS-1 tissue expression seems to depend on tumor cell differentiation (i.e. Ki67, MVD, size), whereas VS-1 plasma level mainly depends on tumor size, which is an accurate surrogate for tumor burden in patients with localized PanNETs.

Discussion

CgA is a well-known marker of endocrine differentiation and currently represents the most used circulating biomarker for NENs. Fragments derived from CgA cleavage have been recently investigated as NET biomarkers (i.e. VS-1, PST), showing promising results (Corsello *et al*, 2018; Andreasi *et al*, 2019; Woltering *et al*, 2019). However, little is known regarding the site of production of these fragments as well as regarding their biological role in the specific setting of PanNENs.

Our group has previously demonstrated the role of CgA-derived fragments in the process of angiogenesis, highlighting the presence of both proangiogenic (i.e. $CgA_{1\text{-}373}$) and antiangiogenic (i.e. VS-1, full-length CgA) factors in several *in vitro* and *in vivo* assays (Veschini *et al*, 2011; Corti *et al*, 2018; Dallatomasina *et al*, 2019). Vascular biology is a crucial aspect in PanNENs, as these neoplasms are highly vascularized as compared with other solid tumors. Also, tumor MVD is a recognized marker of disease aggressiveness and prognosis in patients affected by PanNENs, with low MVD being associated with poorer oncological outcomes (Marion-Audibert *et al*, 2003; Couvelard *et al*, 2005). Therefore, given the involvement of CgA system in tumor vascular biology and the importance of this aspect in NENs, we decided to study the role of CgA-derived fragments in PanNENs, by assessing their site of production, using *in vitro* models, and by correlating their tissue expression with MVD and other markers of aggressiveness.

The present findings show that CgA proteolytic cleavage occurs within the neuroendocrine tumor cells. In this regard, we observed that total-CgA, full-length CgA as well as fragments VS-1 and $CgA_{1\text{-}372/373}$ could be detected not only in cell lines supernatant but also in cell lysate. BON-1, QGP-1 and NT-3 showed different levels of CgA and CgA-derived fragments production and secretion. In particular, QGP-1 had the lowest amount of total-CgA and full-length CgA, whereas neither VS-1 or $CgA_{1\text{-}372/373}$ could be detected in QGP-1 lysate and supernatant. Consistently, a previous study showed that QGP-1 had the lowest mRNA expression of CgA as compared to both BON-1 and NT-3 (Benten *et al*, 2018). Also, QGP-1 stained very weakly for CgA on immunofluorescence (Benten *et al*, 2018). On the other hand, the present data show that NT-3 had the highest level of both full-length CgA and VS-1. This finding is consistent with previous observations reporting a higher expression of neuroendocrine markers (CgA, synaptophysin) in NT-3 as compared with QGP-1 and BON-1 (Benten *et al*, 2018).

The higher neuroendocrine differentiation observed for NT-3 mainly depends on the fact that this cell line derives from a metastatic lymph node of a patient with a well differentiated PanNET (Ki67 15-20%) (Benten *et al*, 2018). Differently, both QGP-1 and BON-1 do not display a well differentiated phenotype, being more similar to poorly differentiated PanNECs (Ki67 >80%) and harbouring mutations (i.e. *TP53*, *RAS*) that are rarely present in PanNETs (Vandamme *et al*, 2015). Therefore, both these cell lines are not good models for slow-growing PanNETs. Finally, we were also able to measure VS-1 in the supernatant of patient-derived islet-like tumoroids, which represent the most reliable *in vitro* model currently available for well differentiated slow-growing PanNETs (April-Monn *et al*, 2020).

Considering CgA cleavage, we observed that $CgA_{1\text{-}372/373}$, which is a product of CgA C-terminal fragmentation, could be detected only in BON-1 lysate and supernatant. On the other hand, VS-1, which derives from CgA N-terminal fragmentation, could be measured in both BON-1 and NT-3, with a higher amount observed in the latter cell line. In this regard, Corsello et al. previously hypothesized that CgA proteolytic cleavage in well differentiated NENs is altered towards the production of the N-terminal peptide VS-1 (Corsello *et al*, 2018). Therefore, the higher VS-1 amount hereby observed for NT-3 might support the hypothesis that CgA N-terminal cleavage is enhanced in well differentiated PanNETs. On the other hand, one might speculate that in the presence of poorly differentiated neoplasms (i.e. BON-1) CgA fragmentation in the C-terminal region is more represented. Of note, our group has shown that PDAC cells can promote C-terminal CgA fragmentation through the activation of plasminogen to plasmin and that this kind of cleavage is associated with worse survival outcomes (Reni *et al*, 2020).

After having demonstrated that CgA cleavage occurs within neuroendocrine tumor cells, immunohistochemistry for CgA and CgA-derived fragments was set up and stainings were scored using a digital pathology software. Overall, we observed that a higher tissue expression of CgA and CgA-derived fragments, especially VS-1, was associated with a more benign biological behaviour of PanNETs (i.e. lower Ki67 proliferative index, smaller tumor size, DAXX/ATRX preserved). Also, a correlation between MVD and VS-1 tissue level was observed, with higher MVD values being associated with higher VS-1 histological scores. On the other hand, the presence of positive CA-9 was associated with lower VS-1 tissue expression.

These findings are apparently in contrast with previous results showing an association between increased VS-1 plasma values and presence of tumor features of aggressiveness (Andreasi *et al*, 2019). For this reason, the correlation between VS-1 plasma levels and VS-1 histological scores was assessed. At first, no correlation between plasma and tissue values was found. However, when plasma levels were corrected for PanNET size, a positive correlation between VS-1 plasma and tissue levels was observed. Tumor size was then identified as the main determinant of VS-1 plasma levels. On the other hand, tumor differentiation was identified as the main determinant of VS-1 tissue level, as expressed by the correlation with MVD and Ki67 proliferative index.

The present data confirm the role of VS-1 as biomarker, given its strong relationship with tumor size and consequently with tumor burden. Also, VS-1 tissue level was identified as a marker of tumor differentiation, as its decreased expression indicated a higher disease aggressiveness in PanNET samples. This result was supported also by data obtained on cell lines, as NT-3, which is the most well differentiated cell line, showed the highest VS-1 level. Therefore, all these observations seem to point towards a role of VS-1 as a marker of differentiation in the setting of PanNENs.

No significant differences between VS-1 and other fragments were observed in terms of correlation with MVD and hypoxia marker CA-9. However, the role of CgA and CgA-derived fragments in PanNEN vascular biology cannot be excluded, as the proangiogenic *versus* antiangiogenic activity of these peptides has been clearly demonstrated in different settings (Dallatomasina *et al*, 2019; Corti *et al*, 2018; Bianco *et al*, 2016b). Of note, the present observations are based IHC, which has the relevant limitation of being a semiquantitative technique. In this study, a continuous score based on the percentage of positive tumor cells and on staining intensity was calculated. However, ratios between CgA and CgA-derived fragments histological scores (i.e. VS-1/total-CgA, $CgA_{1\text{-}372/373}$/total-CgA) could not be assessed and correlated with MVD, given the intrinsic qualitative/semiquantitative nature of IHC. Therefore, further investigation of CgA-derived fragments role, by using a quantitative technique to measure these peptides on tumor tissue, is warranted in order to obtain firm conclusions regarding their involvement in PanNEN vascular biology.

Materials and methods

Patients

Patients' characteristics are reported in **Table 15**. All patient material was used in accordance with the human research act and all the patients signed an institutional broad consent. IHC was performed on PanNET next-generation TMAs including 50 patients who were submitted to surgery at IRCCS San Raffaele Hospital between 2015 and 2018 and additional 12 patients who underwent surgery at the Inselspital, Bern, Switzerland between 2014 and 2018.

Cell culture

BON-1, QGP-1 and NT-3 cell lines were cultured at Bern Institute of Pathology (Switzerland). QGP-1 and NT-3 were cultured in RPMI 1640 medium (Sigma), whereas BON-1 were cultured in DMEM/F12 medium (Sigma). For all cell lines, the medium was supplemented with 100 IU/mL penicillin, 10% FBS, and 0.1 mg/mL streptomycin, and cells were kept in a humidified incubator (5% CO2, 37°C). For NT-3, cell culture flasks were coated with collagen IV in order to achieve better attachment. Growth factors FGF-2 (Gibco PHG0024) and EGF (Gibco PHG0314) were added to NT-3 growth medium. After thawing, cells were cultured for approximately two months.

Cell lysis

Cell lysates were obtained using radioimmunoprecipitation assay (RIPA) buffer, protein concentrations were measured using Bradford assay. Briefly, cell pellets were resuspended in RIPA buffer (150 mM NaCl, 1% Triton X-100, 0.5% sodium deoxycholate, 0.1% SDS, 50 mM Tris pH 8.0, protease inhibitor – 1 tablet per 50 mL) and gently vortexed. The lysate was then sonicated for 0.2 seconds at 40% amplitude (for 3 times) and subsequently centrifuged at 4°C for 15 minutes at 14'000 rpm. Supernatant was collected and protein concentration was measured using Bradford assay. After protein measurement, ELISAs to measure CgA and CgA-derived fragments were performed.

Patient-derived islet-like tumoroids

Primary PanNEN cells were isolated as previously described (April-Monn *et al*, 2020). Isolated primary PanNET cells were maintained in AdvDMEM + GF medium (DMEM-F12, Hepes 10 mM, 5% FBS, 1% L-glutamine (200 mM), 1% penicillin (100 IU/mL),

1% streptomycin (0.1 mg/mL), 1% amphotericin B (0.25 mg/mL) (Merck, Switzerland), 20 ng/mL EGF, 10 ng/mL bFGF, 100 ng/mL PlGF, 769 ng/mL IGF-1) and in 24-well ultra-low attachment plates (Corning, USA) (500 µL/well, 3–5 × 10^5 cells/well) in a humidified cell incubator (21% O2, 5% CO2, 37°C) (April-Monn *et al*, 2020). Supernatant was collected after 15 days from cells plating.

CgA and CgA-derived fragments immunoassays

Total-CgA, full-length CgA (CgA_{1-439}), VS-1 (CgA_{1-76}) and $CgA_{1-372/373}$ were measured in cell lysate, cell supernatant and plasma by using four sandwich ELISAs against different CgA epitopes. Monoclonal antibodies (mAb) B4E11 (against CgA_{68-71}) and 5A8 (against CgA_{54-57}) were used as capturing antibodies (Corti *et al*, 1996). Polyclonal antisera α-76 (against human CgA_{71-76}), α-373 (against human $CgA_{368-373}$), α-439 (against human $CgA_{434-439}$) and α-FRs (against several epitopes in human CgA central region) were raised in rabbits and used as detecting antibodies. Briefly, α-76 binds CgA_{1-76}, but not larger fragments; α-373 binds $CgA_{1-372/373}$, but not larger fragments; α-439 binds only full-length CgA_{1-439}; α-FRs recognizes full-length CgA plus several fragments containing the N-terminal region and all or part of the central region, but not VS-1 (Bianco *et al*, 2016b; Dallatomasina *et al*, 2019).

Immunohistochemistry

2.5 µm sections from next generation TMAs were used for IHC. The immunostainings for all antigens were performed on an automated staining system (Leica Bond RX; Leica Biosystems, Nunningen, Switzerland). The following antibodies were used: CA-9 antibody (1:1500, Abcam, ab15086), CD34 class II antibody (1:100, Dako, M7165), anti-DAXX (1:40, polyclonal rabbit, Sigma), anti-ATRX (1:400, polyclonal rabbit, Sigma). Rabbit polyclonal antibodies described for ELISAs (α -76 1:10000, α-373 1:200, α-439 1:400, and α-FRs 1:1000) were used for VS-1, $CgA_{1-372/373}$, full-length CgA and total-CgA IHC staining, respectively. Antigen retrieval for VS-1 was performed by heating citrate buffer at 95° for 20 minutes. Antigen retrieval for CA-9, CD34, CgA_{1-439} and $CgA_{1-372/373}$ was performed by heating Tris buffer at 95° for 30 minutes. Antigen retrieval for total-CgA was performed by heating Tris buffer at 95° for 40 minutes. Antigen retrieval for DAXX was performed by heating citrate buffer at 100°C for 30 minutes and for ATRX by heating at 95°C Tris buffer for 40 minutes, as previously described (Marinoni *et al*, 2014). Antibody detection was done with the Bond Polymer Refine

Detection kit (Leica Biosystems, DS9800) using 3,3-diaminobenzidine (DAB) as brown chromogen and following the manufacturer's instructions. The samples were counterstained with haematoxylin, dehydrated and mounted with Pertex (Sakura). Slides were scanned on Panoramic 250 Flash (3DHISTECH).

CA-9 staining was scored as positive if at least 5% of tumor cells showed at least a weak cytoplasmic positivity (Schmitt *et al*, 2009). CD34 staining was used to evaluate MVD. Microvessels were manually counted by eye in each TMA punch (diameter 0.6 mm). If the whole area of the punch was not available or a part of the punch contained normal pancreatic tissue, the number of counted microvessels was extrapolated to the whole area. MVD was expressed as number of microvessels per 1 mm^2.

CgA and CgA-derived fragments stainings were scored based on the percentage of positive tumor cells and the intensity of the staining by using QuPath software (Bankhead *et al*, 2017), as described in the paragraph "Immunohistochemistry set-up and scoring for CgA and CgA-derived fragments".

DAXX and ATRX stainings were scored as previously described (Marinoni *et al*, 2014).

Data and samples collection

T, N, M stages were defined according to the current ENETS classification (Rindi *et al*, 2006). Tumor size was defined as the maximum tumor diameter as measured on the final pathology specimen. Tumor grade was classified according to the 2017 WHO classification as G1 (Ki67 < 3%) and G2 (Ki67 3-20%) (Lloyd RV *et al*, 2017). Ki67 proliferative index was assessed by MIB1 antibody staining and expressed as % of cells with positive nuclear staining in 2000 cells counted in the area of highest nuclear labelling (Lloyd RV *et al*, 2017).

Full blood samples were preoperatively collected in 6 mL EDTA tubes. Plasma was obtained after blood centrifugation for 10 minutes (1600xg, room temperature). Plasma samples where then stored for 24-72 hours in a -80°C refrigerator and finally transferred into liquid nitrogen.

Statistical analysis

Continuous variables were reported as median with IQR or as mean with SD. Categorical data were expressed as number and proportion (%). Mann-Whitney U test or Student t test were used to compare continuous variables between two groups, as

appropriate. Spearman bivariate correlation was used to assess the relationship between two continuous variables. Univariate and multivariate linear regression analysis was used to investigate determinants of VS-1 plasma and tissue levels. Statistical analysis was performed using SPSS 25.0 for Mac software (SPSS Inc, Chicago, IL, USA). *P* values were considered significant when equal to or lower than 0.05.

Aim 6 - To investigate CgA and CgA-derived fragments as biomarkers in patients with PDAC, by correlating their plasma levels with survival outcomes.

[The following data have been published in Reni M, Andreasi V, et al. Circulating Chromogranin A Is Cleaved Into Vasoregulatory Fragments in Patients With Pancreatic Ductal Adenocarcinoma. Front Oncol 2020].

Results

Study partecipants

CgA and CgA-derived fragments plasma levels were measured in 172 patients diagnosed with locally advanced or metastatic PDAC and in 37 age-matched healthy controls. Demographics, clinical features and follow-up data of the study cohort are reported in **Table 18**.

Table 18. *Demographics and clinical features of 172 patients with PDAC and 37 healthy subjects.*

	PDAC patients	***Healthy subjects***
Variable	***n 172 (%)***	***n 37 (%)***
Gender		
Female	85 (49)	13 (35)
Male	87 (51)	24 (65)
Age, years*	60 (54-66)	61 (51-71)
Karnofsky Performance Status		
70%	10 (6)	
80%	28 (16)	
90%	88 (51)	
100 %	46 (27)	
Disease stage		
III	65 (38)	
IV	107 (62)	
PPI treatment		
No	75 (44)	
Yes	97 (56)	
Chemotherapy regimen†		
PDXG	24 (14)	
PEXG	148 (86)	
Disease progression		
No	4 (2)	
Yes	168 (98)	
Death		
No	4 (2)	
Yes	168 (98)	
PFS, months*	8 (4-11)	
OS, months*	12 (8-19)	

*Expressed as median (interquartile range) †P: cisplatin; D: docetaxel, X: capecitabine, G: gemcitabine, E: epirubicin *OS*, overall survival; *PFS*, progression-free survival.

CgA and CgA-derived fragments can be measured in healthy subjects

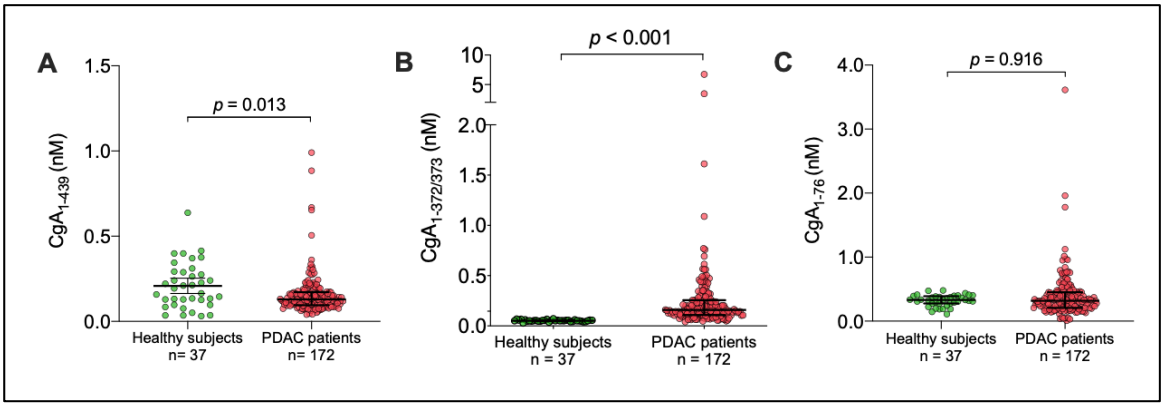
Healthy subjects - The median total-CgA plasma level in healthy subjects was 0.77 nM (IQR 0.62-0.99 nM). Circulating total-CgA comprised both full-length CgA (median 0.19 nM) and CgA-derived fragments (i.e. $CgA_{1-372/373}$, VS-1, $CgA_{1-436/439}$). In healthy subjects, approximately half of total-CgA was represented by $CgA_{1-436/439}$ (median 0.35 nM), which comprises large peptides containing the N-terminal, the central and part of or the entire C-terminal region. On the other hand, a conspicuous amount of circulating total-CgA (50%) consisted of CgA_{1-x} (median 0.41 nM), a family of fragments lacking the entire C-terminal region. Of note, $CgA_{1-372/373}$, which is part of CgA_{1-x}, was almost undetectable in normal subjects (median 0.05 nM) (**Table 19**), thus suggesting that fragments different from $CgA_{1-372/373}$ represented most of CgA_{1-x}. The N-terminal fragment VS-1 could also be measured, suggesting that CgA N- and C-terminal cleavage occurs in normal conditions.

Patients with PDAC - Similarly, CgA and CgA-derived fragments were measured in patients with PDAC. Total-CgA plasma levels were not significantly different between healthy subjects [median 0.77 nM (IQR 0.62-0.99 nM)] and patients with PDAC [median 0.92 nM (IQR 0.61-1.58 nM)] ($p = 0.101$). However, some differences were observed in terms of CgA fragmentation, especially at the C-terminal region. Full-length CgA was significantly higher in healthy subjects as compared with PDAC patients ($p = 0.013$) (**Figure 42A**). On the other hand, $CgA_{1-372/373}$ plasma levels were significantly increased in patients with PDAC ($p < 0.001$) (**Figure 42B**). Finally, similar VS-1 levels were observed in patients and controls ($p = 0.916$) (**Table 19**) (**Figure 42C**).

Table 19. *Comparison of CgA and CgA-derived fragments plasma levels between healthy subjects and patients with PDAC.*

Analyte	**Healthy subjects** *n* = 37	**All patients** *n* = 172	***p***
Total-CgA, nM	0.77 (0.62-0.99)	0.92 (0.61-1.58)	0.101
CgA_{1-439}, nM	0.19 (0.11-0.29)	0.13 (0.10-0.17)	**0.013**
$CgA_{1-436/439}$, nM	0.35 (0.30-0.49)	0.47 (0.32-0.78)	**0.001**
CgA_{1-x}, nM	0.41 (0.32-0.62)	0.44 (0.26-0.87)	0.775
$CgA_{1-372/373}$, nM	0.05 (0.05-0.06)	0.16 (0.11-0.26)	**< 0.001**
CgA_{1-76}, nM	0.33 (0.28-0.39)	0.32 (0.21-0.45)	0.916
CgA_{1-x}/total-CgA	0.55 (0.50-0.61)	0.52 (0.42-0.61)	**0.047**
CgA_{1-439}/total-CgA	0.24 (0.15-0.39)	0.12 (0.09-0.20)	**<0.001**

Figure 42. *Plasma levels of full-length CgA (A), CgA_{1-373} (B) and CgA_{1-76} (C) in normal subjects and in patients with PDAC.*



CgA fragmentation and PPI

Overall, 97 patients (56%) were treated with PPI. The effect of these drugs on circulating CgA and CgA-derived fragments was then assessed (**Table 20**). $CgA_{1-436/439}$ plasma levels were significantly increased in patients assuming PPI as compared to untreated patients (0.49 *versus* 0.42 nM, $p = 0.042$), whereas $CgA_{1-372/373}$ were not significantly different. The CgA_{1-x}/CgA_{total} ratio (i.e. C-terminal fragmentation index) was significantly lower in patients treated with PPI (0.49 *versus* 0.54, $p = 0.032$). Thus, PPI assumption does not seem to be responsible for the increased CgA fragmentation observed in this cohort.

Table 20. *Comparison of CgA and CgA-derived fragments plasma levels in patients with PDAC according to PPI treatment.*

Analyte	**No PPI** *n = 75*	**PPI** *n = 97*	***p***
Total-CgA, nM	0.86 (0.54-1.64)	0.97 (0.67-1.57)	0.184
CgA_{1-439}, nM	0.13 (0.10-0.16)	0.13 (0.09-0.18)	0.938
$CgA_{1-436/439}$, nM	0.42 (0.25-0.76)	0.49 (0.37-0.82)	**0.042**
CgA_{1-x}, nM	0.41 (0.26-0.89)	0.45 (0.25-0.85)	0.900
$CgA_{1-372/373}$, nM	0.17 (0.12-0.24)	0.15 (0.11-0.28)	0.428
CgA_{1-76}, nM	0.32 (0.21-0.44)	0.32 (0.21-0.51)	0.634
CgA_{1-x}/total-CgA	0.54 (0.45-0.62)	0.49 (0.38-0.61)	**0.032**
CgA_{1-439}/total-CgA	0.13 (0.09-0.45)	0.12 (0.09-0.19)	0.304

CgA C-terminal cleavage predicts progression-free survival (PFS) and OS in patients with PDAC

Data regarding chemotherapy regimen, follow-up and survival outcomes are summarized in **Table 18**. Patients with locally advanced neoplasms had a median PFS of 10 months and a median OS of 18 months. Metastatic patients had median PFS and OS of 6 and 10 months, respectively. At univariate survival analysis, only disease stage ($p < 0.001$ for both PFS and OS), Karnofsky performance status ($p = 0.001$ for PFS, $p = 0.003$ for OS), and baseline CA19.9 ($p < 0.001$ for both PFS and OS), but not CgA and CgA-derived peptides plasma levels, were significantly associated with PFS and OS (**Table 21**).

Table 21. *Univariate Cox regression analysis assessing the determinants of PFS and OS in patients with PDAC (n=172).*

	PFS			OS		
Variable	**HR***	**95% CI**	***p***	**HR***	**95% CI**	***p***
Gender			0.604			0.133
Female	1	-		1	-	
Male	1.08	0.80-1.47		1.26	0.93-1.71	
Age			0.058			0.201
≤ 60 years	1	-		1	-	
> 60 years	0.75	0.54-1.01		0.82	0.61-1.11	
Disease stage			**<0.001**			**<0.001**
III	1	-		1	-	
IV	2.36	1.71-3.26		1.90	1.38-2.60	
Karnofsky performance status	0.97	0.95-0.99	**0.001**	0.97	0.95-0.99	**0.003**
CA 19.9	1.02	1.01.1.03	**<0.001**	1.03	1.01-1.04	**<0.001**
Chemotherapy			0.192			
PDXG	1	-		1	-	
PEXG	1.35	0.86-2.13		1.09	0.69-1.70	0.723
PPI treatment			0.652			
No	1	-		1	-	
Yes	0.93	0.69-1.27		1.00	0.74-1.37	0.972
Total-CgA	1.04	0.95-1.14	0.418	1.01	0.92-1.10	0.851
CgA_{1-439}	0.94	0.26-3.36	0.927	0.46	0.12-1.75	0.255
$CgA_{1-436/439}$	1.12	0.86-1.46	0.397	1.01	0.78-1.31	0.944
CgA_{1-x}	1.04	0.93-1.17	0.508	1.01	0.90-1.14	0.830
$CgA_{1-372/373}$	1.13	0.90-1.42	0.297	1.05	0.82-1.35	0.699
CgA_{1-76}	0.82	0.53-1.26	0.361	0.91	0.58-1.44	0.697
CgA_{1-x}/total-CgA	1.54	0.63-3.8	0.340	1.73	0.70-4.30	0.237
CgA_{1-439} /total-CgA	0.54	0.10-2.98	0.481	0.29	0.05-1.64	0.160

CI, confidence interval; *HR*, hazard ratio; *OS*, overall survival; *PDXG*, cisplatin + docetaxel + capecitabine + gemcitabine; *PEXG*, cisplatin+epirubicin+capecitabine+gemcitabine; *PFS*, progression-free survival; *PPI*, proton pump inhibitors.

* HR for every increase of: 10% (performance status); 1000 U/mL (CA 19.9); 1 nM (CgA_{total}, CgA_{1-439}, $CgA_{1-436/439}$, CgA_{1-x}, $CgA_{1-372/373}$, CgA_{1-76}); 1 unit (CgA_{1-x}/CgA_{total}, CgA_{1-439}/CgA_{total})

By multivariate Cox regression analysis, CgA and CgA-derived fragments were significantly associated with PFS and OS (**Table 22**). Higher full-length CgA plasma levels were identified as a protective factor, both in terms of PFS (HR 0.04, $p < 0.001$) and OS (HR 0.03, $p < 0.001$). On the other hand, a high $CgA_{1\text{-}x}/CgA_{total}$ ratio (i.e. index of CgA C-terminal fragmentation) independently predicted poorer OS (HR 3.53, $p = 0.015$). An association with worse survival outcomes was found also for $CgA_{1\text{-}372/373}$ (PFS, HR 1.52, $p = 0.020$) and $CgA_{1\text{-}436/439}$ (OS, HR 1.60, $p = 0.006$).

Table 22. *Multivariate Cox regression analysis assessing the determinants of PFS and OS in patients with PDAC (n=172).*

	PFS			OS		
Variable	**HR***	**95% CI**	***p***	**HR***	**95% CI**	***p***
Gender						
Female	–	–	–	1	-	
Male				1.31	0.96-1.80	0.093
Age						
≤ 60 years	1	-		1	-	
> 60 years	0.60	0.44-0.83	**0.002**	0.69	0.50-0.94	**0.020**
Disease stage						
III	1	-		1	-	
IV	2.82	1.99-3.99	**<0.001**	2.14	1.53-2.99	**<0.001**
Karnofsky performance status	0.96	0.94-0.98	**<0.001**	0.97	0.95-0.99	**0.001**
CA 19.9	1.02	1.01-1.03	**0.007**	1.02	1.01-1.03	**<0.001**
Chemotherapy			**0.006**			
PDXG	1	-		1	-	
PEXG	1.98	1.22-3.21		1.55	0.95-2.52	0.078
PPI treatment						
No	–	–	–	–	–	–
Yes						
Total-CgA	–	–	–	–	–	–
$CgA_{1\text{-}439}$	0.04	0.01-0.24	**<0.001**	0.03	0.01-0.17	**<0.001**
$CgA_{1\text{-}436/439}$	1.40	0.96-2.04	0.080	1.60	1.14-2.23	**0.006**
$CgA_{1\text{-}x}$	–	–	–	–	–	–
$CgA_{1\text{-}372/373}$	1.52	1.07-2.17	**0.020**	–	–	–
$CgA_{1\text{-}76}$	–	–	–	–	–	–
$CgA_{1\text{-}x}$/total-CgA	2.38	0.89-6.38	0.084	3.53	1.28-9.78	**0.015**
$CgA_{1\text{-}439}$ /total-CgA	–	–	–	–	–	–

CI, confidence interval; *HR*, hazard ratio; *OS*, overall survival; *PDXG*, cisplatin + docetaxel + capecitabine + gemcitabine; *PEXG*, cisplatin+epirubicin+capecitabine+gemcitabine; *PFS*, progression-free survival; *PPI*, proton pump inhibitors.

* HR for every increase of: 10% (performance status); 1000 U/mL (CA 19.9); 1 nM (CgA_{total}, $CgA_{1\text{-}439}$, $CgA_{1\text{-}436/439}$, $CgA_{1\text{-}x}$, $CgA_{1\text{-}372/373}$, $CgA_{1\text{-}76}$); 1 unit ($CgA_{1\text{-}x}/CgA_{total}$, $CgA_{1\text{-}439}/CgA_{total}$)

Discussion

The present study shows that CgA fragmentation in the C-terminal region is associated with poorer survival outcomes in patients with locally advanced and metastatic PDAC. In particular, a decrease in $CgA_{1\text{-}439}$ (i.e. full-length protein) and a relative increase in the plasma levels of CgA-derived fragments lacking all or part of the C-terminal region ($CgA_{1\text{-}x}$) was found to be associated with worse prognosis. Interestingly, only the $CgA_{1\text{-}x}$/total-CgA ratio, which is a C-terminal fragmentation index, but not the $CgA_{1\text{-}76}$/total-CgA ratio (N-terminal fragmentation index), was identified as an independent prognostic factor. Therefore, CgA C-terminal fragmentation seems more relevant than CgA N-terminal fragmentation for patients' prognosis in the setting of PDAC.

It is well-known that PPI can induce enterochromaffin-like cells hyperplasia and consequently increase CgA secretion from gastric mucosa (Mosli *et al*, 2012; Giusti *et al*, 2004). Therefore, it might be argued that PPI are responsible for the changes in the circulating pool of $CgA_{1\text{-}439}$ and CgA-derived fragments reported in the present experience. However, we observed that patients assuming PPI had a lower CgA C-terminal fragmentation index (i.e. $CgA_{1\text{-}x}/CgA_{total}$ ratio), as compared with untreated patients. Therefore, PPI administration does not seem to be responsible for the increased CgA fragmentation observed in patients with PDAC.

Consistently, several *in vitro* and *in vivo* studies performed by our group, using PDAC models, suggest that CgA-derived fragments are produced within the tumor by tumor-derived proteases (Reni *et al*, 2020). In particular, human PDAC cell lines can promote the cleavage of exogenous $CgA_{1\text{-}439}$. In this setting, an important role is played by plasminogen activators and plasmin, as no CgA cleavage occurs when plasminogen activator inhibitor-1 (PAI-1) or aprotinin (i.e. inhibitor of plasmin) are added to PDAC cell cultures (Reni *et al*, 2020). CgA fragmentation can be observed also when macrophages or cancer-associated fibroblasts are cultured. Therefore, both tumor cells and other cell types part of the tumor microenvironment may contribute to produce CgA-derived fragments. This hypothesis is further supported by *in vivo* studies showing that the PDAC growth in mice is associated with increased fragmentation of circulating CgA (Reni *et al*, 2020).

According to the present findings, CgA cleavage in PDAC mainly occurs in the C-terminal region. Plasmin is likely to be involved in this process (Jiang *et al*, 2001) and

sites located in CgA C-terminal region are more prone to plasmin cleavage as compared with sites located in CgA N-terminal region (Reni *et al*, 2020). Therefore, it is likely that PDAC promotes CgA cleavage through the activation of plasminogen to plasmin, which then preferentially cleaves CgA in the C-terminal region (Reni *et al*, 2020). Consistently, previous experiences have demonstrated that PDAC cells display an increased expression of urokinase-type plasminogen activator (uPA) and uPA receptor, as compared with normal pancreatic cells, and decreased PAI-1 expression, thus supporting the involvement of this proteolytic system in PDAC (Harvey *et al*, 2003; Xue *et al*, 2008; Warnecke-Eberz *et al*, 2008).

In light of these findings, one might argue that CgA cleavage is not just a cancer-related epiphenomenon, but that it can affect also tumor biology. Several previous observations suggest that CgA cleavage may be involved in the regulation of tumor growth. In this regard, we have previously demonstrated that full-length CgA and VS-1 are able to inhibit angiogenesis, to regulate cell adhesion and to enhance the endothelial barrier function (Gasparri *et al*, 1997; Ferrero *et al*, 2004; Crippa *et al*, 2013). Specifically, CgA_{1-439} and VS-1 can inhibit ECs migration, invasion and VEGF-induced capillary-like structure formation as well as FGF2-induced angiogenesis (Helle & Corti, 2015; Corti *et al*, 2018). VS-1 is also able to inhibit HIF-1α nuclear translocation in ECs (Helle & Corti, 2015; Corti *et al*, 2018). On the other hand, fragments derived from CgA C-terminal cleavage, such as CgA_{1-373} and $CgA_{352-372}$, can induce FGF2 release from ECs and promote angiogenesis (Crippa *et al*, 2013; Theurl *et al*, 2010; Dallatomasina *et al*, 2019). Therefore, circulating CgA and CgA-derived fragments might form a balance of vasoactive factors, finely regulated by N-terminal and C-terminal cleavage. In this setting, CgA degradation by plasmin converts the antiangiogenic full-length CgA into proangiogenic fragments (i.e. CgA_{1-373}) lacking the C-terminal region (Reni *et al*, 2020). Therefore, plasmin-induced CgA fragmentation represents a mechanism for the regulation of PDAC vascular biology.

The predominance of CgA C-terminal fragmentation over N-terminal cleavage leads to increased production of proangiogenic peptides and consequently favors tumor progression, as suggested by the positive correlation between CgA C-terminal fragmentation index and poor prognosis in patients with PDAC. This hypothesis is further corroborated by *in vivo* studies showing that inhibition of CgA cleavage by aprotinin

administration is associated with reduced rate of tumor growth in mice (Reni *et al*, 2020). Also, systemic administration of antibodies against CgA_{1-373} binding site for NRP-1 (Dallatomasina *et al*, 2019), a relevant proangiogenic VEGF coreceptor, significantly reduced tumor growth in PDAC-bearing mice (Reni *et al*, 2020). On the other hand, systemic treatment with exogenous full-length CgA decreased the perfusion of tumors implanted in mice pancreas, at contrast-enhanced ultrasound (Reni *et al*, 2020).

In conclusion, the present findings suggest that the cleavage of circulating CgA at the C-terminal region is enhanced in PDAC and has relevant implications in terms of tumor biology and patients' prognosis. In particular, the decrease in full-length CgA and the increase of proangiogenic fragments lacking the C-terminal region is associated with worse survival outcomes in patients with locally advanced and metastatic PDAC. Therefore, given its potential role in the regulation of tumor vascular biology, CgA system may represent a novel therapeutic target that requires further investigation.

Materials and methods

Patients and plasma samples

Patients with histologically proven locally advanced or metastatic treatment-naïve PDAC were enrolled. Eligibility criteria included: age 18-70 years and Karnofsky performance status > 60, or age 71-75 years and Karnofsky performance status > 70; hemoglobin ≥ 10 g/dL, absolute neutrophil count ≥ 1500/mm^3, platelet count ≥ 100000/mm^3; serum creatinine ≤ 1.5 mg/dL; total bilirubin ≤ 1.5 mg/dL; transaminases less than 3 times the upper limit of normal. This study was approved by the local ethics committee (OSR-Prot. PACT-19) and was conducted at IRCCS San Raffaele Hospital following the principles of good clinical trial practice according to the Declaration of Helsinki. A written informed consent was obtained from each patient.

Five milliliters of peripheral blood were collected at the time of diagnosis, before chemotherapy, in a sterile test-tube and centrifuged at 2500xg for 10 minutes. Plasma samples were stocked in 0.5 mL cryovials and stored at -80ºC.

CgA and CgA-derived fragments immunoassays

CgA_{1-439}, $CgA_{1-436/439}$, $CgA_{1-372/373}$ and CgA_{1-76} and total-CgA were measured in plasma using five sandwich ELISAs based on antibodies against different CgA epitopes. Monoclonal antibodies B4E11 (against CgA epitope 68-71) and 5A8 (against CgA epitope

54-57) were previously described and used as capturing antibodies (Corti *et al*, 1996). Polyclonal antisera against human CgA_{71-76} (α-76), $CgA_{368-373}$ (α-373), or $CgA_{410-439}$ (α-410-439), $CgA_{434-439}$ (α-439) were raised in rabbits and used as detecting antibodies. The antiserum α-76 binds CgA_{1-76}, but not larger fragments; α-373 binds CgA_{1-372} and CgA_{1-373}, but not larger fragments; α410-439 binds CgA_{1-436} and CgA_{1-439}; α-439 binds CgA_{1-439}, but not CgA_{1-436} (Bianco *et al*, 2016b; Dallatomasina *et al*, 2019). A polyclonal antiserum was also raised in rabbits by immunization with recombinant full-length CgA. This antiserum (α-FRs) recognizes epitopes mainly located in CgA central region (90-133, 163-187, 222-256, 315-338) and recognizes full-length CgA as well as several fragments containing the N-terminal region and all or part of the central region, but not CgA_{1-76} (Bianco *et al*, 2016b; Dallatomasina *et al*, 2019).

The assays that were used in the present study can selectively detect: a) full-length CgA (CgA_{1-439} ELISA); b) full-length CgA plus fragments without the C-terminal sequence 437-439 ($CgA_{1-436/439}$ ELISA); c) CgA_{1-372} and CgA_{1-373} ($CgA_{1-372/373}$ ELISA); d) CgA_{1-76} (CgA_{1-76} ELISA); e) full-length CgA plus fragments containing the N-terminal region and part of or the entire central and C-terminal regions, but not CgA_{1-76} (CgA_{total} ELISA) (Bianco *et al*, 2016b). The mixture of large fragments lacking the region 410-430 (collectively called CgA_{1-x}) was calculated as the difference between total-CgA_{total} and $CgA_{1-436/439}$. The specificity of immunoassays performed in the present study is reported in **Table 23**.

Table 23. *Analyte specificity of CgA ELISAs based on different antibodies.*

Assay	**Detected CgA fragments**					
	CgA_{1-439}	**CgA_{1-436}**	**CgA_{1-372}**	**CgA_{1-373}**	**CgA_{1-x}***	**CgA_{1-76}**
CgA_{1-439} ELISA	✓	✗	✗	✗	✗	✗
$CgA_{1-436/439}$ ELISA	✓	✓	✗	✗	✗	✗
$CgA_{1-372/373}$ ELISA	✗	✗	✓	✓	–°	✗
CgA_{1-76} ELISA	✗	✗	✗	✗	✗	✓
CgA_{total} ELISA	✓	✓	✓	✓	✓	✗

* x: any residue of the 133-410 region. CgA_{1-x} includes CgA fragments of different length lacking the 410-439 region and containing the N-terminal region plus part of the central/C-terminal region.

° –: this assay can detect $CgA_{1-372/373}$, which belong to the CgA_{1-x} family, but not larger or shorter fragments.

Statistical analysis

Continuous variables were reported as median and IQR. Categorical data were expressed as number with percentage (%). Continuous variables were compared between two groups using the Student's t test or the Mann-Whitney U test, as appropriate based on variable distribution. Categorical data were compared between two groups using the Chi square test or the Fisher exact test, as appropriate based on expected cell counts. PFS and OS represented the study endpoints. PFS was defined as the time from diagnosis to first evidence of disease progression and it was censored at the last follow-up if no events had occurred. OS was defined as the time from diagnosis to death due to any cause and it was censored at the last follow-up if no events had occurred. Cox proportional hazards models with backward variable selection were used to estimate the predictors of PFS and OS. Statistical analysis was performed using SPSS 25.0 for Mac software (SPSS Inc., Illinois, USA). *P* values < 0.05 were considered significant.

Conclusions

The present project started with the aim to address a crucial unmet clinical need: the lack of a reliable and easily accessible biomarker for diagnosis, follow-up and treatment response evaluation in patients with PanNENs.

In order to reach this purpose, different projects have been carried out, with interesting and clinically relevant findings regarding the role of vasostatin-1 (CgA N-terminal fragment) as possible novel monoanalyte biomarker for PanNENs. At the same time, also a multianalyte biomarker, NETest, was successfully investigated in a surgical cohort, although its broad applicability might be partially limited by the underlying complex statistical analyses and high costs.

This project also focused on the biological role of CgA proteolytic machinery in the setting of pancreatic neoplasms. CgA and CgA-derived fragments were investigated in the setting of PDAC, where their impact on survival outcomes and their involvement in tumor biology were demonstrated. In particular, CgA cleavage at the C-terminal region was enhanced in patients with PDAC, whereas CgA cleavage at the N-terminal region seems more relevant in PanNENs, with vasostatin-1 plasma level being a reliable marker of tumor burden. Based on IHC data, no clear relationship between CgA-derived fragments and PanNEN vascularization parameters was observed. However, previous results from *in vitro* and *in vivo* studies demonstrate that these peptides are deeply involved in the process of angiogenesis. Therefore, further investigation with quantification of CgA-derived fragments in tumor tissue might help to prove that they are not just a disease epiphenomenon but that they have a biological role also in the setting of PanNENs.

References

Andreasi V, Muffatti F, Guarneri G, Falconi M & Partelli S (2020) Surgical Principles in the Management of Pancreatic Neuroendocrine Neoplasms. *Curr Treat Options Oncol* 21: 48

Andreasi V, Partelli S, Manzoni M, Muffatti F, Colombo B, Corti A & Falconi M (2019) Association between preoperative Vasostatin-1 and pathological features of aggressiveness in localized nonfunctioning pancreatic neuroendocrine tumors (NF-PanNET). *Pancreatology* 19: 57–63

April-Monn SL, Wiedmer T, Magdalena S, Maire RS, Schiavo Lena M, Trippel M, Di Domenico A, Muffatti F, Andreasi V, Capurso G, *et al* (2021) 3D Primary Cell Culture: A Novel Preclinical Model For Pancreatic Neuroendocrine Tumors (PanNETs). *Neuroendocrinology* 111:2 73–287

Bachetti T, Ferrari Bardile A, Aloi TL, Colombo B, Assi E, Savino G, Vercelli A, Colombo R & Corti A (2017) Plasma levels of vasostatin-1, a chromogranin A fragment, are associated with carotid artery maximum stenosis: A pilot study. *Int J Cardiol* 236: 438–443

Baekdal J, Krogh J, Klose M, Holmager P, Langer SW, Oturai P, Kjaer A, Federspiel B, Hilsted L, Rehfeld JF, *et al* (2020) Limited Diagnostic Utility of Chromogranin A Measurements in Workup of Neuroendocrine Tumors. *Diagnostics (Basel, Switzerland)* 10: 881

Bailey P, Chang DK, Nones K, Johns AL, Patch A-M, Gingras M-C, Miller DK, Christ AN, Bruxner TJC, Quinn MC, *et al* (2016) Genomic analyses identify molecular subtypes of pancreatic cancer. *Nature* 531: 47–52

Bankhead P, Loughrey MB, Fernández JA, Dombrowski Y, McArt DG, Dunne PD, McQuaid S, Gray RT, Murray LJ, Coleman HG, *et al* (2017) QuPath: Open source software for digital pathology image analysis. *Sci Rep* 7: 16878

Banks P & Helle K (1965) The release of protein from the stimulated adrenal medulla. *Biochem J* 97: 40C-41C

Basturk O, Yang Z, Tang LH, Hruban RH, Adsay V, McCall CM, Krasinskas AM, Jang K-T, Frankel WL, Balci S, *et al* (2015) The high-grade (WHO G3) pancreatic neuroendocrine tumor category is morphologically and biologically heterogenous and includes both well differentiated and poorly differentiated neoplasms. *Am J Surg*

Pathol 39: 683–690

Baudin E, Gigliotti A, Ducreux M, Ropers J, Comoy E, Sabourin JC, Bidart JM, Cailleux AF, Bonacci R, Ruffie P, *et al* (1998) Neuron-specific enolase and chromogranin A as markers of neuroendocrine tumours. *Br J Cancer* 78: 1102–1107

Belloni D, Scabini S, Foglieni C, Veschini L, Giazzon A, Colombo B, Fulgenzi A, Helle KB, Ferrero ME, Corti A, *et al* (2007) The vasostatin-I fragment of chromogranin A inhibits VEGF-induced endothelial cell proliferation and migration. *FASEB J Off Publ Fed Am Soc Exp Biol* 21: 3052–3062

Beltran H, Romanel A, Conteduca V, Casiraghi N, Sigouros M, Franceschini GM, Orlando F, Fedrizzi T, Ku S-Y, Dann E, *et al* (2020) Circulating tumor DNA profile recognizes transformation to castration-resistant neuroendocrine prostate cancer. *J Clin Invest* 130: 1653–1668

Benten D, Behrang Y, Unrau L, Weissmann V, Wolters-Eisfeld G, Burdak-Rothkamm S, Stahl FR, Anlauf M, Grabowski P, Möbs M, *et al* (2018) Establishment of the first well-differentiated human pancreatic neuroendocrine tumor model. *Mol Cancer Res*

Bergenfelz A, Luts L, Jensen TB & Sundler F (2000) Pancreastatin plasma levels in patients with primary hyperparathyroidism. *World J Surg* 24: 1579–1583

Bettini R, Partelli S, Boninsegna L, Capelli P, Crippa S, Pederzoli P, Scarpa A & Falconi M (2011) Tumor size correlates with malignancy in nonfunctioning pancreatic endocrine tumor. *Surgery* 150: 75–82

Bianco M, Gasparri A, Generoso L, Assi E, Colombo B, Scarfò L, Bertilaccio MTS, Scielzo C, Ranghetti P, Dondossola E, *et al* (2016a) Inhibition of chronic lymphocytic leukemia progression by full-length chromogranin A and its N-terminal fragment in mouse models. *Oncotarget* 7: 41725–41736

Bianco M, Gasparri AM, Colombo B, Curnis F, Girlanda S, Ponzoni M, Bertilaccio MTS, Calcinotto A, Sacchi A, Ferrero E, *et al* (2016b) Chromogranin A Is Preferentially Cleaved into Proangiogenic Peptides in the Bone Marrow of Multiple Myeloma Patients. *Cancer Res* 76: 1781–1791

Birrer DL, Golcher H, Casadei R, Haile SR, Fritsch R, Hussung S, Brunner TB, Fietkau R, Meyer T, Grützmann R, *et al* (2021) Neoadjuvant Therapy for Resectable Pancreatic Cancer: A New Standard of Care. Pooled Data from Three Randomized Controlled Trials. *Ann Surg* doi: 10.1097/SLA.0000000000005126 Online ahead of

print

Bodei L, Ambrosini V, Herrmann K & Modlin I (2017) Current Concepts in (68)Ga-DOTATATE Imaging of Neuroendocrine Neoplasms: Interpretation, Biodistribution, Dosimetry, and Molecular Strategies. *J Nucl Med* 58: 1718–1726

Bodei L, Kidd MS, Singh A, van der Zwan WA, Severi S, Drozdov IA, Malczewska A, Baum RP, Kwekkeboom DJ, Paganelli G, *et al* (2020) PRRT neuroendocrine tumor response monitored using circulating transcript analysis: the NETest. *Eur J Nucl Med Mol Imaging* 47: 895–906

Bodei L, Sundin A, Kidd M, Prasad V & Modlin IM (2015) The status of neuroendocrine tumor imaging: from darkness to light? *Neuroendocrinology* 101: 1–17

Bossuyt PM, Reitsma JB, Bruns DE, Gatsonis CA, Glasziou PP, Irwig L, Lijmer JG, Moher D, Rennie D, de Vet HCW, *et al* (2015) STARD 2015: an updated list of essential items for reporting diagnostic accuracy studies. *BMJ* 351: h5527

Calle EE, Rodriguez C, Walker-Thurmond K & Thun MJ (2003) Overweight, obesity, and mortality from cancer in a prospectively studied cohort of U.S. adults. *N Engl J Med* 348: 1625–1638

Capretti G, Nappo G, Smiroldo V, Cereda M, Branciforte B, Spaggiari P, Carrara S, Preatoni P, Gavazzi F, Ridolfi C, *et al* (2019) The number of metastatic lymph nodes is a useful predictive factor for recurrence after surgery for nonmetastatic nonfunctional neuroendocrine neoplasm of the pancreas. *Gastroenterol Res Pract* 2019:6856329

Chaudhuri AA, Chabon JJ, Lovejoy AF, Newman AM, Stehr H, Azad TD, Khodadoust MS, Esfahani MS, Liu CL, Zhou L, *et al* (2017) Early Detection of Molecular Residual Disease in Localized Lung Cancer by Circulating Tumor DNA Profiling. *Cancer Discov* 7: 1394–1403

Chauhan A, Kohn E & Del Rivero J (2020) Neuroendocrine Tumors-Less Well Known, Often Misunderstood, and Rapidly Growing in Incidence. *JAMA Oncol* 6: 21–22

Chen F, Zhang Y, Gibbons DL, Deneen B, Kwiatkowski DJ, Ittmann M & Creighton CJ (2018) Pan-Cancer Molecular Classes Transcending Tumor Lineage Across 32 Cancer Types, Multiple Data Platforms, and over 10,000 Cases. *Clin cancer Res* 24: 2182–2193

Chung H, Corti A, Crippa L, Schneider F, Metz-Boutigue M-H & Garnero P (2012)

Development of an immunoassay for the derived-peptide of chromogranin A, vasostatin-I (1-76): assessment of severity in patients with sepsis. *Biomarkers* 17: 430–434

Cives M & Strosberg JR (2018) Gastroenteropancreatic Neuroendocrine Tumors. *CA Cancer J Clin* 68: 471–487

Conroy T, Desseigne F, Ychou M, Bouche O, Guimbaud R, Becouarn Y, Adenis A, Raoul J-L, Gourgou-Bourgade S, de la Fouchardiere C, *et al* (2011) FOLFIRINOX versus gemcitabine for metastatic pancreatic cancer. *N Engl J Med* 364: 1817–1825

Corsello A, Di Filippo L, Massironi S, Sileo F, Dolcetta Capuzzo A, Gemma M, Carlucci C, Cusini C, Colombo B, Dallatomasina A, *et al* (2018) Vasostatin-1: A novel circulating biomarker for ileal and pancreatic neuroendocrine neoplasms. *PLoS One* 13: e0196858

Corti A, Longhi R, Gasparri A, Chen F, Pelagi M & Siccardi AG (1996) Antigenic regions of human chromogranin A and their topographic relationships with structural/functional domains. *Eur J Biochem* 235: 275–280

Corti A, Marcucci F & Bachetti T (2018) Circulating chromogranin A and its fragments as diagnostic and prognostic disease markers. *Pflugers Arch* 470: 199–210

Couvelard A, O'Toole D, Turley H, Leek R, Sauvanet A, Degott C, Ruszniewski P, Belghiti J, Harris AL, Gatter K, *et al* (2005) Microvascular density and hypoxia-inducible factor pathway in pancreatic endocrine tumours: negative correlation of microvascular density and VEGF expression with tumour progression. *Br J Cancer* 92: 94–101

Crippa L, Bianco M, Colombo B, Gasparri AM, Ferrero E, Loh YP, Curnis F & Corti A (2013) A new chromogranin A-dependent angiogenic switch activated by thrombin. *Blood* 121: 392–402

Cristofanilli M, Budd GT, Ellis MJ, Stopeck A, Matera J, Miller MC, Reuben JM, Doyle G V, Allard WJ, Terstappen LWMM, *et al* (2004) Circulating tumor cells, disease progression, and survival in metastatic breast cancer. *N Engl J Med* 351: 781–791

Curnis F, Dallatomasina A, Bianco M, Gasparri A, Sacchi A, Colombo B, Fiocchi M, Perani L, Venturini M, Tacchetti C, *et al* (2016) Regulation of tumor growth by circulating full-length chromogranin A. *Oncotarget* 7: 72716–72732

Cwikla JB, Bodei L, Kolasinska-Cwikla A, Sankowski A, Modlin IM & Kidd M (2015)

Circulating Transcript Analysis (NETest) in GEP-NETs Treated With Somatostatin Analogs Defines Therapy. *J Clin Endocrinol Metab* 100: E1437–45

Dallatomasina A, Gasparri AM, Colombo B, Sacchi A, Bianco M, Daniele T, Esposito A, Pastorino F, Ponzoni M, Marcucci F, *et al* (2019) Spatiotemporal Regulation of Tumor Angiogenesis by Circulating Chromogranin A Cleavage and Neuropilin-1 Engagement. *Cancer Res* 79: 1925–1937

Dam G, Grønbæk H, Sorbye H, Thiis Evensen E, Paulsson B, Sundin A, Jensen C, Ebbesen D, Knigge U & Tiensuu Janson E (2020) Prospective Study of Chromogranin A as a Predictor of Progression in Patients with Pancreatic, Small-Intestinal, and Unknown Primary Neuroendocrine Tumors. *Neuroendocrinology* 110: 217–224

Das S & Dasari A (2021) Epidemiology, Incidence, and Prevalence of Neuroendocrine Neoplasms: Are There Global Differences? *Curr Oncol Rep* 23: 43

Dasari A, Shen C, Halperin D, Zhao B, Zhou S, Xu Y, Shih T & Yao JC (2017) Trends in the Incidence, Prevalence, and Survival Outcomes in Patients With Neuroendocrine Tumors in the United States. *JAMA Oncol* 3: 1335–1342

Dindo D, Demartines N & Clavien P-A (2004) Classification of surgical complications: a new proposal with evaluation in a cohort of 6336 patients and results of a survey. *Ann Surg* 240: 205–213

Di Domenico A, Wiedmer T, Marinoni I & Perren A (2017) Genetic and epigenetic drivers of neuroendocrine tumours (NET). *Endocr Relat Cancer* 24: R315–R334

Elias D, Lefevre JH, Duvillard P, Goéré D, Dromain C, Dumont F & Baudin E (2010) Hepatic metastases from neuroendocrine tumors with a ‘thin slice’ pathological examination: they are many more than you think. *Ann Surg* 251: 307–310

Falconi M, Eriksson B, Kaltsas G, Bartsch DK, Capdevila J, Caplin M, Kos-Kudla B, Kwekkeboom D, Rindi G, KlÖppel G, *et al* (2016) ENETS consensus guidelines update for the management of patients with functional pancreatic neuroendocrine tumors and non-functional pancreatic neuroendocrine tumors. *Neuroendocrinology* 103: 153–171

Ferrero E, Scabini S, Magni E, Foglieni C, Belloni D, Colombo B, Curnis F, Villa A, Ferrero ME & Corti A (2004) Chromogranin A protects vessels against tumor necrosis factor alpha-induced vascular leakage. *FASEB J* 18: 554–556

Filosso PL, Kidd M, Roffinella M, Lewczuk A, Chung K-M, Kolasinska-Cwikla A, Cwikla J, Lowczak A, Doboszynska A, Malczewska A, *et al* (2018) The utility of blood neuroendocrine gene transcript measurement in the diagnosis of bronchopulmonary neuroendocrine tumours and as a tool to evaluate surgical resection and disease progression. *Eur J cardio-thoracic Surg* 53: 631–639

Frank R & Hargreaves R (2003) Clinical biomarkers in drug discovery and development. *Nat Rev Drug Discov* 2: 566–580

Frilling A, Akerstrom G, Falconi M, Pavel M, Ramos J, Kidd M & Modlin IM (2012) Neuroendocrine tumor disease: an evolving landscape. *Endocr Relat Cancer* 19: R163–R185

Frilling A, Clift AK, Frampton AE, Bomanji J, Kaemmerer D, Al-Nahhas A, Alsafi A, Kidd M, Modlin IM, Hoersch D, *et al* (2021) A combination of surgery, theranostics, and liquid biopsy - a personalised oncologic approach to treatment of patients with advanced metastatic neuroendocrine neoplasms. *Int J Med Sci* 18: 2166–2175

Fujino M, Aishima S, Shindo K, Oda Y, Morimatsu K, Tsutsumi K, Otsuka T, Tanaka M & Oda Y (2016) Expression of glucose transporter-1 is correlated with hypoxia-inducible factor 1alpha and malignant potential in pancreatic neuroendocrine tumors. *Oncol Lett* 12: 3337–3343

Fuksiewicz M, Kowalska M, Kolasińska-Ćwikła A, Ćwikła JB, Sawicki Ł, Roszkowska-Purska K, Drygiel J & Kotowicz B (2018) Prognostic value of chromogranin A in patients with GET/NEN in the pancreas and the small intestine. *Endocr Connect* 7: 803–810

Garcia-Carbonero R, Sorbye H, Baudin E, Raymond E, Wiedenmann B, Niederle B, Sedlackova E, Toumpanakis C, Anlauf M, Cwikla JB, *et al* (2016) ENETS Consensus Guidelines for High-Grade Gastroenteropancreatic Neuroendocrine Tumors and Neuroendocrine Carcinomas. *Neuroendocrinology* 103: 186–194

Gasparri A, Sidoli A, Sanchez LP, Longhi R, Siccardi AG, Marchisio PC & Corti A (1997) Chromogranin A fragments modulate cell adhesion. Identification and characterization of a pro-adhesive domain. *J Biol Chem* 272: 20835–20843

Genç CG, Jilesen AP, Partelli S, Falconi M, Muffatti F, Van Kemenade FJ, Van Eeden S, Verheij J, Van Dieren S, Van Eijck CHJ, *et al* (2018) A New Scoring System to Predict Recurrent Disease in Grade 1 and 2 Nonfunctional Pancreatic

Neuroendocrine Tumors. *Ann Surg* 267:1148–1154

Genc CG, Jilesen APJ, Nieveen van Dijkum EJM, Klumpen H-J, van Eijck CHJ, Drozdov I, Malczewska A, Kidd M & Modlin I (2018) Measurement of circulating transcript levels (NETest) to detect disease recurrence and improve follow-up after curative surgical resection of well-differentiated pancreatic neuroendocrine tumors. *J Surg Oncol* 118: 37–48

Giovinazzo F, Schimmack S, Svejda B, Alaimo D, Pfragner R, Modlin I & Kidd M (2013) Chromogranin A and its fragments as regulators of small intestinal neuroendocrine neoplasm proliferation. *PLoS One* 8: e81111

Giusti M, Sidoti M, Augeri C, Rabitti C & Minuto F (2004) Effect of short-term treatment with low dosages of the proton-pump inhibitor omeprazole on serum chromogranin A levels in man. *Eur J Endocrinol* 150: 299–303

Guarneri G, de Mestier L, Landoni L, Partelli S, Gaujoux S, Andreasi V, Nessi C, Dokmak S, Fontana M, Dousset B, *et al* (2021) Prognostic Role of Examined and Positive Lymph Nodes after Distal Pancreatectomy for Non-Functioning Neuroendocrine Neoplasms. *Neuroendocrinology* 111: 728–738

Gut P, Czarnywojtek A & Ruchała M (2020) Chromogranin A assessment in patients with neuroendocrine neoplasm of the small bowel and carcinoid syndrome treated with somatostatin analogues. *Adv Clin Exp Med* 29: 1319–1324

Hamilton NA, Liu T-C, Cavatiao A, Mawad K, Chen L, Strasberg SS, Linehan DC, Cao D & Hawkins WG (2012) Ki-67 predicts disease recurrence and poor prognosis in pancreatic neuroendocrine neoplasms. *Surgery* 152: 107–113

Han X, Zhang C, Tang M, Xu X, Liu L, Ji Y, Pan B & Lou W (2015) The value of serum chromogranin A as a predictor of tumor burden, therapeutic response, and nomogram-based survival in well-moderate nonfunctional pancreatic neuroendocrine tumors with liver metastases. *Eur J Gastroenterol Hepatol* 27: 527–535

Harvey SR, Hurd TC, Markus G, Martinick MI, Penetrante RM, Tan D, Venkataraman P, DeSouza N, Sait SNJ, Driscoll DL, *et al* (2003) Evaluation of urinary plasminogen activator, its receptor, matrix metalloproteinase-9, and von Willebrand factor in pancreatic cancer. *Clin cancer Res* 9: 4935–4943

Hashim YM, Trinkaus KM, Linehan DC, Strasberg SS, Fields RC, Cao D & Hawkins

WG (2014) Regional lymphadenectomy is indicated in the surgical treatment of pancreatic neuroendocrine tumors (PNETs). *Ann Surg* 259: 197–203

Helle KB & Corti A (2015) Chromogranin A: a paradoxical player in angiogenesis and vascular biology. *Cell Mol Life Sci* 72: 339–348

Hijioka M, Ito T, Igarashi H, Fujimori N, Lee L, Nakamura T, Jensen RT & Takayanagi R (2014) Serum chromogranin A is a useful marker for Japanese patients with pancreatic neuroendocrine tumors. *Cancer Sci* 105: 1464–1471

Howe JR, Merchant NB, Conrad C, Keutgen XM, Hallet J, Drebin JA, Minter RM, Lairmore TC, Tseng JF, Zeh HJ, *et al* (2020) The North American Neuroendocrine Tumor Society Consensus Paper on the Surgical Management of Pancreatic Neuroendocrine Tumors. *Pancreas* 49: 1–33

Howlader N, Noone AM, Krapcho M, Miller D, Brest A, Yu M, Ruhl J, Tatalovich Z, Mariotto A, Lewis DR, Chen HS, Feuer EJ CK ed. (2019) SEER Cancer Statistics Review, 1975-2016, National Cancer Institute.

Hsieh JC-H, Chen G-Y, Jhou DD-W, Chou W-C, Yeh C-N, Hwang T-L, Lin H-C, Chu H-C, Wang H-M, Yen T-C, *et al* (2019) The Prognostic Value of Circulating Tumor Cells in Asian Neuroendocrine Tumors. *Sci Rep* 9: 19917

Huang X, Gao P, Song Y, Sun J, Chen X, Zhao J, Xu H & Wang Z (2015) Meta-analysis of the prognostic value of circulating tumor cells detected with the CellSearch System in colorectal cancer. *BMC Cancer* 15: 202

Hulka B (1990) Overview of biological markers. In *Biological Markers in Epidemiology*, Hulka, B; Griffith, J; Wilcosky T (ed) pp 3–15. New York: Oxford University Press

Jiang Q, Taupenot L, Mahata SK, Mahata M, O'Connor DT, Miles LA & Parmer RJ (2001) Proteolytic cleavage of chromogranin A (CgA) by plasmin. Selective liberation of a specific bioactive CgA fragment that regulates catecholamine release. *J Biol Chem* 276: 25022–25029

Jilesen APJ, Busch ORC, van Gulik TM, Gouma DJ & Nieveen van Dijkum EJM (2014) Standard pre- and postoperative determination of chromogranin a in resectable non-functioning pancreatic neuroendocrine tumors--diagnostic accuracy: NF-pNET and low tumor burden. *Dig Surg* 31: 407–414

Jun E, Kim SC, Song KB, Hwang DW, Lee JH, Shin SH, Hong SM, Park K-M & Lee Y-J (2017) Diagnostic value of chromogranin A in pancreatic neuroendocrine tumors

depends on tumor size: A prospective observational study from a single institute. *Surgery* 162: 120–130

Khan MS, Kirkwood A, Tsigani T, Garcia-Hernandez J, Hartley JA, Caplin ME & Meyer T (2013a) Circulating tumor cells as prognostic markers in neuroendocrine tumors. *J Clin Oncol* 31: 365–372

Khan MS, Kirkwood AA, Tsigani T, Lowe H, Goldstein R, Hartley JA, Caplin ME & Meyer T (2016a) Early Changes in Circulating Tumor Cells Are Associated with Response and Survival Following Treatment of Metastatic Neuroendocrine Neoplasms. *Clin cancer Res* 22: 79–85

Khan MS, Luong T V, Watkins J, Toumpanakis C, Caplin ME & Meyer T (2013b) A comparison of Ki-67 and mitotic count as prognostic markers for metastatic pancreatic and midgut neuroendocrine neoplasms. *Br J Cancer* 108: 1838–1845

Khan MS, Tsigani T, Rashid M, Rabouhans JS, Yu D, Luong TV, Caplin M & Meyer T (2011) Circulating tumor cells and EpCAM expression in neuroendocrine tumors. *Clin Cancer Res* 17: 337–345

Khan TM, Garg M, Warner RRP, Uhr JH & Divino CM (2016b) Elevated Serum Pancreastatin Is an Indicator of Hepatic Metastasis in Patients With Small Bowel Neuroendocrine Tumors. *Pancreas* 45: 1032–1035

Kidd M, Drozdov I & Modlin I (2015) Blood and tissue neuroendocrine tumor gene cluster analysis correlate, define hallmarks and predict disease status. *Endocr Relat Cancer* 22: 561–575

Kim JY, Lee SH, An S, Kim SJ, Sung Y-N, Song K-B, Hwang DW, Kim SC & Hong S-M (2018) Carbonic anhydrase 9 expression in well-differentiated pancreatic neuroendocrine neoplasms might be associated with aggressive behavior and poor survival. *Virchows Arch* 472: 739–748

Kimura W, Kuroda A & Morioka Y (1991) Clinical pathology of endocrine tumors of the pancreas. Analysis of autopsy cases. *Dig Dis Sci* 36: 933–942

Kishi S, Sakamoto K, Mori M, Isogawa A & Shiba T (2012) Asymptomatic insulinoma: a case report and autopsy series. *Diabetes Res Clin Pract* 98: 445–451

Kleeff J, Korc M, Apte M, La Vecchia C, Johnson CD, Biankin A V, Neale RE, Tempero M, Tuveson DA, Hruban RH, *et al* (2016) Pancreatic cancer. *Nat Rev Dis Prim* 2: 16022

Kuo EJ & Salem RR (2013) Population-level analysis of pancreatic neuroendocrine tumors 2 cm or less in size. *Ann Surg Oncol* 20: 2815–2821

Landoni L, Marchegiani G, Pollini T, Cingarlini S, D'Onofrio M, Capelli P, De Robertis R, Davi M V, Amodio A, Impellizzeri H, *et al* (2019) The Evolution of Surgical Strategies for Pancreatic Neuroendocrine Tumors (Pan-NENs): Time-trend and Outcome Analysis From 587 Consecutive Resections at a High-volume Institution. *Ann Surg* 269: 725–732

Langstein HN, Norton JA, Chiang V, O'Dorisio TM, Maton PN, Marx SJ & Jensen RT (1990) The utility of circulating levels of human pancreatic polypeptide as a marker for islet cell tumors. *Surgery* 108: 1106–1109

Laskaratos F-M, Liu M, Malczewska A, Ogunbiyi O, Watkins J, Luong TV, Mandair D, Caplin M & Toumpanakis C (2020) Evaluation of circulating transcript analysis (NETest) in small intestinal neuroendocrine neoplasms after surgical resection. *Endocrine* 69: 430–440

Lee JC, Taylor C V, Gaucher SP, Toneff T, Taupenot L, Yasothornsrikul S, Mahata SK, Sei C, Parmer RJ, Neveu JM, *et al* (2003) Primary sequence characterization of catestatin intermediates and peptides defines proteolytic cleavage sites utilized for converting chromogranin a into active catestatin secreted from neuroendocrine chromaffin cells. *Biochemistry* 42: 6938–6946

Lee SH, Jo JH, Kim YJ, Lee HS, Chung MJ, Park JY, Bang S, Park SW & Song SY (2019) Plasma Chromogranin A as a Prognostic Marker in Pancreatic Ductal Adenocarcinoma. *Pancreas* 48: 662–669

Li S-C, Essaghir A, Martijn C, Lloyd R V, Demoulin J-B, Oberg K & Giandomenico V (2013) Global microRNA profiling of well-differentiated small intestinal neuroendocrine tumors. *Mod Pathol* 26: 685–696

Lim M, Erdman P, Cho S, Mathew A, Fleisher M & Thoren KL (2019) Evaluation of CisBio ELISA for Chromogranin A Measurement. *J Appl Lab Med* 4: 11–18

Liu E, Paulson S, Gulati A, Freudman J, Grosh W, Kafer S, Wickremesinghe PC, Salem RR & Bodei L (2019) Assessment of NETest Clinical Utility in a U.S. Registry-Based Study. *Oncologist* 24: 783–790

Lloyd, RV, Osamura, RY, Kloppel, G, Rosai J ed. (2017) WHO Classification of Tumours of Endocrine Organs 4th ed. Lyon: IARC Press

Mahata SK & Corti A (2019) Chromogranin A and its fragments in cardiovascular, immunometabolic, and cancer regulation. *Ann N Y Acad Sci* 1455: 34–58

Malaguarnera M, Cristaldi E, Cammalleri L, Colonna V, Lipari H, Capici A, Cavallaro A, Beretta M, Alessandria I, Luca S, *et al* (2009) Elevated chromogranin A (CgA) serum levels in the patients with advanced pancreatic cancer. *Arch Gerontol Geriatr* 48: 213–217

Malczewska A, Bodei L, Kidd M & Modlin IM (2019a) Blood mRNA Measurement (NETest) for Neuroendocrine Tumor Diagnosis of Image-Negative Liver Metastatic Disease. *J Clin Endocrinol Metab* 104: 867–872

Malczewska A, Kidd M, Matar S, Kos-Kudla B & Modlin IM (2018) A Comprehensive Assessment of the Role of miRNAs as Biomarkers in Gastroenteropancreatic Neuroendocrine Tumors. *Neuroendocrinology* 107: 73–90

Malczewska A, Oberg K, Bodei L, Aslanian H, Lewczuk A, Filosso PL, Wójcik-Giertuga M, Rydel M, Zielińska-Leś I, Walter A, *et al* (2019b) NETest Liquid Biopsy Is Diagnostic of Lung Neuroendocrine Tumors and Identifies Progressive Disease. *Neuroendocrinology* 108: 219–231

Malczewska A, Witkowska M, Makulik K, Bocian A, Walter A, Pilch-Kowalczyk J, Zajęcki W, Bodei L, Oberg KE & Kos-Kudła B (2019c) NETest liquid biopsy is diagnostic of small intestine and pancreatic neuroendocrine tumors and correlates with imaging. *Endocr Connect* 8: 442–453

Marchegiani G, Landoni L, Andrianello S, Masini G, Cingarlini S, D'Onofrio M, De Robertis R, Davì M, Capelli P, Manfrin E, *et al* (2019) Patterns of Recurrence after Resection for Pancreatic Neuroendocrine Tumors: Who, When, and Where? *Neuroendocrinology* 108:161–171

Marinoni I, Kurrer AS, Vassella E, Dettmer M, Rudolph T, Banz V, Hunger F, Pasquinelli S, Speel EJ & Perren A (2014) Loss of DAXX and ATRX are associated with chromosome instability and reduced survival of patients with pancreatic neuroendocrine tumors. *Gastroenterology* 146: 453–460.e5

Marion-Audibert AM, Barel C, Gouysse G, Dumortier J, Pilleul F, Pourreyron C, Hervieu V, Poncet G, Lombard-Bohas C, Chayvialle JA, *et al* (2003) Low microvessel density is an unfavorable histoprognostic factor in pancreatic endocrine tumors. *Gastroenterology* 125: 1094–1104

Marotta V, Nuzzo V, Ferrara T, Zuccoli A, Masone M, Nocerino L, Del Prete M, Marciello F, Ramundo V, Lombardi G, *et al* (2012) Limitations of Chromogranin A in clinical practice. *Biomarkers* 17: 186–191

Massironi S, Rossi RE, Casazza G, Conte D, Ciafardini C, Galeazzi M & Peracchi M (2014) Chromogranin A in diagnosing and monitoring patients with gastroenteropancreatic neuroendocrine neoplasms: a large series from a single institution. *Neuroendocrinology* 100: 240–249

Modlin IM, Aslanian H, Bodei L, Drozdov I & Kidd M (2014) A PCR blood test outperforms chromogranin A in carcinoid detection and is unaffected by proton pump inhibitors. *Endocr Connect* 3: 215–223

Modlin IM, Bodei L & Kidd M (2016a) Neuroendocrine tumor biomarkers: From monoanalytes to transcripts and algorithms. *Best Pract Res Clin Endocrinol Metab* 30: 59–77

Modlin IM, Drozdov I & Kidd M (2013) The identification of gut neuroendocrine tumor disease by multiple synchronous transcript analysis in blood. *PLoS One* 8: e63364

Modlin IM, Frilling A, Salem RR, Alaimo D, Drymousis P, Wasan HS, Callahan S, Faiz O, Weng L, Teixeira N, *et al* (2016b) Blood measurement of neuroendocrine gene transcripts defines the effectiveness of operative resection and ablation strategies. *Surgery* 159: 336–347

Modlin IM, Gustafsson BI, Moss SF, Pavel M, Tsolakis A V & Kidd M (2010) Chromogranin A--biological function and clinical utility in neuro endocrine tumor disease. *Ann Surg Oncol* 17: 2427–2443

Modlin IM, Kidd M, Bodei L, Drozdov I & Aslanian H (2015) The clinical utility of a novel blood-based multi-transcriptome assay for the diagnosis of neuroendocrine tumors of the gastrointestinal tract. *Am J Gastroenterol* 110: 1223–1232

Modlin IM, Kidd M, Falconi M, Filosso PL, Frilling A, Malczewska A, Toumpanakis C, Valk G, Pacak K, Bodei L, *et al* (2021a) A multigenomic liquid biopsy biomarker for neuroendocrine tumor disease outperforms CgA and has surgical and clinical utility. *Ann Oncol* S0923-7534(21)03975-2

Modlin IM, Kidd M, Frilling A, Falconi M, Filosso PL, Malczewska A & Kitz A (2021b) Molecular Genomic Assessment using a blood-based mRNA signature (NETest) is Cost Effective and Predicts Neuroendocrine Tumor Recurrence with 94% accuracy.

Ann Surg 274:481–490

Modlin IM, Kidd M, Malczewska A, Drozdov I, Bodei L, Matar S & Chung K-M (2018) The NETest: The Clinical Utility of Multigene Blood Analysis in the Diagnosis and Management of Neuroendocrine Tumors. *Endocrinol Metab Clin North Am* 47: 485–504

Modlin IM, Kidd M, Oberg K, Falconi M, Filosso PL, Frilling A, Malczewska A, Salem R, Toumpanakis C, Laskaratos F-M, *et al* (2021c) Early Identification of Residual Disease After Neuroendocrine Tumor Resection Using a Liquid Biopsy Multigenomic mRNA Signature (NETest). *Ann Surg Oncol* doi: 10.1245/s10434-021-10021-1 Online ahead of print

Mosli HH, Dennis A, Kocha W, Asher LJ & Van Uum SHM (2012) Effect of short-term proton pump inhibitor treatment and its discontinuation on chromogranin A in healthy subjects. *J Clin Endocrinol Metab* 97: E1731-5

Nehar D, Lombard-Bohas C, Olivieri S, Claustrat B, Chayvialle J-A, Penes M-C, Sassolas G & Borson-Chazot F (2004) Interest of Chromogranin A for diagnosis and follow-up of endocrine tumours. *Clin Endocrinol (Oxf)* 60: 644–652

Neoptolemos JP, Stocken DD, Friess H, Bassi C, Dunn JA, Hickey H, Beger H, Fernandez-Cruz L, Dervenis C, Lacaine F, *et al* (2004) A randomized trial of chemoradiotherapy and chemotherapy after resection of pancreatic cancer. *N Engl J Med* 350: 1200–1210

Nobels FR, Kwekkeboom DJ, Coopmans W, Schoenmakers CH, Lindemans J, De Herder WW, Krenning EP, Bouillon R & Lamberts SW (1997) Chromogranin A as serum marker for neuroendocrine neoplasia: comparison with neuron-specific enolase and the alpha-subunit of glycoprotein hormones. *J Clin Endocrinol Metab* 82: 2622–2628

Nolting S, Kuttner A, Lauseker M, Vogeser M, Haug A, Herrmann KA, Hoffmann JN, Spitzweg C, Goke B & Auernhammer CJ (2012) Chromogranin a as serum marker for gastroenteropancreatic neuroendocrine tumors: a single center experience and literature review. *Cancers (Basel)* 4: 141–155

O'Dorisio TM, Krutzik SR, Woltering EA, Lindholm E, Joseph S, Gandolfi AE, Wang Y-Z, Boudreaux JP, Vinik AI, Go VLW, *et al* (2010) Development of a highly sensitive and specific carboxy-terminal human pancreastatin assay to monitor

neuroendocrine tumor behavior. *Pancreas* 39: 611–616

Oberg K (2011) Circulating biomarkers in gastroenteropancreatic neuroendocrine tumours. *Endocr Relat Cancer* 18 Suppl 1: S17–25

Öberg K (2021) Molecular Genomic Blood Biomarkers for Neuroendocrine Tumors: The Long and Winding Road from Berzelius and Bence Jones to a Neuroendocrine Destination. *Neuroendocrinology* 111: 297–303

Oberg K, Califano A, Strosberg JR, Ma S, Pape U, Bodei L, Kaltsas G, Toumpanakis C, Goldenring JR, Frilling A, *et al* (2020) A meta-analysis of the accuracy of a neuroendocrine tumor mRNA genomic biomarker (NETest) in blood. *Ann Oncol* 31: 202–212

Oberg K, Krenning E, Sundin A, Bodei L, Kidd M, Tesselaar M, Ambrosini V, Baum RP, Kulke M, Pavel M, *et al* (2016) A Delphic consensus assessment: imaging and biomarkers in gastroenteropancreatic neuroendocrine tumor disease management. *Endocr Connect* 5: 174–187

Oberg K, Modlin IM, De Herder W, Pavel M, Klimstra D, Frilling A, Metz DC, Heaney A, Kwekkeboom D, Strosberg J, *et al* (2015) Consensus on biomarkers for neuroendocrine tumour disease. *Lancet Oncol* 16: e435–e446

Paik WH, Ryu JK, Song BJ, Kim J, Park JK, Kim Y-T & Yoon YB (2013) Clinical Usefulness of Plasma Chromogranin A in Pancreatic Neuroendocrine Neoplasm. *J Korean Med Sci* 28: 750–754

Partelli S, Andreasi V, Muffatti F, Schiavo Lena M & Falconi M (2020a) Circulating Neuroendocrine Gene Transcripts (NETest): A Postoperative Strategy for Early Identification of the Efficacy of Radical Surgery for Pancreatic Neuroendocrine Tumors. *Ann Surg Oncol* 27:3928–3936

Partelli S, Bartsch DK, Capdevila J, Chen J, Knigge U, Niederle B, Nieveen van Dijkum EJM, Pape U-F, Pascher A, Ramage J, *et al* (2017) ENETS Consensus Guidelines for Standard of Care in Neuroendocrine Tumours: Surgery for Small Intestinal and Pancreatic Neuroendocrine Tumours. *Neuroendocrinology* 105: 255–265

Partelli S, Gaujoux S, Boninsegna L, Cherif R, Crippa S, Couvelard A, Scarpa A, Ruszniewski P, Sauvanet A & Falconi M (2013) Pattern and Clinical Predictors of Lymph Node Involvement in Nonfunctioning Pancreatic Neuroendocrine Tumors (NF-PanNETs). *JAMA Surg* 148: 932–939

Partelli S, Giannone F, Schiavo Lena M, Muffatti F, Andreasi V, Crippa S, Tamburrino D, Zamboni G, Rubini C, Doglioni C, *et al* (2019) Is the Real Prevalence of Pancreatic Neuroendocrine Tumors Underestimated? A Retrospective Study on a Large Series of Pancreatic Specimens. *Neuroendocrinology* 109: 165–170

Partelli S, Javed AA, Andreasi V, He J, Muffatti F, Weiss MJ, Sessa F, La Rosa S, Doglioni C, Zamboni G, *et al* (2018) The number of positive nodes accurately predicts recurrence after pancreaticoduodenectomy for nonfunctioning neuroendocrine neoplasms. *Eur J Surg Oncol* 44: 778–783

Partelli S, Landoni L, Andreasi V, Nessi C, Muffatti F, Crippa S, Cingarlini S, Bassi C & Falconi M (2020b) Pattern of disease recurrence and treatment after surgery for nonfunctioning well-differentiated pancreatic neuroendocrine tumors. *Surgery* 168: 816–824

Pavel M, Jann H, Prasad V, Drozdov I, Modlin IM & Kidd M (2017) NET Blood Transcript Analysis Defines the Crossing of the Clinical Rubicon: When Stable Disease Becomes Progressive. *Neuroendocrinology* 104: 170–182

Pregun I, Herszenyi L, Juhasz M, Miheller P, Hritz I, Patocs A, Racz K & Tulassay Z (2011) Effect of proton-pump inhibitor therapy on serum chromogranin a level. *Digestion* 84: 22–28

Puliani G, Di Vito V, Feola T, Sesti F, Centello R, Pandozzi C, Tarsitano MG, Verrico M, Lenzi A, Isidori AM, *et al* (2021) NETest: a systematic review focusing on the prognostic and predictive role. *Neuroendocrinology* doi:10.1159/000518873 Online ahead of print

Pulvirenti A, Javed AA, Landoni L, Jamieson NB, Chou JF, Miotto M, He J, Gonen M, Pea A, Tang LH, *et al* (2019a) Multi-institutional Development and External Validation of a Nomogram to Predict Recurrence after Curative Resection of Pancreatic Neuroendocrine Tumors. *Ann Surg* doi: 10.1097/SLA.0000000000003579. Online ahead of print

Pulvirenti A, Pea A, Chang DK & Jamieson NB (2020) Clinical and Molecular Risk Factors for Recurrence Following Radical Surgery of Well-Differentiated Pancreatic Neuroendocrine Tumors. *Front Med* 7: 385

Pulvirenti A, Rao D, Mcintyre CA, Gonen M, Tang LH, Klimstra DS, Fleisher M, Ramanathan L V, Reidy-Lagunes D & Allen PJ (2019b) Limited role of

Chromogranin A as clinical biomarker for pancreatic neuroendocrine tumors. *HPB (Oxford)* 21: 612–618

Qiu W, Christakis I, Silva A, Bassett RLJ, Cao L, Meng QH, Gardner Grubbs E, Zhao H, Yao JC, Lee JE, *et al* (2016) Utility of chromogranin A, pancreatic polypeptide, glucagon and gastrin in the diagnosis and follow-up of pancreatic neuroendocrine tumours in multiple endocrine neoplasia type 1 patients. *Clin Endocrinol (Oxf)* 85: 400–407

Reni M, Andreasi V, Gasparri AM, Dugnani E, Colombo B, Macchini M, Bianco M, Dallatomasina A, Citro A, Assi E, *et al* (2020) Circulating Chromogranin A Is Cleaved Into Vasoregulatory Fragments in Patients With Pancreatic Ductal Adenocarcinoma. *Front Oncol* 10: 613582

Ricci C, Partelli S, Landoni L, Rinzivillo M, Ingaldi C, Andreasi V, Nessi C, Muffatti F, Fontana M, Tamburrino D, *et al* (2021) Sporadic non-functioning pancreatic neuroendocrine tumours: multicentre analysis. *Br J Surg* 108: 811–816

Rindi G, Klersy C, Albarello L, Baudin E, Bianchi A, Buchler MW, Caplin M, Couvelard A, Cros J, de Herder WW, *et al* (2018) Competitive Testing of the WHO 2010 versus the WHO 2017 Grading of Pancreatic Neuroendocrine Neoplasms: Data from a Large International Cohort Study. *Neuroendocrinology* 107: 375–386

Rindi G, Kloppel G, Alhman H, Caplin M, Couvelard A, de Herder WW, Erikssson B, Falchetti A, Falconi M, Komminoth P, *et al* (2006) TNM staging of foregut (neuro)endocrine tumors: a consensus proposal including a grading system. *Virchows Arch* 449: 395–401

Rinzivillo M, Partelli S, Prosperi D, Capurso G, Pizzichini P, Iannicelli E, Merola E, Muffatti F, Scopinaro F, Schillaci O, *et al* (2018) Clinical Usefulness of (18)F-Fluorodeoxyglucose Positron Emission Tomography in the Diagnostic Algorithm of Advanced Entero-Pancreatic Neuroendocrine Neoplasms. *Oncologist* 23: 186–192

Roldo C, Missiaglia E, Hagan JP, Falconi M, Capelli P, Bersani S, Calin GA, Volinia S, Liu C-G, Scarpa A, *et al* (2006) MicroRNA expression abnormalities in pancreatic endocrine and acinar tumors are associated with distinctive pathologic features and clinical behavior. *J Clin Oncol* 24: 4677–4684

Rossi RE, Garcia-Hernandez J, Meyer T, Thirlwell C, Watkins J, Martin NG, Caplin ME & Toumpanakis C (2015) Chromogranin A as a predictor of radiological disease

progression in neuroendocrine tumours. *Ann Transl Med* 3: 118

Scarpa A, Chang DK, Nones K, Corbo V, Patch A-M, Bailey P, Lawlor RT, Johns AL, Miller DK, Mafficini A, *et al* (2017) Whole-genome landscape of pancreatic neuroendocrine tumours. *Nature* 543: 65–71

Schmitt AM, Schmid S, Rudolph T, Anlauf M, Prinz C, Kloppel G, Moch H, Heitz PU, Komminoth P & Perren A (2009) VHL inactivation is an important pathway for the development of malignant sporadic pancreatic endocrine tumors. *Endocr Relat Cancer* 16: 1219–1227

Schneider F, Bach C, Chung H, Crippa L, Lavaux T, Bollaert P-E, Wolff M, Corti A, Launoy A, Delabranche X, *et al* (2012) Vasostatin-I, a chromogranin A-derived peptide, in non-selected critically ill patients: distribution, kinetics, and prognostic significance. *Intensive Care Med* 38: 1514–1522

Schwartz LH, Litiere S, de Vries E, Ford R, Gwyther S, Mandrekar S, Shankar L, Bogaerts J, Chen A, Dancey J, *et al* (2016) RECIST 1.1-Update and clarification: From the RECIST committee. *Eur J Cancer* 62: 132–137

Shah D, Lamarca A, Valle JW & McNamara MG (2021a) The Potential Role of Liquid Biopsies in Advancing the Understanding of Neuroendocrine Neoplasms. *J Clin Med* 10: 403

Shah MH, Goldner WS, Benson AB, Bergsland E, Blaszkowsky LS, Brock P, Chan J, Das S, Dickson P V, Fanta P, *et al* (2021b) Neuroendocrine and Adrenal Tumors, Version 2.2021, NCCN Clinical Practice Guidelines in Oncology. *J Natl Compr Canc Netw* 19: 839–868

Shanahan MA, Salem A, Fisher A, Cho CS, Leverson G, Winslow ER & Weber SM (2016) Chromogranin A predicts survival for resected pancreatic neuroendocrine tumors. *J Surg Res* 201: 38–43

Sherman SK, Maxwell JE, O'Dorisio MS, O'Dorisio TM & Howe JR (2014) Pancreastatin predicts survival in neuroendocrine tumors. *Ann Surg Oncol* 21: 2971–2980

Siegel RL, Miller KD, Fuchs HE & Jemal A (2021) Cancer Statistics, 2021. *CA Cancer J Clin* 71: 7–33

Singh S, Chan DL, Moody L, Liu N, Fischer HD, Austin PC & Segelov E (2018a) Recurrence in Resected Gastroenteropancreatic Neuroendocrine Tumors. *JAMA*

Oncol 4: 583–585

Singh S, Moody L, Chan DL, Metz DC, Strosberg J, Asmis T, Bailey DL, Bergsland E, Brendtro K, Carroll R, *et al* (2018b) Follow-up Recommendations for Completely Resected Gastroenteropancreatic Neuroendocrine Tumors. *JAMA Oncol* 4: 1597–1604

Siravegna G, Marsoni S, Siena S & Bardelli A (2017) Integrating liquid biopsies into the management of cancer. *Nat Rev Clin Oncol* 14: 531–548

Srirajaskanthan R, Kayani I, Quigley AM, Soh J, Caplin ME & Bomanji J (2010) The role of 68Ga-DOTATATE PET in patients with neuroendocrine tumors and negative or equivocal findings on 111In-DTPA-octreotide scintigraphy. *J Nucl Med* 51: 875–882

Stronge RL, Turner GB, Johnston BT, McCance DR, McGinty A, Patterson CC & Ardill JES (2008) A rapid rise in circulating pancreastatin in response to somatostatin analogue therapy is associated with poor survival in patients with neuroendocrine tumours. *Ann Clin Biochem* 45: 560–566

Strosberg D, Schneider EB, Onesti J, Saunders N, Konda B, Shah M, Dillhoff M, Schmidt CR & Shirley LA (2018) Prognostic Impact of Serum Pancreastatin Following Chemoembolization for Neuroendocrine Tumors. *Ann Surg Oncol* 25: 3613–3620

Sundin A & Rockall A (2012) Therapeutic monitoring of gastroenteropancreatic neuroendocrine tumors: the challenges ahead. *Neuroendocrinology* 96: 261–271

Syversen U, Ramstad H, Gamme K, Qvigstad G, Falkmer S & Waldum HL (2004) Clinical significance of elevated serum chromogranin A levels. *Scand J Gastroenterol* 39: 969–973

Takahashi Y, Akishima-Fukasawa Y, Kobayashi N, Sano T, Kosuge T, Nimura Y, Kanai Y & Hiraoka N (2007) Prognostic value of tumor architecture, tumor-associated vascular characteristics, and expression of angiogenic molecules in pancreatic endocrine tumors. *Clin Cancer Res* 13:187–196

Taupenot L, Harper KL & O'Connor DT (2003) The chromogranin-secretogranin family. *N Engl J Med* 348: 1134–1149

Theurl M, Schgoer W, Albrecht K, Jeschke J, Egger M, Beer AGE, Vasiljevic D, Rong S, Wolf AM, Bahlmann FH, *et al* (2010) The neuropeptide catestatin acts as a novel angiogenic cytokine via a basic fibroblast growth factor-dependent mechanism. *Circ*

Res 107: 1326–1335

Thorns C, Schurmann C, Gebauer N, Wallaschofski H, Kumpers C, Bernard V, Feller AC, Keck T, Habermann JK, Begum N, *et al* (2014) Global microRNA profiling of pancreatic neuroendocrine neoplasias. *Anticancer Res* 34: 2249–2254

Tie J, Wang Y, Tomasetti C, Li L, Springer S, Kinde I, Silliman N, Tacey M, Wong H-L, Christie M, *et al* (2016) Circulating tumor DNA analysis detects minimal residual disease and predicts recurrence in patients with stage II colon cancer. *Sci Transl Med* 8: 346ra92

Tombetti E, Colombo B, Di Chio MC, Sartorelli S, Papa M, Salerno A, Bozzolo EP, Tombolini E, Benedetti G, Godi C, *et al* (2016) Chromogranin-A production and fragmentation in patients with Takayasu arteritis. *Arthritis Res Ther* 18: 187

Tran CG, Sherman SK, Scott AT, Ear PH, Chandrasekharan C, Bellizzi AM, Dillon JS, O'Dorisio TM & Howe JR (2021) It Is Time to Rethink Biomarkers for Surveillance of Small Bowel Neuroendocrine Tumors. *Ann Surg Oncol* 28: 732–741

van Treijen MJC, Korse CM, van Leeuwaarde RS, Saveur LJ, Vriens MR, Verbeek WHM, Tesselaar MET & Valk GD (2018) Blood Transcript Profiling for the Detection of Neuroendocrine Tumors: Results of a Large Independent Validation Study. *Front Endocrinol (Lausanne)* 9: 740

Tseng C-M, Cheng T-Y, Chen T-B, Tien Y-W, Chen C-C, Lin J-T & Wang H-P (2018) Low accuracy of chromogranin A for diagnosing early-stage pancreatic neuroendocrine tumors. *Oncol Lett* 15: 8951–8958

Valicherla GR, Hossain Z, Mahata SK & Gayen JR (2013) Pancreastatin is an endogenous peptide that regulates glucose homeostasis. *Physiol Genomics* 45: 1060–1071

Vandamme T, Peeters M, Dogan F, Pauwels P, Van Assche E, Beyens M, Mortier G, Vandeweyer G, de Herder W, Van Camp G, *et al* (2015) Whole-exome characterization of pancreatic neuroendocrine tumor cell lines BON-1 and QGP-1. *J Mol Endocrinol* 54: 137–147

Veschini L, Crippa L, Dondossola E, Doglioni C, Corti A & Ferrero E (2011) The vasostatin-1 fragment of chromogranin A preserves a quiescent phenotype in hypoxia-driven endothelial cells and regulates tumor neovascularization. *FASEB J*: 3906–3914

Waldum HL, Arnestad JS, Brenna E, Eide I, Syversen U & Sandvik AK (1996) Marked increase in gastric acid secretory capacity after omeprazole treatment. *Gut* 39: 649–653

Walter T, Chardon L, Chopin-laly X, Raverot V, Caffin A-G, Chayvialle J-A, Scoazec J-Y & Lombard-Bohas C (2012) Is the combination of chromogranin A and pancreatic polypeptide serum determinations of interest in the diagnosis and follow-up of gastro-entero-pancreatic neuroendocrine tumours? *Eur J Cancer* 48: 1766–1773

Warnecke-Eberz U, Prenzel KL, Baldus SE, Metzger R, Dienes HP, Bollschweiler E, Hoelscher AH & Schneider PM (2008) Significant down-regulation of the plasminogen activator inhibitor 1 mRNA in pancreatic cancer. *Pancreas* 36: 173–177

Watanabe T (2021) The Emerging Roles of Chromogranins and Derived Polypeptides in Atherosclerosis, Diabetes, and Coronary Heart Disease. *Int J Mol Sci* 22: 6118

Woltering EA, Beyer DT, Thiagarajan R, Ramirez RA, Wang Y-Z, Ricks MJ & Boudreaux JP (2016) Elevated Plasma Pancreastatin, but Not Chromogranin A, Predicts Survival in Neuroendocrine Tumors of the Duodenum. *J Am Coll Surg* 222: 534–542

Woltering EA, Voros BA, Beyer DT, Thiagarajan R, Ramirez RA, Mamikunian G & Boudreaux JP (2019) Plasma Pancreastatin Predicts the Outcome of Surgical Cytoreduction in Neuroendocrine Tumors of the Small Bowel. *Pancreas* 48: 356–362

Wu JT, Erickson AJ, Tsao KC, Wu TL & Sun CF (2000) Elevated serum chromogranin A is detectable in patients with carcinomas at advanced disease stages. *Ann Clin Lab Sci* 30: 175–178

Xue A, Scarlett CJ, Jackson CJ, Allen BJ & Smith RC (2008) Prognostic significance of growth factors and the urokinase-type plasminogen activator system in pancreatic ductal adenocarcinoma. *Pancreas* 36: 160–167

Yao JC, Hassan M, Phan A, Dagohoy C, Leary C, Mares JE, Abdalla EK, Fleming JB, Vauthey J-N, Rashid A, *et al* (2008) One hundred years after 'carcinoid': epidemiology of and prognostic factors for neuroendocrine tumors in 35,825 cases in the United States. *J Clin Oncol* 26: 3063–3072

Yao JC, Pavel M, Phan AT, Kulke MH, Hoosen S, St Peter J, Cherfi A & Oberg KE

(2011) Chromogranin A and neuron-specific enolase as prognostic markers in patients with advanced pNET treated with everolimus. *J Clin Endocrinol Metab* 96: 3741–3749

Zaidi MY, Lopez-Aguiar AG, Switchenko JM, Lipscomb J, Andreasi V, Partelli S, Gamboa AC, Lee RM, Poultsides GA, Dillhoff M, *et al* (2019) A Novel Validated Recurrence Risk Score to Guide a Pragmatic Surveillance Strategy after Resection of Pancreatic Neuroendocrine Tumors: An International Study of 1006 Patients. *Ann Surg* 270:422–433

Zakka K, Nagy R, Drusbosky L, Akce M, Wu C, Alese OB, El-Rayes BF, Kasi PM, Mody K, Starr J, *et al* (2020) Blood-based next-generation sequencing analysis of neuroendocrine neoplasms. *Oncotarget* 11: 1749–1757

